SLAC-R-324

SLAC–324
CONF–8709224
UC–34D
(E)

PROCEEDINGS OF
THE B–MESON FACTORY WORKSHOP
Stanford, CA
September 8–9, 1987

Program Directors:
Elliott D. Bloom
Alfred Fridman

Ed. by Laura Friedsam

February 1988

Prepared for the Department on Energy
under contract number DE–AC03–76SF00515

Printed in the United States of America. Available from National Technical Information Service, U.S. Department of Commerce, 5285 Port Royal Road, Springfield, VA 22161. Price: Printed copy A04, Microfiche A01.

Foreword

A B–meson factory workshop was held at SLAC during September 8–9, 1987. It was planned as a natural follow-on to the **International Symposium on the Production and Decay of Heavy Flavors** held the previous week on the Stanford University campus. This workshop was one in an informal series extending over the previous year. Physicists from ten countries gathered to discuss and study the possibilities for machines and experiments which might greatly extend knowledge about the production and decay of B–mesons. Many of the lectures presented strong arguments that such an extension would lead to new information about CP violation as well as marked improvement of our knowledge of a number of areas of the "Standard Model" and "beyond." The format of this workshop was more like a mini conference with not much time for new work to be done. As in a number of the workshops of the recent past on this subject, the majority of attendees were highly motivated toward the creation of new advanced facilities for B–meson studies. Thus much useful information was passed through informal contact outside the formal lectures.

Interestingly, none of the scenarios discussed had the appearance of the "Holy Grail" of B physics, seeming more as needed developments along a very difficult road toward the goal of a measurement of CP violation in the B–meson system. It is clear that the road will be a long one, and most hoped for strong and lasting commitments toward an eventual understanding of these fascinating and deep phenomena.

We would like to thank all who worked so hard to make this workshop a success. The speakers were all highly motivated and well prepared; all but two wrote up their talks. Of course the speakers are the essence of an interesting and exciting conference. In addition, we would like to thank Nina Adelman and Laura Friedsam and staff for organizing and running the meeting, and Laura for editing these proceedings. Without a good humored and hardworking staff there is certainly no meeting. Finally, we would like to thank the SLAC administration for their cooperation and support, and in particular, the SLAC Director, Burton Richter, for his useful and informative welcoming address.

Elliott Bloom

Alfred Fridman

TABLE OF CONTENTS

THE SIN PROJECT

KLAUS WILLE
University of Dortmund, Germany

Abstract

Future experiments in the b–meson region require a luminosity of $L > 1 \times 10^{33}$ cm^{-2} sec^{-1} at 5 GeV which is more than one order of magnitude higher than presently available values. For the design of the b–meson factory described in this paper an e^+e^- storage ring was chosen. The two beams are mainly guided in two different rings allowing an operation with many bunches. The collision takes place in two interaction points head-on without any crossing angle. A mini beta scheme with superconductive quadrupoles provides the required small beam waist. Long electrostatic plates or fast rf-magnets on both sides of the interaction points are used for beam separation.

1. Introduction

The design of an ideal b–meson factory presented in this paper is based on the classical storage ring concept. Since e^+e^- storage rings have been in operation for many years, many experiences have been collected, and therefore, no serious risks or significant technical problems are expected. Presently, an electron storage ring seems to be the best solution for this purpose. This is important to avoid a substantial delay in constructing the b–meson factory.

The luminosity of an e^+e^- storage ring produced by n bunches per beam with a bunch current I_b is given by the well-known formula

$$L = \frac{n\ I_b^2}{4\pi\ e^2\ f_u\ \sigma_x^*\ \sigma_z^*} \quad , \tag{1}$$

where e is the charge of an electron and f_u the revolution frequency. For a beam energy E the transverse bunch dimensions in the Interaction Point (IP) may be expressed by $\sigma_{xz}^* = E\hat{\sigma}_{xz}^* = E\ (\hat{\epsilon}_{xz}\ \beta_{xz}^*)^{1/2}$ where $\hat{\sigma}_{xz}^*$ are the values at 1 GeV. In an ideal flat storage ring there exists only a natural horizontal emittance ϵ_{xo}. Because of imperfections in a real machine one has also a nonnegligible emittance in the vertical direction. This fact is normally expressed by the emittance coupling $k = \epsilon_z/\epsilon_x$ with $k > 0$. The emittances in both planes are given by the following simple relations

$$\epsilon_x = \frac{\epsilon_{xo}}{1+k} \qquad \text{and} \qquad \epsilon_z = \frac{k\ \epsilon_{xo}}{1+k} \quad . \tag{2}$$

During collision the particles of one bunch are focused by the space-charge forces of the opposite bunch which causes in the linear approximation a tune shift ΔQ. As found in most of the e^+e^- storage rings, a maximum tune shift of $\Delta Q_{\max} \approx 0.025$ is available during normal machine runs. Higher values are possible after very careful orbit corrections. Since ΔQ is proportional to the bunch current I_b, one cannot collide higher currents than

$$I_{\max}[\text{mA}] = 698.5\ \frac{f_u\ E^3\ (\hat{\sigma}_x^* + \hat{\sigma}_z^*)\ \hat{\sigma}_{xz}^*}{\beta_{xz}^*}\ \Delta Q_{xz} \quad . \tag{3}$$

This current limitation due to space-charge effects is the main limitation of the luminosity of a storage ring. Usually, for a given beam current, the tune shift ΔQ is different in both planes. This is not the best case from the luminosity point of view. For maximum luminosity, however, one has to fulfill the constraint $\Delta Q_x = \Delta Q_z = \Delta Q$. With this constraint, we can calculate the required emittance coupling using Eq. (2). We get

$$k = \frac{\beta_z^*}{\beta_x^*} = \frac{\epsilon_z}{\epsilon_x} \tag{4}$$

and the resulting bunch current limit becomes

$$I_{\max} = 698.5\ f_u\ E^3\ \epsilon_{xo}\ \Delta Q \quad . \tag{5}$$

With this simple expression we can finally write the optimized luminosity as

$$L = 1.513 \times 10^{32}\ \frac{n\ f_u\ E^4(1+k)\epsilon_{xo}}{\beta_z^*}\ \Delta Q^2 \quad . \tag{6}$$

2. Design Criteria of the B–Meson Factory

Following Eq. (6) one has, for a given energy E, five independent parameters to play with: ϵ_{xo}, β_z^*, n, ΔQ and k. In most of the e^+e^- storage rings the emittance coupling is rather small ($k \ll 1$). Therefore, the luminosity is mainly determined by the relation

$$L \sim \frac{n\ (1+k)\ \epsilon_{xo}}{\beta_z^*}\ \Delta Q^2 \approx \frac{n\ \epsilon_{xo}}{\beta_z^*}\ \Delta Q^2 \quad . \tag{7}$$

From this formula one can directly derive the constraints for high luminosity in an e^+e^- storage ring:

(1) a very small vertical beta function β_z^* in the IP

(2) the emittance ϵ_{xo} has to be as large as possible

(3) the storage ring should run with many bunches per beam ($n > 1$)

(4) the maximum tune shift ΔQ has to be as large as possible.

1. Lower limit for the vertical beta function β_z^*

The beta function in the IP must not be unlimitedly small. If $s = 0$ is the position of the IP, the beta function in this region is given by

$$\beta_z(s) = \beta_z^* + \frac{s^2}{\beta_z^*} \tag{8}$$

which is a consequence of Liouville's theorem. An extremely small value of β_z^* would cause a strong divergence of the beam in the IP. In other words, the beta function changes significantly along the bunch during collision. This leads, because of the space-charge effect, to a strong reduction of the maximum tune shift ΔQ and, consequently, to a much smaller luminosity. Therefore, in the range of $-\sigma_s < s < \sigma_s$, where σ_s is the bunchlength, the beta function has to be almost constant ($\beta_z(s) \approx \beta_z^*$). More precisely, one has to fulfill the following empirical relation

$$\frac{\beta_z(\sigma_s)}{\beta_z^*} = 1 + \left(\frac{\sigma_s}{\beta_z^*}\right)^2 < 1.5 \ \rightarrow\ \beta_z^* > 1.5\ \sigma_s \quad . \tag{9}$$

We assume an accelerator system running with a frequency of $f_{\text{rf}} = 500$ MHz which is from the present knowledge a good compromise between efficiency and cost. With this system the bunchlength is $\sigma_s \approx 2$ cm. Therefore, the lower limit for the vertical beta function is $\boldsymbol{\beta_z^* \geq 3}$ **cm**. This is, however, an extremely small value compared to the rest of the ring and it is therefore necessary to have a very strong focusing in the interaction region. Such an insertion providing a very small beam waist in the IP is called a "Mini Beta Scheme."[1]

One major problem of a small β_z^* value is caused by (8), the extremely large beta functions in the first vertically focusing quadrupoles mounted a certain distance away from the IP. Corresponding to the relation $\sigma = \sqrt{\epsilon\ \beta(s)}$, the beam dimensions in this quads become very large, limiting the aperture of the machine. Another problem is the resulting high chromaticity which describes the energy dependence of the tune and is defined by the relation $\xi := \Delta Q/(\Delta p/p)$. In an e^+e^- storage ring with mini beta insertions a significant portion of the chromaticity is produced by the first strong focusing quads next to the IP. It may be expressed by the relation

$$\xi = \frac{-1}{4\pi} \int_{\mathrm{QUAD}} \beta(s)\ k(s)\ ds \quad . \tag{10}$$

In order to avoid the "head tail" instability, a compensation of the chromaticity by use of sextupole magnets is required. High chromaticity makes strong sextupoles necessary. Strong sextupoles, however, reduce because of their nonlinear fields the so called "dynamic aperture."[2] The consequence is a short beam lifetime and smaller maximum currents. One can partly overcome this problem with a proper sextupole distribution. The best solution is an arrangement of two or more different sextupole "families," where the magnets of one particular family have a distance of half a betatron wavelength. Under these conditions most of the beam distortions caused by the sextupoles are nearly compensated. As shown in several storage rings, stable dynamic apertures of the order of $A_{\mathrm{dyn}} \approx 50$ mm are possible.

A magnet lattice with a rather low natural chromaticity is undoubtedly the best situation to start with. Therefore, a mini beta insertion has to be used with a very small distance between the IP and the first focusing quadrupole. For the b–meson factory a distance of only 0.6 m is chosen. This concept reduces, because of (8) and (10), the chromaticity significantly. The vertical and horizontal beta functions in the IP are $\beta_x^* = 1.00$ m and $\beta_z^* = 0.03$ m, respectively. The magnet arrangement of the mini beta insertion is sketched in Fig. 1.

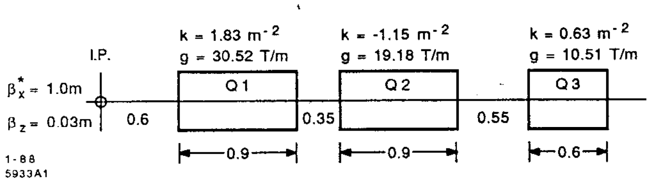

Fig. 1. The mini beta insertion for the b–meson factory.

At least the first vertically focusing quadrupole will be mounted inside the particle detector. It is important to mention here that all quadrupoles with a gradient of $g = \partial B_z/\partial x >$ 20 T/m are superconductive magnets.

2. Upper limit of the emittance ϵ_{xo}

In modern storage rings the horizontal aperture is of the order of $A_{\max} \approx 50$ mm and is limited either by the mechanical dimension of the vacuum chamber or more often by dynamic effects due to nonlinear magnetic fields. The upper limit of the emittance can be easily derived from the relation $A_{\max} = N\ \sigma_{\max} = N\ \sqrt{\epsilon_{xo}\ \beta_{\max}}$ where N is the number of standard deviations (STD) available for the beam. The maximum possible emittance therefore becomes

$$\epsilon_{\max} = \frac{A_{\max}^2}{N^2\ \beta_{\max}} \quad . \tag{11}$$

A beam lifetime of $\tau > 1$ hour requires a least $N = 7$ STD, but because of orbit distortions and mechanical tolerances this number should not be smaller than $N = 10$. Therefore, a large emittance is only possible with relatively small beta functions around the ring. For the b–meson factory the maximum beta function must not exceed the value $\beta_{\max} = 30$ m. Because of this constraint, the distance between the IP and the first vertically focusing quadrupole was set to $d = 0.6$ m. The resulting maximum emittance is, according to Eq. (11), $\boldsymbol{\epsilon_{\max} = 8.3 \times 10^{-7}}$ **m rad.**

3. Upper limit of the number of bunches

As seen in Eq. (1), the luminosity of a storage ring is proportional to the number n of bunches per beam. Generally one can get a large number of bunches by filling all buckets around the ring. This, however, would lead to a large number of uniformly distributed collision points around a standard single ring; but because of the space-charge effect the beams must not collide outside the IP's. Therefore, a beam separation is required. Since the b–meson factory has to run stable and reliable with the highest possible luminosity, one has to choose the best conditions for the storage ring. In particular, a very good orbit for both beams and an effective feedback system against the instabilities are necessary. Taking this into account two separated rings with combined insertions in the interaction region seems to be the best solution for this purpose (Fig. 2). As shown in DORIS I[3] it is extremely important to avoid any crossing angle between the colliding beams which would cause strong additional transverse space-charge forces, reducing the luminosity significantly.

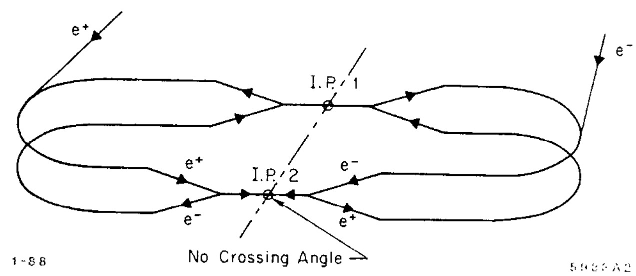

Fig. 2. Sketch of the double ring with head-on collision.

The beam separation on both sides of the IP's may be done either by time, by use of fast rf-magnets, or by charge, by use of electrostatic fields. Unfortunately, both principles provide an extremely small bending angle. Therefore, rather long driftspaces are required. In order to avoid beam-beam interaction inside this driftspace, the bunch spacing has to be of the order of 40 m. Assuming a machine circumference of l = 518.4 m, a maximum number of $\mathbf{n = 12}$ bunches per beam is possible. Since the harmonic number $q = f_{rf}/f_u$ has the value $q = 864 = 2^5 \times 3^3$ following bunch numbers per beam are possible : $n = 1,2,3,4,6,8,9,12$.

4. Upper limit of the tune shift ΔQ

There are several effects limiting the maximum tune shift ΔQ and consequently the maximum colliding beam currents. Because of the nonlinear space charge forces between the two beams, synchrotron sidebands of the betatron oscillations are generated. These oscillations are called "synchro-betatron resonances."[4] The strength of the resonances grows with the beam current. It is obvious that this effect reduces the stable area in the tune diagram drastically. At the maximum possible current the free space in the diagram is totally filled by the beam. This is the limit for the tune shift.

At the space-charge limit, the particles in the electron beam do not have the gaussian charge distribution any longer, as is the case without interaction. Usually, the tails of the distribution contain more particles than the ideal gaussian distribution. Therefore, more particles are lost at the limit of the dynamic aperture.

Most of the electron-positron storage rings have, during normal experimental runs, a maximum tune shift of

$$\Delta Q_{\max} \approx 0.025 \quad . \tag{12}$$

This value is possible without special procedures. Therefore one can take this empirical value for all luminosity calculations providing a rather conservative estimate.

There are, however, cures to get higher tune shifts. First of all, a careful alignment of all magnets around the machine is required as well as an effective orbit correction. But because of the systematic errors of the positron monitors and the position errors of the magnets, the standard orbit correction is not sufficient. An empirical fine tune of the orbit can increase the tune shift and the luminosity significantly as demonstrated at PETRA[5] and PEP.[6]

Under all circumstances a large dynamic aperture helps a lot to reduce the space-charge effects. Therefore, this is a very important point one has to look at during the machine design. Based on knowledge and experience presently available, it should be possible to replace the empirical procedure by an improved orbit correction scheme which automatically finds the highest possible tune shift. With this technique a maximum tune shift of **$\Delta Q \approx 0.05$** will be available.

2. Magnet Lattice of the B–Meson Factory

Following the principals described above, one can give a summary of the most important design criteria for a circular b–meson factory:

- The energy of the storage ring should range from $E = 4$ GeV to a maximum value of $E = 7$ GeV.
- The injection into the storage ring has to be possible at any working energy. This gives the highest injection efficiency and a high-integrated luminosity.
- In order to achieve a sufficiently large emittance for a given size of the vacuum pipe, the beta function around the ring should be of the order of $\beta_{\max} < 30$ m. Larger beta values are acceptable only in the interaction quads.
- A large variation of the emittance ϵ_{xo} is required to fit the beam parameters at different energies for the best luminosity.
- The beam optics should provide also a sufficient variation of the vertical beta function β_z^* in the IP.
- The dispersion has to be $D \equiv 0$ in the interaction region, in the rf-cavities and, if possible, in the injection region.
- The dynamic aperture should be almost as large as the mechanical aperture given by the beam pipes. Therefore, a very effective and properly designed sextupole arrangement is required. One also has to take the correction of higher harmonic magnetic fields into account.
- Finally, the storage ring has to provide additional free straight sections for wigglers, undulators, etc.

Using the design criteria described above a magnet lattice for the b–meson factory has been developed. The aim of the study was to find a lattice which allows the variation of different optics parameters of the machine almost without changing all other parameters and in particular without changing the hardware of the storage ring. The philosophy of the scheme which has been finally found is sketched in Fig. 3.

The optics structure in the arcs consists of eight standard FODO cells. The focusing in this region defines the emittance ϵ_x and the tune Q_x and Q_z. Here also the dispersion is different from zero whereas it vanishes in all other places. The matching of the dispersion on both ends of the FODO structure is done by use of the "missing magnet" insertion as described in Ref. 7. Because of the limited number of FODO cells only one cell can be used on each side to suppress the dispersion. Therefore, the two horizontal focusing quads in these cells are tuned independently.

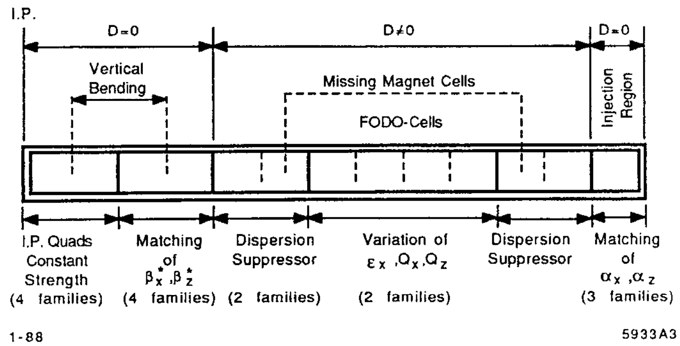

Fig. 3. Philosophy of the magnet lattice.

The injection is placed around the middle of the arc. For matching, three quadrupole families are available. Only two families would be sufficient, but it seems to be helpful to have one additional free parameter to find proper injection optics.

The interaction region contains four quadrupole families with constant magnet strength for all different optics. The variation of the beta functions β_x^* and β_z^* in the IP is done by the four adjacent quadrupoles between the interaction region and the FODO structure.

The basic problem is the layout of the vertical beam separation at the end of the interaction region. Generally one can use electrostatic plates as well as fast rf-magnets. Unfortunately both techniques provide only a rather weak bending. Therefore, 8 m long elements have been chosen. In Fig. 4 the solution with the electrostatic plates is drawn. With this device a homogeneous field of about 3×10^6 V/m should be possible bending a 7 GeV beam by the required angle of $\alpha = 3.6$ mrad. The vertically defocusing quadrupole Q4 adds another 1.9 mrad. At the entrance of the first vertical bending magnet VM1 the beam distance with respect to the horizontal interaction plane is 60 mm.

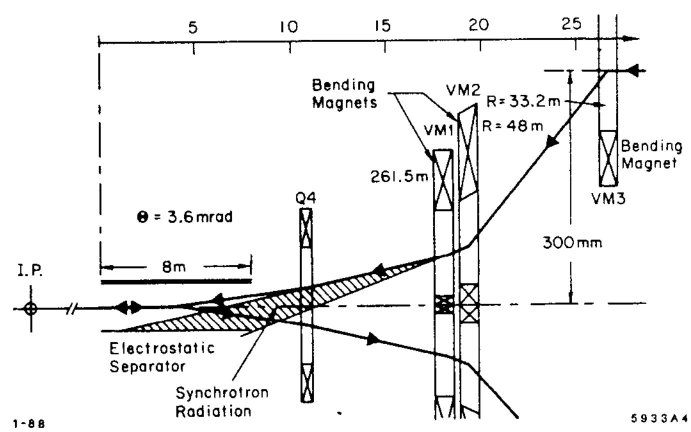

Fig. 4. The vertical beam separation of the b–meson factory.

The synchrotron radiation produced by the first vertical bending magnet VM1 hits the electrostatic plates which cannot be cooled efficiently. Therefore, this magnet is very weak (bending radius $R = 261.5$ m) and the resulting radiation power is of the order of 10 Watts/m along the plates. This amount seems to be tolerable. The main vertical bending is finally done by use of the magnets VM2 and VM3. The vertical spacing between the two rings is 0.6 m.

A careful design of the plates, taking the synchrotron radiation and the higher order mode losses into account, is necessary to get a reliable beam separation without beam loss over many hours or even days. This problem obviously needs further R&D. On the other hand, the multi-bunch scheme of CESR[8] has demonstrated the electrostatic separation can work reliably under realistic beam conditions.

The extremely high beam currents of the b–meson factory of the order of 500 mA, however, may cause serious problems with the electrostatic separation. Therefore, we also have to look at a solution with a fast rf-magnet. A preliminary study has shown that a strip line magnet of 8 m length seems to be the best solution. The principal of the magnet is sketched in Fig. 5. It is a shortened $\lambda/2$-resonator with capacitive loads on both ends. The electric field is zero in the center of the magnet where the magnet field has its maximum. Therefore, the bending is mainly caused by the magnetic field. The bending angle is given by the relation

$$z' = \frac{2\ e\ B_0}{k\ m_e\ c} \times \sin\ k \times 1 \qquad \text{with} \qquad k = \frac{2\pi}{\lambda} \quad . \tag{13}$$

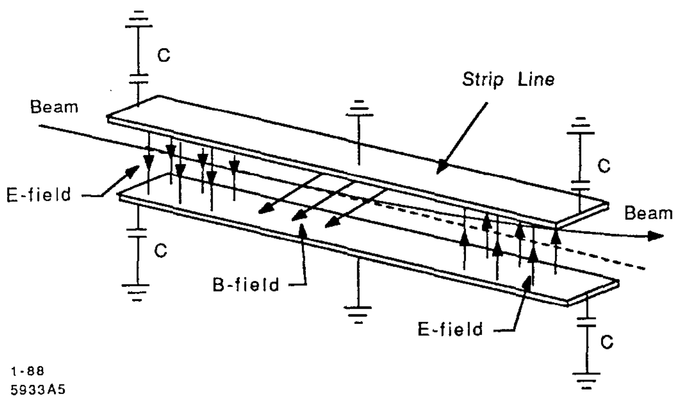

Fig. 5. Sketch of the rf-magnet using strip line technique.

This formula shows that the maximum angle is achieved for a magnet length of $1 = \lambda/4$. As a design example, a strip line with a conductor width of W = 100 mm and a distance of d = 50 mm between the parallel conductors has been chosen. The resulting impedance is $Z_0 = 125\ \Omega$. The driver amplifier has an output power of $P_{rf} = 2.6$ kW and operates at a frequency of 9.26 MHz. Assuming copper conductors, this power is sufficient to bend the beam by the required angle of $\Theta = 3.6$ mrad. The voltage across the magnet ends is $U_{max} = 21$ kV which is relatively moderate. Compared to the electrostatic separators the rf-magnet has the advantage of a low sensitivity against synchrotron radiation and a simple cooling. Both techniques should be studied experimentally and a final decision whether to construct the electrostatic plates or the rf-magnet should be made later after the laboratory tests.

The beta functions and the dispersion of one quadrant of the b-meson factory are plotted in Fig. 6. The standard optics with a vertical beta function of $\beta_z^* = 0.03$ m is shown. As required, the values do not exceed the maximum limit of β_{max} = 30 m around the ring. The following table lists the most important optical parameters of the present design of the b–meson factory. The first column shows the standard optics and the second one a more sophisticated "micro beta optics." Both optics have exactly the same magnet structure.

The chromaticity is compensated by two families of sextupoles (SF and SD) mounted close to the quadrupoles in the FODO cells. The integrated strength of the sextupoles is $m \cdot 1_{SF} = -0.483\ m^{-2}$ and $m \cdot 1_{SD} = 1.115\ m^{-2}$, respectively which is rather moderate. As proved with tracking simulations the dynamic aperture is almost not restricted by the sextupoles. Besides the energy acceptance of the lattice is significantly larger than $\pm 1\%$.

List of the most important optical parameters of the b–meson factory: (E = 5 GeV per beam)

		Standard Optics	"Micro–β"
circumference	1[m]	2×518.4	
number of bends		2×48	
bending radius	R[m]	24.828	
maximum energy	E[GeV]	7.00	
energy loss/turn	ΔE [MeV]	2.28	
horiz. beta function	β_x^* [m]	1.00	1.00
vert. beta function	β_z^* [m]	0.03	0.015
tune	Q_x	8.184	8.248
	Q_z	9.254	9.441
chromaticity	ξ_x	−13.21	−13.42
	ξ_z	−19.53	−30.56
mom. comp. factor	α	2.15×10^{-2}	
emittance	ϵ [m rad]	$2 \times 10^{-7} \ldots 10 \times 10^{-7}$	
energy spread	$\Delta E/E$	8.42×10^{-4}	

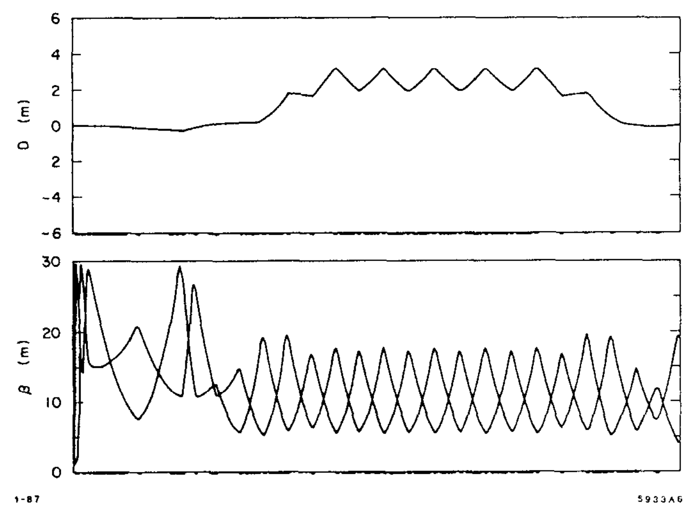

Fig. 6. Standard optics of the b–meson factory.

3. The rf–System and Instabilities

The accelerating frequency is set to f_{rf} = 500 MHz. Per ring a total number of ten five-cell cavities of the PETRA type[9] are necessary to get sufficient luminosity up to a center of mass energy of 13 GeV. A straight section without dispersion for two such cavities is available in each quadrant in the optical matching region. At an energy of E = 5.3 GeV the energy loss per turn due to synchrotron radiation is ΔE = 2.88 MeV. Assuming a current of I = 485 mA per beam, a rf power of P_{rf} = 1600 kW per ring is required.

The beam has a maximum number of 12 bunches with a bunch current of 40 mA. This high current obviously will cause transverse and longitudinal instabilities as found in different storage rings.[10] Therefore, one has to apply all cures either to avoid instabilities or to add artificial dampening by use of proper feedback systems. From this point of view, an extremely

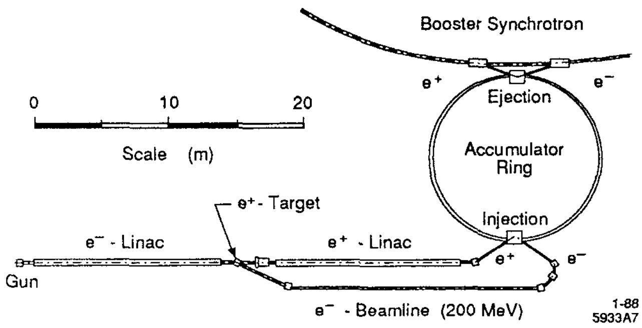

Fig. 7. The linac and the accumulator ring for electrons and positrons.

smooth vacuum chamber without sudden changes of the cross section has to be designed as proposed for the ESRF.[11] This design will provide the required low chamber impedance. The cavities are another problem. The PETRA types, as used for the first studies of the b–meson factory, have a high shunt impedance and, consequently, a high accelerating voltage for a given rf-power. The high shunt impedance, however, is because of the strong beam loading not the most important requirement for the b–factory. The problem of the instabilities is the real crucial point. Therefore, we have to look for cavities with very effective mode dampening. A reduced shunt impedance is tolerable under these conditions. At present, a cavity sized as the superconductive types with the mode couplers, but made by normal conductive material such as copper, seems to be the best solution.[12] Such a design would combine the advantage of high mode dampening with the high reliability of conventional techniques.

In addition, an active feedback system has to be used in order to get rid of the coherent unstable bunch oscillations. This system has to act on the different bunches independently. Different systems have been successfully applied at many storage rings. For the b–meson factory we have foreseen a concept proposed by R. D. Kohaupt.[13] This concept has been tested at PETRA recently and has demonstrated a high effectivity.

4. The Injection System

Since, finally, only the integrated luminosity over a longer time counts for the experiments, a very fast and effective injection is required. Therefore, the energy of the storage ring has to be kept constant at the operating energy. The b–meson factory is consequently equipped with a booster synchrotron providing electron beams up to the maximum energy of 7 GeV. This booster synchrotron is a standard design based on a FODO structure as used for DESY II.[14]

In order to get high single bunch currents, an accumulator ring is arranged between the 200 MeV linacs and the booster synchrotron as shown in Fig. 7. The design of the accumulator ring is based on the concept of PIA at DESY.[15] For the b–meson factory both the positrons and the electrons are accumulated in the ring simultaneously. The entire view of the b–meson factory with preaccelerators and buildings is sketched in Fig. 8.

5. Luminosity of the B–Meson Factory

As shown in Eq. (6), the luminosity of an electron-positron storage ring depends on different machine parameters as emittance ϵ_{xo}, tune shift ΔQ, beta function β_z^* and the bunch number n. Generally it is very difficult to tune these parameters

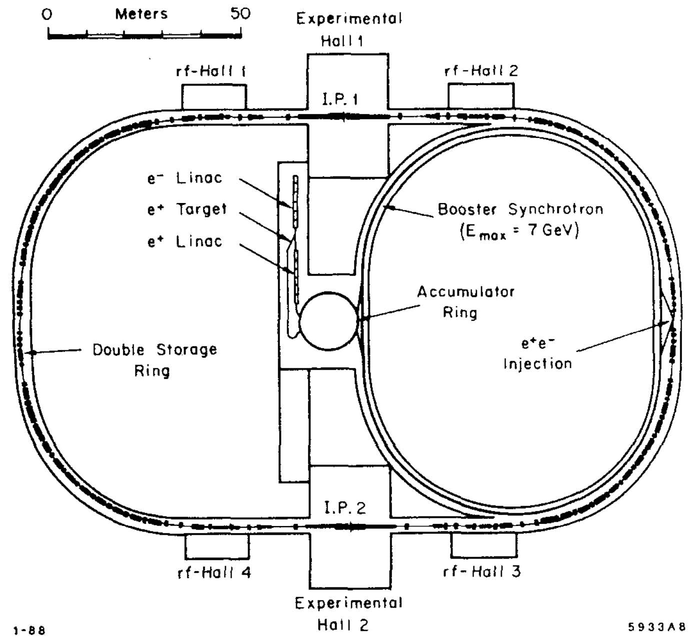

Fig. 8. View of the b–meson factory.

to the best values from the luminosity point of view simultaneously. Usually the resulting beam current is extremely high and will cause strong vacuum problems due to synchrotron radiation and higher order mode losses as well as instabilities. Due to this reason, the highest possible luminosity of a storage ring is available after a longer operation time of at least one year. This time is necessary to get familiar with the machine and to find the limitations of the beam current and the luminosity. Improvement programs cannot start before a careful commissioning of the machine and effective studies of the beam dynamics and the beam-beam effects. Because of this reason, the b–meson factory will start with moderate parameters first which will be available approximately one year after finishing the construction work.

The different luminosities corresponding to the different stages of improvement are plotted in Fig. 9. Most of the curves are based on calculations with a maximum rf-power of P_{rf} = 1.6 MW per ring. The maximum energy with sufficient luminosity is E_{max} = 13 GeV. With a rf-power of P_{rf} = 2.5 MW per ring the energy increased to $E_{max} \approx 14$ GeV. Using the standard optics ($\beta_x^* = 1.0$ m, $\beta_z^* = 0.03$ m), 8 bunches per beam and a moderate tune shift of $\Delta Q = 0.025$, one achieves the lowest luminosity curve in Fig. 9 with a maximum of L = 3.5×10^{32} cm^{-2} sec^{-1} at $E = 5.4$ GeV. This is roughly the value one can count on during the first year of experimental runs.

Improved magnet alignment and orbit control as well as a better understanding of the machine and the beam instabilities will raise the tune shift to $\Delta Q = 0.05$ and, consequently, the luminosity to values around $\boldsymbol{L = 1 \times 10^{33}}$ **cm^{-2} sec^{-1}** after two or more years of operation. This value is the design luminosity of the b–meson factory presented in this paper. Nevertheless, further improvements are possible using the microbeta optics with $\beta_z^* = 0.015$ m and 12 bunches per beam. The resulting luminosity is $L \approx 2 \ldots 3 \times 10^{33}$ cm^{-2} sec^{-1}. Because of Eq. (9), the bunch length has to be reduced to approximately $\sigma_s \approx 1$ cm which increases the higher order mode losses and the vacuum problems significantly. It is therefore not possible to guarantee these high values.

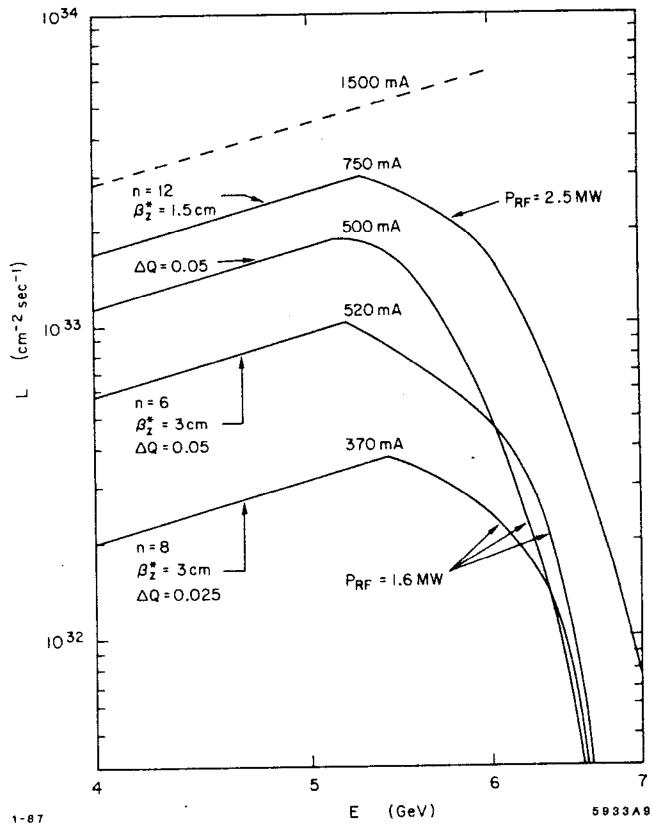

Fig. 9. The luminosity of the b–meson factory.

References

(1) K. Steffen, Internal Report, DESY M–79/23, May 1979; K. Wille, DORIS II/III, *A 5.8 GeV e^+e^- Storage Ring with High Luminosity*, DESY 81–047, August 1981.

(2) H. Wiedemann, *Chromatic Corrections in Large Storage Rings*, PEP–Note 220, 1976, SLAC.

(3) A. Piwinski, Proc. of the 1977 Part. Acc. Conf., Chicago, 1977.

(4) H. Mais and G. Ripken, *Theory of Coupled Synchro-Betatron Oscillations*, DESY, Internal Report M–82–05, 1982.

(5) A. Piwinski, DESY, private communication.

(6) M. Donald, SLAC, private communication.

(7) R. Brinkmann, *Insertions*, DESY HERA 87–01, 1987.

(8) N. B. Mistry, R. Talman, CBN 82–34, 1982.

(9) H. Gerke and M. Musfeldt, *The Radiofrequency System for the PETRA Storage Ring*, Internal Report, DESY M–79/33, 1979.

(10) See, J. L. Laclare, XIth Intern. Conf. on High Energy Accelerators, Geneva, 1980.

(11) L. Farvacque and A. Ropert, ESRF–MAC–05–05, Grenoble, 1987.

(12) Proch, DESY, private communication.

(13) R. D. Kohaupt, DESY Report 86–121, 1986.

(14) G. Hemmie et al., 1987 Particle Acc. Conf., Washington, D.C., 1987.

(15) A. Febel and G. Hemmie, Internal Report DESY M–79/13, 1979.

THE PEP OPTION*

E. D. Bloom

Stanford Linear Accelerator Center, Stanford University, Stanford, California 94305

1. Introduction and Motivation

How to learn about the "next" energy scale has been a major occupation of particle physicists over the past few years. The SSC is one such obvious attempt, though perhaps not the most imaginative one (and certainly not the most economical). A lesson from history may have relevance to this question. The weak interaction has been very helpful in determining the electroweak scale, as well as determining the phenomenology of the electroweak interactions. Figure 1 reproduces one of the arguments, circa the early 1960's, which led to the conclusion that 100 GeV was the "natural" scale of the weak interaction. Extensive and (frequently) precision experiments at the available mass scale (E^{∞}_{cm} ~ 0.5–30 GeV) over the next 20 years, using a variety of techniques, then led to a firm prediction of the W and Z masses, detailed knowledge of their decays, and the relatively economical machine designed to observe them at CERN in the 1980's. It is possible that history can repeat by using CP violation as a similar tool to explore the "next" mass scale.

The framework which we now consider CP violation is the KM matrix of the standard model with three quark-lepton generations. In this model, CP violation is the result of the one irreducible phase in the KM matrix; indeed, three generations and the KM matrix were developed in large part to provide an explanation of CP violation in the early 1970's. At the present time, there seem to be two possibilities: the mass scale of CP violation is electroweak, or the mass scale is much larger. If the relevant mass scale which correctly describes CP violation is on the order of the present electroweak scale, one expects large CP violations in the B–meson system explainable in the context of the KM matrix. The ability to observe CP violation, if the standard model is correct, is considerably enhanced if the recent ARGUS collaboration results on B^0_d mixing are confirmed. ARGUS has obtained,[1]

$$X_d = \Delta M/\Gamma(B^0_d) = 0.78 \pm 0.16,$$

as compared to theoretical predictions in the range $X_d < 0.2$.[2]

The mixing is calculated using the real part of the box diagram of Fig. 2,[3]

$$\Delta M/\Gamma = (32\pi/3)\, \mathrm{Re}\{V_{tb}V_{td}^{*}\}/|V_{cb}|^2\, (B_B f_B^2\, \eta_2 m_t^2/m_b^4)\,.$$

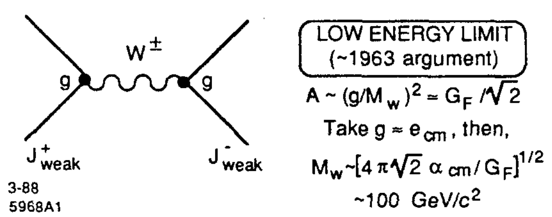

Fig. 1. Lowest order weak interaction theory extrapolated in the early 60's to estimate the mass scale of weak interactions.

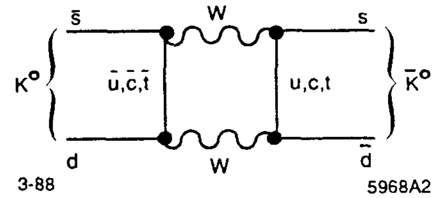

Fig. 2. Second order box diagram used in the calculation of CP violation in the standard model.

The theoretical unknowns are the KM matrix elements, V_{tb} and V_{td}, the B–meson structure constant ($B_B^{1/2} f_B$), the QCD correction η_2, and the mass of the top quark, m_t. The large ARGUS mixing result and the B–lifetime measurements[4] (~10^{-12} sec.) imply a larger than predicted V_{td}, and smaller than predicted V_{cb}, respectively, as well as m_t > 50 GeV[5] (just about the mass lower limit measured by UA-1).[6]

Experimental estimates of ϵ and ϵ', from measurements of CP violation in the K^0–system,[7] where,

$$\eta_{\pm} \equiv \mathrm{amp}(K_L \to \pi^+\pi^-)/\mathrm{amp}(K_s \to \pi^+\pi^-) = \epsilon + \epsilon' = 2.279(26) \times 10^{-3}\, e^{i\{44.6 \pm (1.2)\}}$$

and,

$$\eta_{00} \equiv \mathrm{amp}(K_L \to \pi^0\pi^0)/\mathrm{amp}(K_s \to \pi^0\pi^0) = \epsilon - 2\epsilon' = 2.29(4) \times 10^{-3}\, e^{i\{55^{\circ}(6)\}}\ ,$$

then imply a large KM phase, $\delta \approx 100^{\circ}$.[8] Figure 3 shows the approximate values of s_2, s_3, and δ (KM matrix representation) inferred from the experiments.[8]

The large mixing, measured for B_d, and predicted for B_s, then implies an incredibly large CP violation in B–decays, on the order of 10%–50%.[5] A striking manifestation of CP violation is predicted to be a large difference in time evolution between initially B^0– and $\underline{B}^0$–mesons as they decay into particular final states. The reactions,

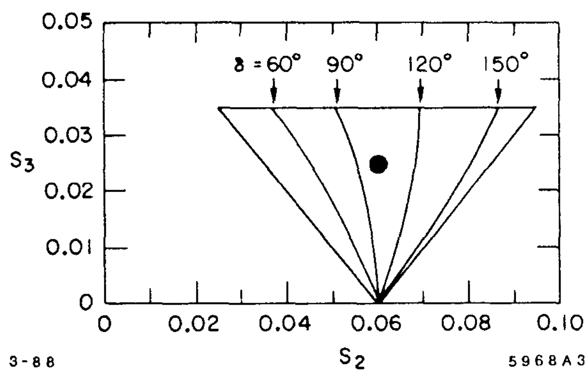

Fig. 3. The allowed range of KM parameters as determined using b–quark lifetime and leptonic branching ratio. The "best" value is somewhat loosely chosen at the dot.

* Work supported by the Department of Energy, contract DE-AC03-76F00515.

$$B^0_d \to \psi + K_s,\ B^0_d \to \psi + K^*,\ \text{and},\ B^0_s \to \psi + \phi\ ,$$

look particularly accessible and promising for realizing a CP violation at this time.

What if the standard model is wrong? Then, there is probably a new mass scale and CP violation is its prophet. An example of such a model is the "minimal" left-right symmetric model involving a very heavy right-handed W.[9] Figure 4 shows the box diagrams relevant to this model. Assume that box 1 $\equiv$ I, is relatively real, and that the entire CP violation in the K^0–system is due to box 2. Note that only two generations are included in the calculation, and thus we are effectively assuming that KM contributes nothing, or is irrelevant to CP violation ($\delta = 0$). In addition, we assume equal left- and right-handed Cabbibo angles. It can be shown,[9]

$$\text{box 2} \;=\; I \times [M(W_L)M(W_R)]^2 \times \underline{430} \times e^{i\varphi}\ ,$$

where $M(W_{L,R})$ are the left- and right-handed W masses, respectively, $\underline{430}$ is a numerical factor which depends on the detailed structure of the theory, and φ is a CP violating phase induced by right-handed W exchange.

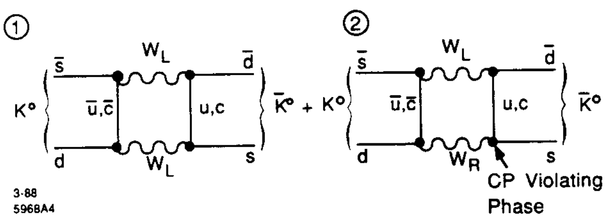

Fig. 4. Box diagrams contributing to $\Delta M(K^0)$ and ϵ in left-right symmetric model. #2 contributes CP violating phase. Note that only two generations are involved in the model.

Assuming the entire CP violating effect is due to the diagrams of Fig. 4, we obtain, by comparing to experiment,

$$\Delta M_{LRS}(K^0) = \mathcal{R}e\{\text{box2}\} = I \times [M(W_L)M(W_R)]^2 \times 430 \times \cos\vartheta \le \text{box1}$$

$$\epsilon_{LRS}(K^0) = \mathcal{I}m\{\text{box2}\} = [M(W_L)/M(W_R)]^2 \times 430 (2\sqrt{2}) \times \sin\vartheta = 2\times 10^{-3}.$$

These conditions imply that, 2 TeV $\le W_R \le$ 20 TeV.[9] In this case, CP violation in the B–system would be comparable to that in the K–system as the B–mass is still very small compared to $M(W_R)$. Very high precision CP violation experiments would then be needed in the B–system, as they are now needed in the K–system, to explore the source of the violation.

Both scenarios above promise many fruitful years of physics to come from a careful and systematic study of the B–system, if a sufficient number of B–decays are available. This last point, however, presents a severe challenge to the experimentalist.

2. Where to "B"

The question of which B–meson sources, coupled with which detection techniques, loom as the major challenges in the future of B–meson studies.[10] There are two general areas of possibilities, proton machines and e^+e^- colliders. I will briefly discuss both sets of possibilities and then reflect in more detail on e^+e^- colliders, which is my area of specialization. Details for the proton machine option are give in B. Cox's talk at this workshop.[11]

2a. Protons or Electrons

High energy proton machines, both fixed target and colliders, presently have some advantages as compared to e^+e^- colliders. First and most importantly, there exists the potential to produce very large numbers of B–mesons per unit running time. As Table 1 shows, up to 10^9 B's might be produced per day of running at the SSC, with lesser amounts from presently available machines. In addition, decay lengths for B's of a few mm may allow measurement of decay vertices with relative ease if radiation problems can be overcome. However, as outlined in Table 1, these potential advantages are presently all but neutralized by a number of disadvantages. Although $\sigma_{tot} \sim$ 50 mb, $\sigma(b\underline{b})/\sigma_{tot}$ is very small and thus the $b\underline{b}$ events are very difficult to extract with reasonable efficiency (even in Monte Carlo land). The trigger will be crucial here.[11] In addition, large multiplicities generated from the $b\underline{b}$ part of the event, coupled with many additional particles not associated with the $b\underline{b}$, exacerbate the problem of B–finding. Finally, the question of radiation damage from high doses near the target (or IP for colliders) presents a severe technological challenge.

Table 1. Comparison of hadronic experiments

	TeV II Few Years	TeV II Improved	TeV Coll Few Years	TeV Coll Improved	SSC
E_{cm}(GeV)	40	40	2,000	2,000	40,000
$\sigma(b\underline{b})/\sigma_{tot}$	10^{-6}	10^{-6}	10^{-4}	10^{-4}	10^{-3}
$\mathcal{L}_{day}(pb^{-1})^*$	3	30	.03	0.3	limited by rate
Interactions 200 days	10^{13}	10^{14}	10^{12}	10^{13}	10^{14}
$\#B\underline{B}$/200 days	10^7	10^8	3×10^7	10^9	10^{11}
$\gamma\beta c\tau$ (mm)	7	7	2	2	3
$<n_{ch}>_{detector}$	8	8	100	100	50
Solid angle	0.2π	0.2π	$\sim 4\pi$	$\sim 4\pi$	$\sim \pi$

* Approximate Lumi limit producing 10^7 interactions/sec max in some cases.

Presently, conceived advantages and disadvantages for e^+e^- colliders are essentially orthogonal to those for proton machines. Although detection of B's is not simple here, experience has shown that the $\sigma(b\underline{b})/\sigma_{tot} \sim$ 0.1–.25 makes the problem rather straightforward, and new detectors presently being built at Cornell, LEP, and SLAC will improve matters considerably. As shown in Table 2, a small beam pipe radius is projected for a number of machines allowing improved lifetime measurements and flavor tagging. However, <u>the</u> question at e^+e^- colliders is rate. Figure 5 and Table 2 illustrate the problem. Even at the peak of the Z^0, where $\sigma_{bb} \sim$ 6 nb, rate is severely limiting. The problem is luminosity, or the lack thereof, for presently available or building e^+e^- colliders. It seems clear that if CP violation is to be explored by e^+e^- collider experiments, factors of 100–1000 in luminosity are needed over presently operating machines, depending on E_{cm} and machine design, i.e., symmetric or asymmetric beam energies. Table 2 shows projected operating luminosities for a number of machines. Some of these machines are well along, while others are just at the conceptual stage. Through state-of-the-art and beyond, none of the machines in the table have the integrated luminosity to do anything but scratch the region of interesting limits on CP violation in the B–system.

2b. Energy and Kinematics

Not only is the question of $\mathcal{L}$ vs σ_{tot}, i.e., production rate, a crucial issue for e^+e^- colliders, E_{cm} and movement of the center-of-

Table 2. e^+e^- collider parameters

	CESR (1990's)	SIN* (1995?)	SBF* (1995?)	SLC (1990's)	LEP (1990's)	Lin Coll (2000?)
E_{cm}(GeV)	10(4S)	10(4S)	10–26	93(Z^0)	93(Z^0)	10–20
$\sigma(b\underline{b})/\sigma_{tot}$	0.25	0.25	0.25–0.1	0.15	0.15	0.25–0.1
σ_{tot}(nb)	3.9	3.9	3.9–0.5	40	40	3.9–0.7
$\mathcal{L}_{day}$(pb^{-1})	10	30	180(E_{max})	0.2^+	0.6	$45–450^+$
#$B\underline{B}$/200 days	2×10^6	6×10^6	$\geq1.6\times10^6$	2×10^5	6×10^5	10^7
$\gamma\beta c\tau(mm)_{Lund}$	0.01	0.01	0.01–0.5	2.4	2.4	0.01–0.4
$R_{beampipe}$(cm)	2-6	2-6	2–4	1-3	6-8	1-3
$<n_{ch}>_{detector}$	6	6	6–10	20	20	6–10

* New proposal for e^+e^- storage ring collider optimized for Υ(4S).

\# Conceptual design for a major upgrade to PEP, the Stanford Beauty Factory (see Sections 3–4 of this report).

\+ For linear colliders $<L> = L_{peak}/2$, for storage rings $<L> = L_{peak}/3$.

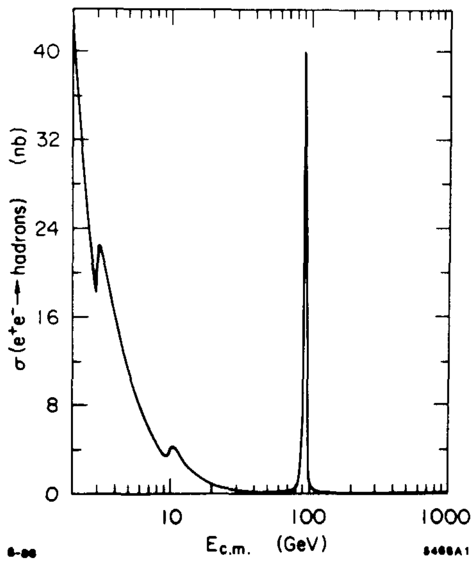

Fig. 5. Approximate σ_{tot} vs E_{cm} for e^+e^- collisions.

mass are also important. The latter points relate to the measurement of CP violation though the spectacular signature of unequal partial widths, i.e., decay length vs time for certain combinations of final states for B^0 vs $\underline{B}^0$. For example, this phenomenon is predicted to occur for a CP self-conjugate decay mode, f, common to B^0 and $\underline{B}^0$,[12] and yields disparate time dependent partial widths for B^0 and [$\underline{B}^0$] given by,

$$\Gamma(B^0[\underline{B}^0](t)\text{->}f[\underline{f}]) \propto e^{-\Gamma t}\{(1 + \cos \Delta mt) \times |\rho_f|^2[1]+$$

$$(1\text{-}\cos \Delta mt) \times 1[|\rho_f|^2]\text{-}[+](2 \sin \Delta mt) \times \mathrm{Im}((p/q)\rho_f)\},$$

where, $\rho_f = A(B^0 \text{->} f)/A(\underline{B}^0 \text{->} f)$, $p/q = (1+\epsilon)/(1-\epsilon)$, and the authors of Ref. 12 have set $\Delta\Gamma = 0$, and $|p|^2 = |q|^2$ for simplicity, and with the expectation that these approximations are accurate. An example of such a decay is $B^0 \text{->} \psi K^0_s$, though the size of the CP violation in each particular case is a matter of some conjecture.[5]

Figure 6 shows examples of events from the decay,[13]

$$B^0 \text{->} D^0\pi^+\pi^- \text{->} K^+\pi^-\pi^+\pi^-,$$

and its charge conjugate as seen at different E_{cm} and for the case of, E_{beam} = 12.2 GeV on E_{beam} = 2.0 GeV with E_{cm} = 10 GeV, i.e., asymmetric Υ(4S) production. As the figure qualitatively demonstrates, either symmetric production well into the continuum or asymmetric production at the Υ(4S) (or other resonances with low Q, e.g., the Υ(5S) for $B^0_s\underline{B}^0_s$ production) is needed to enable observation of the spectacular CP violating effects associated with decay length interference.

In addition to enabling the start of the search for CP violation in the B–system, some of the machines whose properties are outlined in Table 2 have impressive yields of other heavy flavors. The latter is shown in Table 3, where large yields of τ's and charm are shown for the Υ(4S) and continuum machines. As the branching ratio to $\tau\underline{\tau}$ from the Z^0 is only a few percent, machines presently planned for the Z^0 are not competitive for τ physics.

The efficiency of identification of $B\underline{B}$ pairs and the correct assignment of decay products to the B and $\underline{B}$ are of paramount importance in CP violation experiments. Much of the present deficit in rate at e^+e^- colliders might be made up by clever detection and tagging strategies. The problems at a stationary Υ(4S) are formidable in this respect; however, it is not so clear at this time whether asymmetric production at lower masses or symmetric production in the continuum optimize efficiencies at signifi-

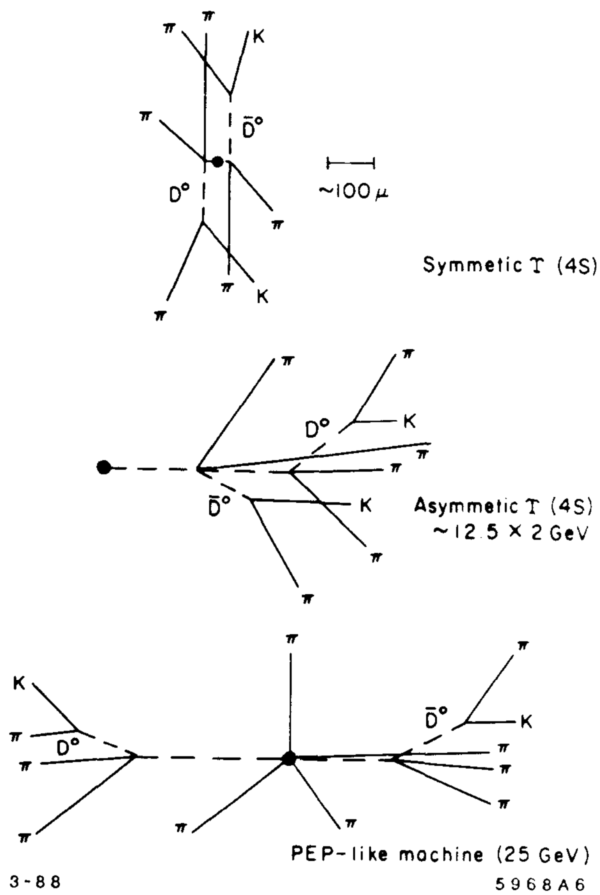

Fig. 6. Simulations of a prototypical $B\underline{B}$–decay as seen in different machines, both symmetric and asymmetric.

Table 3. Heavy flavor yields from e^+e^- colliders

	CESR (1990's)	SIN (1995?)	SBF (1995?)	SLC (1990's)	LEP (1990's)	Lin Coll (2000 ?)
# $B\underline{B}$/200 days	2×10^6	6×10^6	1.6×10^6	2×10^5	6×10^5	10^7
# $C\underline{C}$/200 days	2×10^6	6×10^6	6×10^6	1.6×10^6	5×10^6	4×10^7
# $\tau\underline{\tau}$/200 days	1.7×10^6	5×10^6	4.5×10^6	4.8×10^4	1.5×10^5	3×10^7
Note: $f_s = 0.02$ @ Z^0, $f_s = 0.21$ in the continuum.						

cantly different levels. Considerably more work with data and Monte Carlo has to be done for a rational decision to be made. Some work[14] has been done comparing stationary $\Upsilon(4S)$ production to that in the continuum, and a summary is shown in Figs. 7–10.

Some of the figures were generated from Ref. 14 which used an early version of the Lund Monte Carlo[15] for E_{cm} between the $\Upsilon(4S)$ and 60 GeV; a smooth extrapolation to the Z^0 at E_{cm} of 92 GeV was then made (shown as dashed lines in two of the figures). As the work of Ref. 14 used the Lund symmetric B-fragmentation function, the results, sensitive to fragmention function, were redone for the entire energy range with a more accurate model[16]. Figure 7 defines the general topology of the $B\underline{B}$-events with most of the B jet and $\underline{B}$ jet on opposite sides of the IP and a few extra π's produced at the event vertex. Figure 8a shows n_{ch}, the charged multiplicity in the $\underline{B}$ jet summed with the prompt charged particles vs E_{cm}. Figure 8b shows n_c/B, the number of charged particles per B with momentum > 1 GeV/c, vs E_{cm}. Figure 9 shows $<\beta\gamma>$ for the B's and the average impact parameter, $<\delta>$, for decay particles with $|\mathbf{p}|$ > 1 GeV/c, vs E_{cm}. Although $<\beta\gamma>$ grows linearly with E_{cm}, $<\delta>$ increases much more slowly for E_{cm} > 20 GeV. Note that a "typical" e^+e^- storage ring beam size is about $20\times350\,\mu$ (vertical × horizontal) with "mini-β," while the SLC beam size will be $\sim 2\times2\,\mu$.

Figures 10a–c continue with a more quantitative description of the general topology of the $B\underline{B}$-events. Figure 10a shows the distribution in rapidity with respect to the sphericity axis for $B\underline{B}$-events with E_{cm} = 29 GeV. The solid line is the distribution for all charged particles, the dashed line for the charged particles from a B-decay in each event. Figure 10b shows $<n_{na}>$, the mean number of charged particles not associated with the B-decay, but within the B-decay rapidity region. Figure 10c shows the fraction of tracks with momentum > 1 GeV/c emitted into the hemisphere of the opposite $\underline{B}$. Clearly, as E_{cm} increases to about 25 GeV a rapid improvement

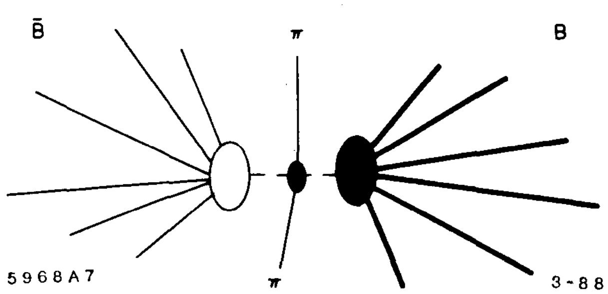

Fig. 7. Representation of a $B\underline{B}$-event at $E_{cm} \sim 25$ GeV. The π's at the e^+e^- vertex come from the central rapidity region and can be removed by a simple rapidity cut. The vertices associated with the B- and $\underline{B}$-decays are then revealed.

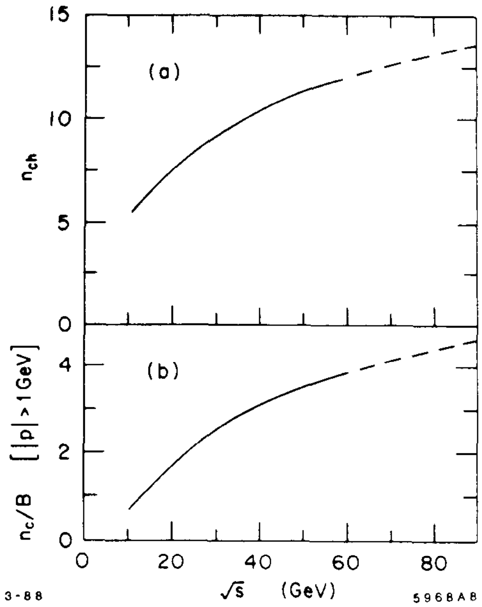

Fig. 8. a) n_{ch}, the charged multiplicity in the $\underline{B}$ jet summed with the prompt charged π's vs E_{cm}. The solid line is from the Lund M.C.,[16] the data point is from the TPC/2γ collaboration.[17] b) n_c/B, the number of charged particles with $|\mathbf{p}|$ > 1 GeV/c, vs E_{cm}. The solid line is from the Lund M.C.[16]

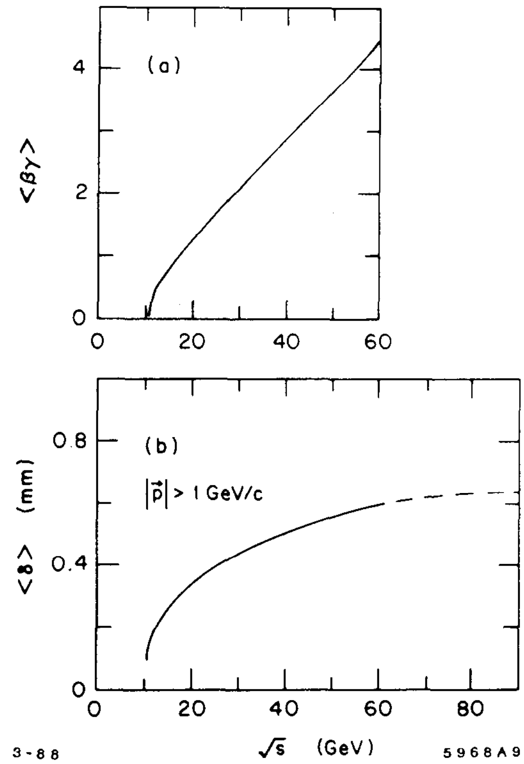

Fig. 9. a) $<\beta\gamma>$ for the B's, vs E_{cm}. b) $<\delta>$, the average impact parameter for particles decaying from B's with momentum greater than 1 GeV/c, vs E_{cm}. The solid lines are from Ref. 14, dashed line is an extrapolation.

in the isolation of the B and $\underline{B}$ jets occurs with only a mild increase of multiplicity. In addition, $<\delta>$ increases dramatically over this range. However, as one proceeds to higher E_{cm}, isolation and $<\delta>$ improvement saturate while multiplicity continues to increase. It thus seems that for symmetric colliders, E_{cm} in the range 20–30 GeV yield the best topological features for a broad range of B physics which involves B– and $\underline{B}$–separation and lifetime determination, features important to CP violation measurements. As mentioned previously, asymmetric and symmetric collider configurations are still in need of a detailed comparison.

The ability to verticize a B$\underline{B}$–event is a crucial aspect of CP violation measurements. Much work has yet to be done before such capability is available, with the development of two-dimensional and low mass vertex tracking within 1–2 cm of the IP essentially a prerequisite. Vertex tracker (VT) resolutions of $\sim 20\ \mu$ in both dimensions will be required, as well as material thickness of less than $\sim$ 0.5% of a radiation length for the VT

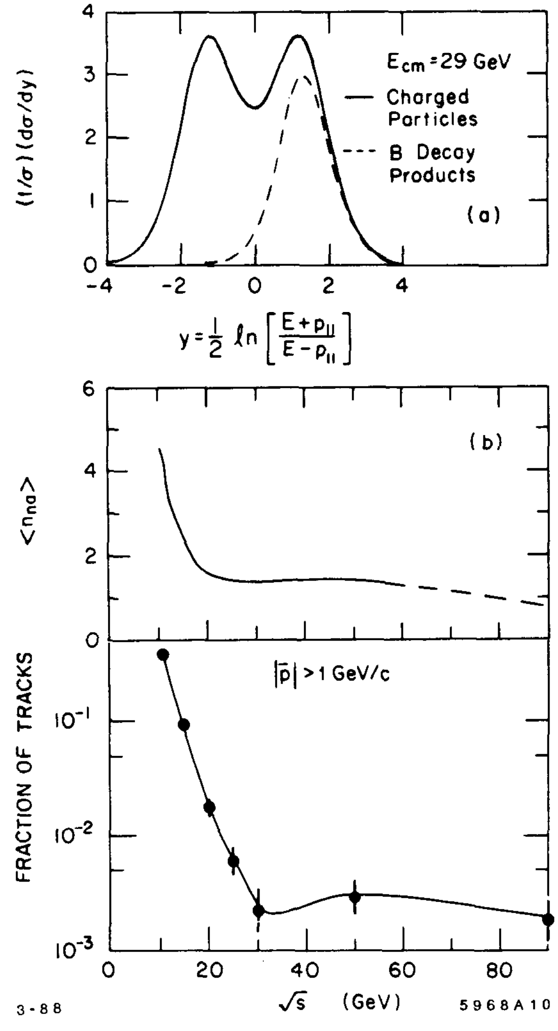

Fig. 10. a) Distribution in rapidity, y, with respect to the sphericity axis for B$\underline{B}$–events with E_{cm} = 29 GeV. The solid line is the distribution for all charged particles, the dashed line for the charged particles from a B–decay in each event.[14] b) $<n_{na}>$, the mean number of charged particles not associated with the B–decay, but in the B–decay y region.[14] The dashed part of the curve is extrapolated. c) "Fraction of Tracks" with $|p| > 1$ GeV/c emitted into the hemisphere of the opposite $\underline{B}$.[16] The errors on the points indicate the statistical uncertainty of the Monte Carlo.

and beam pipe combination. Note that for the case of a 500 MeV/c particle 0.5% rl, $\theta_z \sim 90^{\circ}$ at 1 cm from the IP, the position error from multiple scattering is $\Delta x \sim 20\ \mu$ at the IP. Higher momentum for the particles determining the vertex will be helpful, and so strategies which tag on high energy leptons, as that in Ref. 17, may be important.

Figure 11 shows such a B$\underline{B}$–event where one B–decays to $\psi(\ell^+\ell^-)$ + $K^*(K\pi)$, and the other B is tagged by a lepton with $E_l >$ 1 GeV (perhaps with a K depending on efficiency). As the B–meson inclusive decay to ψ is large, at about 1.25%, the decay of a B to lepton pairs from a ψ is about 0.2%. Given the results of Ref. 18, and considering a Stanford Beauty Factory (SBF) at design luminosity (see Table 1), and a new detector optimized to this type of physics (including VT), one estimates that in a year of data taking (200 days): about 6000 $\psi \to \ell^+\ell^-$ are produced, half of which are detected; about 350 $B^0_d \to \psi(\ell^+\ell^-)\,K\pi$ are fully reconstructed (including vertex); taking $B^0_s/B^0_d \sim 0.5$, about 150 $B^0_s \to \psi(\ell^+\ell^-)\ \phi(KK)$ are fully reconstructed; and finally, assuming a 0.1% branching ratio, one expects 200 fully reconstructed $B^0_d \to \psi(\ell^+\ell^-)$ K_s–decays. If the opposite B($\underline{B}$) semi-inclusive tag (including vertex) has a 50% efficiency, a CP violation measurement may be possible using the time dependence of decay for B vs $\underline{B}$. Given present day speculations on the size of the CP violation in these channels ($\sim$10%–50%),[5] about a five-year run could be sufficient to see an effect. Note that the detector alluded to above is well beyond what is now available.

3. Machine Design Considerations

The results of the previous section indicate that a good machine design for the observation of CP violation in B–meson decay is a very high luminosity e^+e^- symmetric storage ring operating at $E_{cm} \sim$ 20–25 GeV. As SLAC has a machine of the appropriate radius, it is worthwhile to consider some improvements to the present HiLum PEP machine which might possibly achieve the desired level of performance. The two ideas I will discuss involve multiple bunch machines, much like the SIN proposal in spirit.[19] Indeed, the general design criteria used are very similar to those used by K. Wille in his talk at this workshop, and those used for the SIN proposal; this is not an accident.[19]

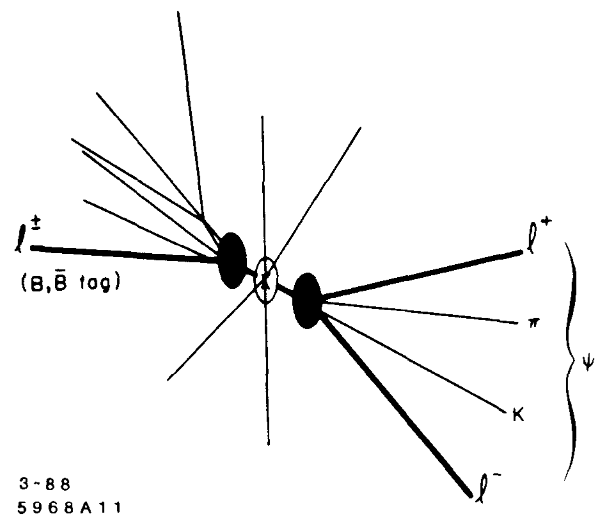

Fig. 11. B$\underline{B}$–event with one B–vertex tagged by ψ decay to $\ell^+\ell^-$ and the other B identified as B or $\underline{B}$ via a lepton tag. A CP violation measurement is possible using time dependence of difference of decay vertices for B vs $\underline{B}$.

There are a few basic criteria. The storage ring should have many bunches; the beam should fill the available physical aperture at all operating energies; there should be only one IR, or two at the most, where the beams collide; there should be a small β^*_y at the IR. These considerations result from the following formula,

$$\mathcal{L} \propto (nf_u) \times \epsilon_{x0} \times (\Delta\nu)^2/\beta^*_y ,$$

where, nf_u is the number of bunches, n, times the revolution frequency, f_u, (nf_u is independent of machine size for the same interbunch spacing), ϵ_{x0} is the natural horizontal emittance of the beam, and $\Delta\nu$ is the linear tune shift.

Assuming that the single bunch characteristics transfer to the multi-bunch case (no easy feat), the reason for the first factor is evident. More bunches means more luminosity (maybe even linearly with the number of bunches). Multi-bunching has been made to work by the CESR group at Cornell.[20] The second factor, ϵ_{x0}, should be made as large as possible with cost being the limiting consideration. The larger ϵ_{x0}, the larger the vacuum pipe, magnet apertures, and other apertures have to be. Also, for machines where rf power is a limitation, larger ϵ_{x0} typically means more power. For machines which will operate at E_b appreciably less than E^{max}_b, wiggler magnets should be used to fill the available physical aperture at the lower E_b.[21] The question of maximum $\Delta\nu$, the third factor, is related to the number of IR's, and will be discussed below. Finally, the influence of β^*_y is clear.

The question of maximal $\Delta\nu$ is important for achieving high $\mathcal{L}$. Figure 12 shows accumulated machine data plotted,[22] $\Delta\nu/\gamma(\times 10^7)$ vs $1/(n\rho)$, where, $\gamma = E_b/m_e$, and ρ is the machine bending radius. The plot shows data from many machines, and from the old (6 IR) PEP with 1 and 3 bunches per beam. These data imply (fitted line) that $\Delta\nu$ increases, $\propto (n\rho)^{-1/2}$, as the amount of energy radiated between collisions increases, $\propto(n\rho)^{-1}$, all other variables equal (e.g., E_b). That is, as one increases the damping time between collisions, the attainable $\Delta\nu$ increases. There are those that believe there is also theoretical evidence for this scaling law as well.[23] Such a scaling law favors machines with fewer IR's, with one IR being optimum. The newly completed HiLum PEP has but one IR and will yield an important test of the scaling law with $\Delta\nu \sim 0.08$ expected at $E_b = 14.5$ GeV. This value is shown on the figure as, n = 3, 1 IR, HiLum PEP (projected). The scaling law also favors the use of wiggler magnets that do not only fill the aperture of the storage ring, but also excite maximum damping consistent with available rf power. The installation of such wigglers at PEP, motivated by their utility for the synchrotron radiation program, has been previously suggested.[24]

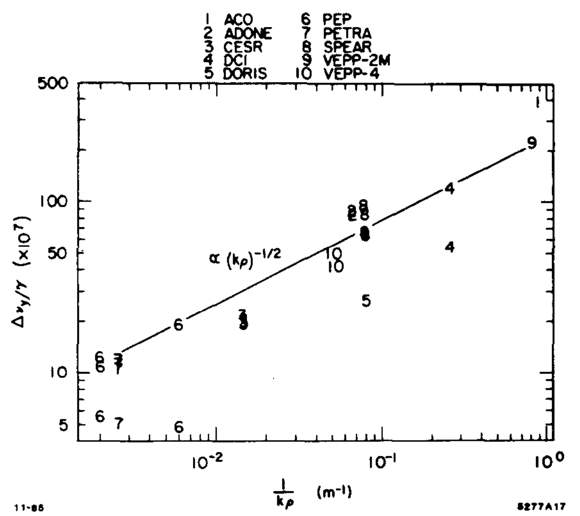

Fig. 12. Empirical scaling of the maximum vertical linear tune shifts with machine bend radius, ρ, and number of bunches per beam, n.[22] In particular, values are indicated for old PEP for n = 1 and n = 3, as well as the projected value for HiLum PEP (and SBF). The projection is made using the fit to the data shown in the figure as a solid line.

The design numbers that appear later in this report have been obtained from the following formulae which work reasonably well for existing machines,[19]

$$(I^{bunch})_{max} = 698.5 f_u E_b \epsilon_{x0} \Delta\nu ,$$

and,

$$\mathcal{L}_{peak} = 1.51 \times 10^{32}[nf_u E_b^2(1+\kappa^2)^2 \epsilon_{x0}(\Delta\nu)^2 \beta^*_y] ,$$

where, E_b is the beam energy, and κ is the horizontal-vertical beam coupling, $\kappa = (\epsilon_y/\epsilon_x)^{1/2} = (\beta^*_y/\beta^*_x)^{1/2}$. Note that in the above formulae $\Delta\nu_x = \Delta\nu_y = \Delta\nu$ is assumed. For many existing machines "optimal" coupling is $\kappa \sim 0.2$. We also assume that ϵ_{xo} "fills the aperture," i.e., ϵ_{xo} is constant, as a function of E_b; this was not assumed in Ref. 19. Filling the machine aperture at $E_b < E^{Max}_b$ can be done with wiggler magnets placed at proper locations in the machine lattice.[21]

Figure 13 shows a schematic layout of a two ring machine with one IR. Following the design of K. Wille,[10] a zero crossing angle is taken at the IP. In order to accomplish a zero crossing geometry a combination of electric or time varying magnetic, and static magnetic guide fields are needed. Static magnetic guide fields alone bend the e^- and e^+ beam in the same direction, as the e^- and e^+ are moving in opposite directions (this is why single ring storage rings work). Figure 14a shows the geometry needed and illustrates the principle of operation of an rf separator.[25] Figure 14b[19] shows a possible geometry using electrostatic separator plates. As is discussed by Wille,[25] both techniques need further development with a decision for one scheme or the other based on the results of experiments.

3b. Scaling from the SIN design to a Stanford Beauty Factory (SBF)

Figure 15 shows a plan view of the proposed SIN B–Meson factory.[17] The facility includes $e^{\pm}$ sources, an accumulator ring, a booster synchrotron allowing injection to a maximum of 7 GeV, a double ring storage ring which is 520 m in circumference, and two experimental halls enclosing 2 IR's. This machine will be a

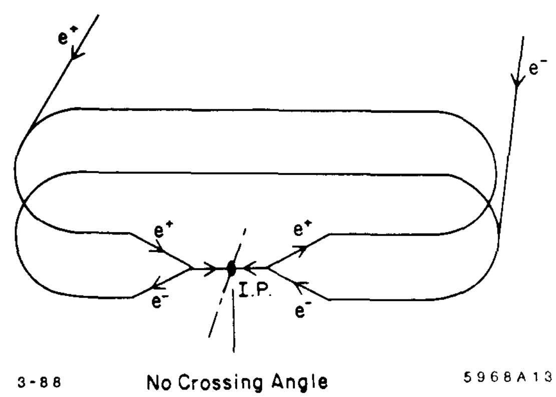

Fig. 13. A schematic layout of a two ring e^+e^- storage ring with one IR. This concept has a zero crossing angle at the one IR.

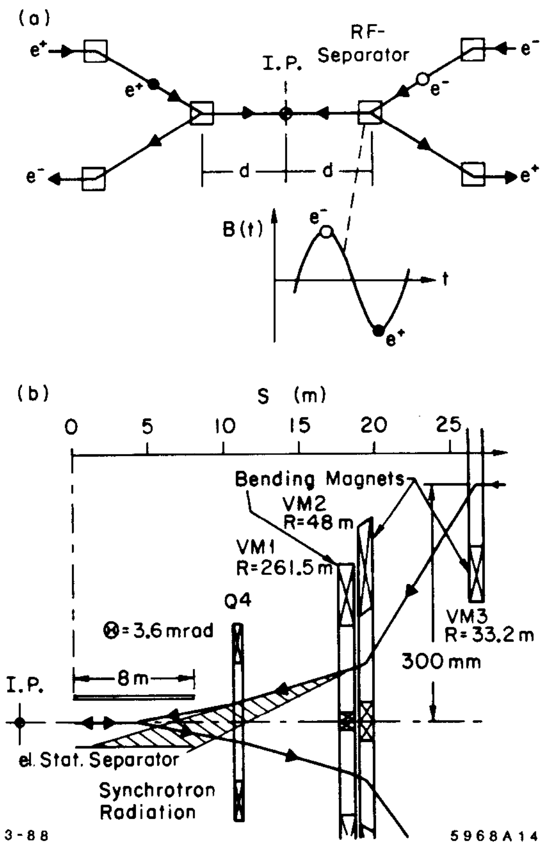

Fig. 14. a) Geometry needed for a zero angle crossing IR. Also shown is the principle of operation of an rf magnetic separator. b) A more detailed geometry from the SIN proposal for a zero angle crossing IR using electrostatic separator plates.

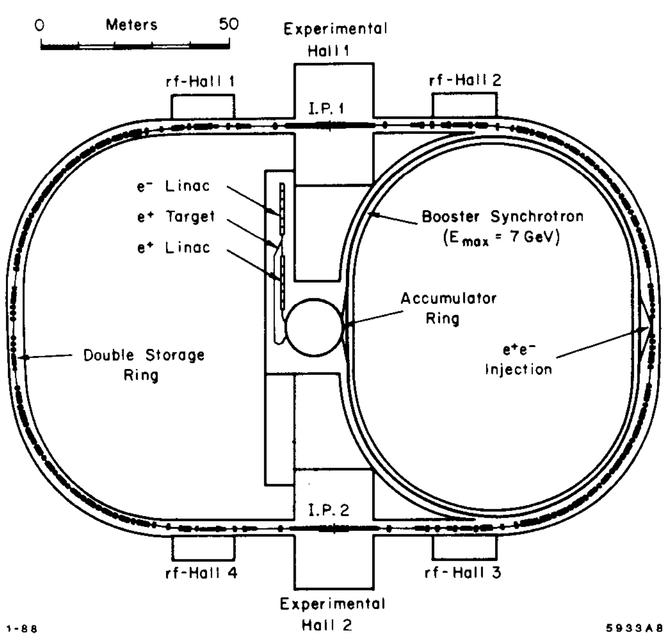

Fig. 15. The proposed SIN facility.[19] Included are an e^- linac, e^+ target and linac used to accelerate $e^{\pm}$ to an energy of about 200 MeV. The two beams are then accumulated and compressed in a damping ring or accumulator ring. A booster synchrotron is then needed to inject at energy to the main storage rings. Finally, a double ring storage ring with two IR's completes the facility. At least one totally new detector is also being proposed.

symmetric collider intended for optimum operation at the $\Upsilon(4S)$. It will be a multiple bunch machine, ultimately operating with 12 bunches per beam (interbunch spacing of 43 m), with currents up to 0.75 A per beam.

In order to scale this design to $E_{cm} \sim 25$ GeV, we will consider the major points mentioned in Section 3a.

First, the number of bunches. A minimum bunch spacing of 20–40 m is dictated by the rise time of the feedback systems needed to control the multi-bunch instabilities, and the geometry of the IR. The collisions should be head-on to avoid the problems that DORIS I had. The long straight sections of Hi-Lum PEP are particularly amenable to a double ring upgrade as

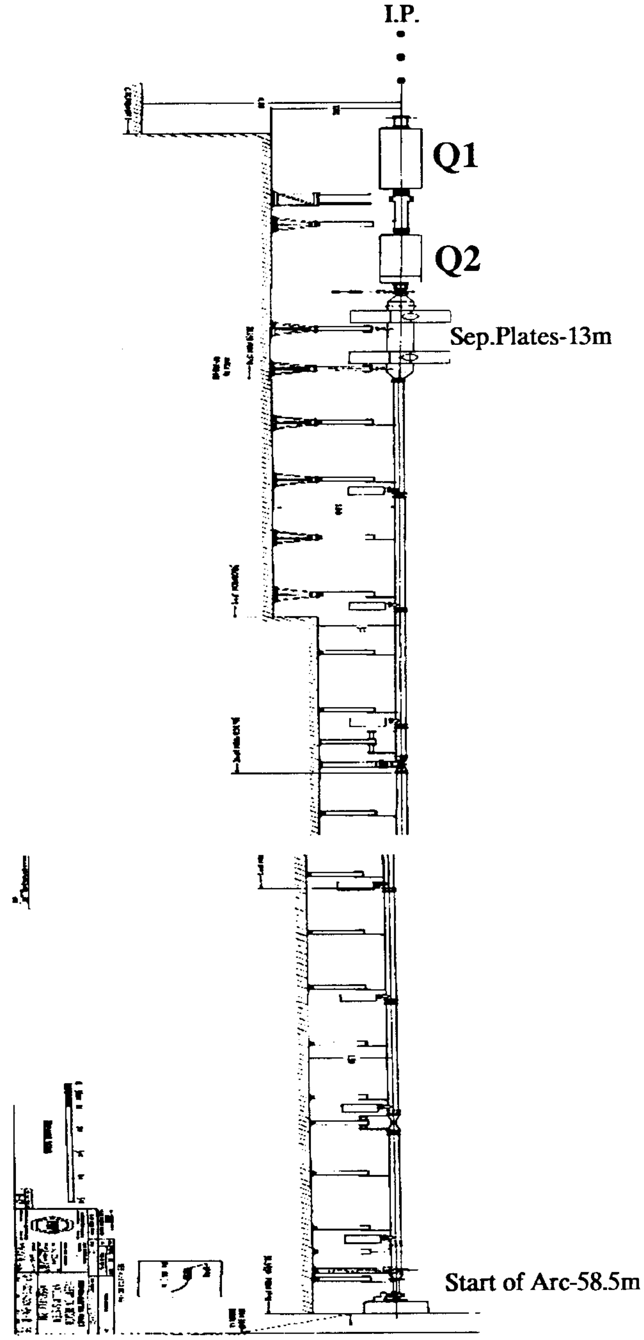

Fig. 16. A PEP straight section shown from Q1, the first quad after the IP, to the start of the bending arcs at 58.5 m from the IP. This section corresponds to all IR's except IR 2 which has an additional quad, Q2.5.

there is considerable room for matching the arcs to the IR's. With a separation of 31 m, 70 bunches can be put uniformly in a double ring machine. In addition, the very long straight sections of 117 m, see Fig. 16, allow an initial phase of multi-bunching to be done without a double ring (SBF_0). For separation in the straight sections only (there is not enough aperture in the arcs) the present PEP ring can be used. This scheme allows 15 bunches per beam placed in three groups of five bunches with each bunch in a group separated by 20 m from the next. The single ring multi-bunch PEP, SBF_0, has about five times fewer bunches and thus five times lower $\mathcal{L}$ than a double ring; however, this scheme is relatively inexpensive to build, and could yield a factor of five in $\mathcal{L}$ over the present HiLum PEP.

Second, the aperture. The SIN machine is planned to have quite a large emittance allowing $\epsilon_{x0} = 8.3 \times 10^{-7}$ m-rad.[19] This is accomplished by keeping $\beta \leq 30$ m in the ring, rather than by having a larger than normal physical aperture. For the SBF calculations we will use the present HiLum PEP emittance, $\epsilon_{x0} = 1.2 \times 10^{-7}$ m-rad. Note that ϵ_{x0} is defined by $\sigma_x \approx \surd(\epsilon_{x0}\beta_x)$, ($\eta = 0$). Wigglers are needed to bring beam size to the aperture limit at $E^b < 14.5$ GeV, and to assure the tune shift limit of the design. Figure 17 shows a schematic of a three pole wiggler with trim sections at either end which allow a match into the machine lattice.

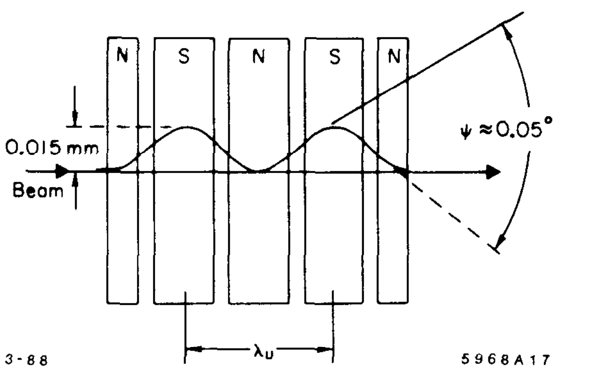

Fig. 17. Schematic of a three pole wiggler magnet with trim magnets on either end to allow matching into the storage ring lattice. Ψ is the maximum angle of bend of the beam as it wiggles through the magnets, and λ_μ is the wavelength of the "wiggle."

The use of wiggler magnets has been extensively discussed in Refs. 21 and 24. I will review the basic principles of operation below. The increase in emittance, $\epsilon^w_{x0}/\epsilon_{x0}$, is given by,

$$\epsilon^w_{x0}/\epsilon_{x0} \approx [1 + (<H_w>L_w/(<H_0>L_0)) \times (\rho_0/\rho_w)^3]/[1+(\rho_0/\rho_w)^2],$$

where, ρ_0 is the main bend radius of the storage ring, ρ_w is the wiggler magnet bend radius, L_0 is the length of the machine bends, and L_w is the effective length of the wiggler. The H's are more complicated, with H_0 being a complex function of the machine lattice.[26] H_w is reasonably approximated by,

$$<H_w> \sim <\eta^2/\beta>_w,$$

where the average is taken over the length of the wigglers. Note that for the old PEP, $<H_w>/<H_0> \sim 1$.

The stored beam's damping time is given by,

$$\tau_w/\tau_0 \sim [1+ (L_w/L_0)*(\rho_0/\rho_w)^2]^{-1},$$

where, τ_0 is the damping time of the beam without wigglers. In order to damp the beam more quickly rf power is needed. The energy loss per turn, U0, increases as wiggler strength is increased, and,

$$U0_w/U0 = \tau_0/\tau_w.$$

The above formulae show that by adjusting η and β at the wiggler location, one can tune the tradeoff between beam size and damping time over a wide range, however, at a cost of additional rf power.

Third, the maximum tune shift. As DORIS II has achieved $\Delta\nu_{max} \sim 0.025$, Wille[25] has been conservative in his design specs in specifying $\Delta\nu_{max} \sim 0.025$ as the initially achievable tune shift for the proposed SIN machine. This machine will be operating in the same energy regime, and has other features reminiscent of DORIS II. However, Wille projects that $\Delta\nu_{max} \sim 0.05$ will be possible eventually. PEP has achieved $\Delta\nu_{max} \sim 0.05$ in its old carnation and the scaling laws discussed in Section 3a imply that, using wigglers for E_b, 14.5 GeV, $\Delta\nu_{max} \sim 0.08$ will be possible for the SBF (and SBF_0).

Fourth, the β^*_y. Figure 18a shows the low beta insertion for the proposed SIN machine. This design is state-of-the art with two superconducting quads required (per side), and only 0.6 m between the face of the last superconducting quad and the IP. β^*_y is quite modest at 3 cm and cannot be made much smaller as dictated by the natural bunch length for storage rings with rf frequency in the 350–500M MHz range; β^*_y should be no smaller than $\sim 1.5 \times \sigma_z$. Figure 18b shows a possible IR arrangement for the SBF (and SBF^0). With the first major quads at 2.75 m, a 3 cm β^*_y is possible. In addition, a very smooth beam pipe, and minimal length of rf cavities are needed in all machines of this type due to the high currents and the possible effects of beam bunch lengthening.

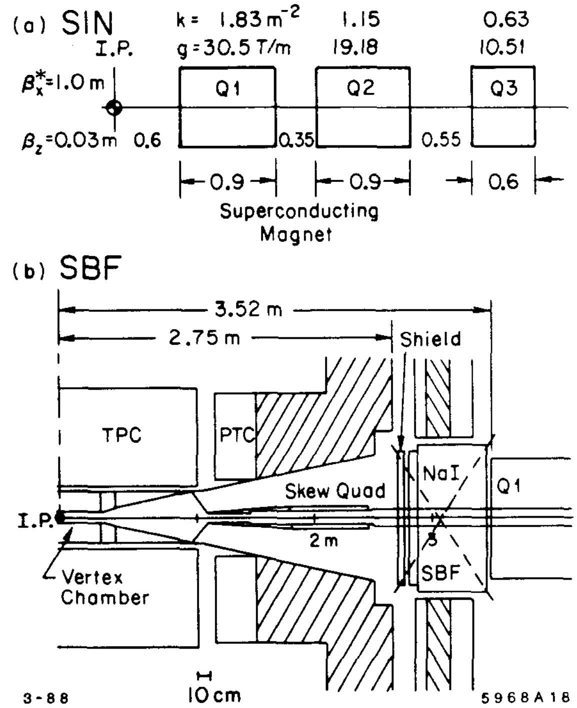

Fig. 18. a) Preliminary design of the SIN IR.[19] This design requires two (pairs) of superconducting quads with the face of the nearest quad at 0.6 m from the IP. b) Concept for the SBF IR. The first large quad is a standard PEP Q1 at a distance of 2.75 m from the IP. This should allow for $\beta^*_y \sim 3$ cm as is the case for SIN. The present TPC/2γ forward detector will have to be redesigned to accomodate the new Q1 location.

Finally, superior injection is required so as to allow rapid filling of the storage ring. The stored current goals for the SIN proposal are, $I_{max} \sim 0.75$ A per beam, while for the fullblown SBF concept $I_{max} \sim 0.85$ A per beam. In the case of the SBF, injection at 5×10^9 particles per pulse, at a 60 Hz injection rate, with 50% capture efficiency will take ~ 4 min per beam. As the proposed SIN ring has a circumference with is about four times smaller, it would required about 1 min per beam with the same rate. For topping off (both machines will fill at energy without the need for ramping (divide the times by ~2). The SBF_0 would need about five times less time than the SBF, or about the same as the SIN proposal. DORIS II has actually achieved impressive filling rates, with topping off typically requiring only one or two minutes. Figure 19 shows a typical day's record when the system is fully operational. However, the three new machines discussed here have injection requirements which are an order of magnitude or more greater than DORIS II. Powerful injectors are required or much longer times will be taken for fills.

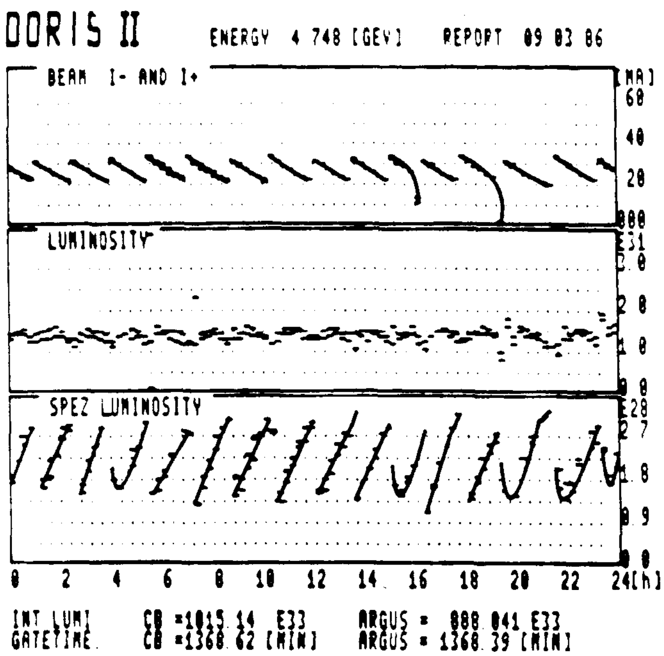

3-88 5968A19

Fig. 19. A typical day of injection at DORIS II when the injection system is fully operational. This quality of injection was not unusual after the initial bugs in the storage ring were found (took about 1.5 years of operational experience).

4. Luminosity Estimates

Figure 20 shows the design luminosity for the SIN proposal. Wille expects the luminosity to increase in stages as more is learned and improvements are made.[26] The bottom curve in the figure is expected within the first year of operation, with subsequently higher levels achieved as operating experience is gained. Finally, after some years of operation, $\mathcal{L}_{peak} \sim 3\times10^{33}$ cm^{-2} sec^{-1}, is projected at the Υ(4S).

The SBF can also be staged. Initially, the SBF_0 can be built, at modest cost, and operational experience with multi-bunch and high currents will be gained. If and when it appears possible and desirable to gain an additional factor of about five in luminosity the SBF is a candidate design. Table 4 gives some parameters of SBF_0 and SBF. At E_B = 12.5 GeV, $\mathcal{L}_{peak} \sim 10^{33}$ is projected for the SBF_0, and $\mathcal{L}_{peak} \sim 6\times10^{33}$ for the SBF. The large

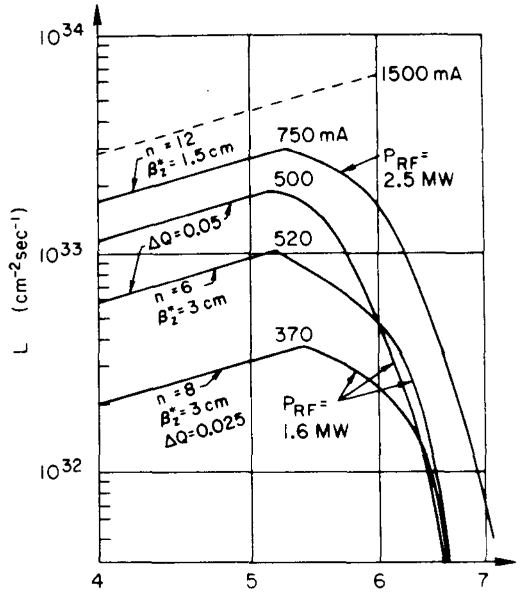

3-88 5968A20

Fig. 20. The design luminosity for the proposed SIN machine. Improvement of $\mathcal{L}$ is expected in stages as more is learned and machine improvements are made. The bottom curve is expected within the first year of operation, with subsequently higher levels achieved as operating experience is gained. Finally, with n = 12, $\Delta\nu$ = 0.05 ($\Delta Q \equiv \Delta\nu$), $\beta^*_y(\equiv\beta^*_z)$ = 1.5 cm, and I_{beam} = 0.75A, $\mathcal{L}_{peak} \sim 3 \times10^{33}$ cm^{-2}sec^{-1} is projected.

Table 4. Parameters for e^+e^- storage rings based on improvements to PEP. The present HiLum PEP is compared to the SBF^0 and SBF. The parameters discussed in the text are used to calculate projected performance.

	HiLum PEP	SBF_0	SBF
circumference (m)	2200	2200	2200
#rings	1	1	2
#IR'S	1	1	1
n	3	15	70
β^*_y	4	3	3
$\Delta\nu$	0.07 (@12.5)	0.08	0.08
Wigglers	no	yes	yes
L_{peak} ($\times$ 10^{32} cm^{-2} sec^{-1})			
@12.5 GeV/beam	1.4	13.2	61.6
@5.4 GeV Υ(4S)	NA	2.4	11.1
<L> (pb^{-1}/day)			
@12.5 GeV/beam	4.0	38.0	177.3
@5.4 GeV Υ(4S)	NA	6.8	31.9
P_{beam} (MW)			
@12.5 GeV	0.3	4.0	18.8
@5.4 GeV Υ(4S)	NA	0.7	3.4
I_{bunch} (ma)			
@12.5 GeV	8.3	11.9	11.9
@5.4 GeV Υ(4S)	NA	5.1	5.1
I_{beam} (ma)			
@ 12.5 GeV	24.9	178.9	834.9
@5.4 GeV Υ(4S)	NA	75.9	354.0
B$\underline{\text{B}}$ pairs/200 days($\times$ 10^6)			
@ 12.5 GeV	0.04	0.35	1.6
@5.4 GeV Υ(4S)	NA	1.4	6.4

rf power required for the SBF and perhaps the SBF^0 as well, may demand the use of LEP type klystrons and superconducting cavities. The klystrons are now "off the shelf" items obtained from Philips (Cat. #YK1350), are rated for 1 MW output power, and have a central frequency of 352.21 MHz, the PEP rf frequency, Figure 21 shows a schematic of the Philips tube. In addition, superconducting cavities at the same frequency should also be available from European industrial sources in a couple of years (as a small add-on to LEP's).

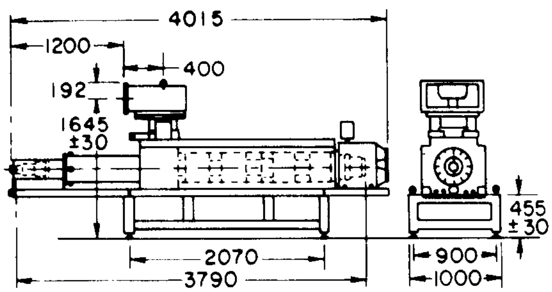

Fig. 21. Philips YK 1350 continuous-wave high-power klystron. Water cooled, high efficiency, fixed frequency (353.31 MHz), 1 MW klystron in metal-ceramic construction. Cost per klystron is ~ \$1m installed with power supply. Dimensions in the figure are in cm.

5. Conclusions

The chance to gain insight into a possibly new mass scale, plus many other physics opportunities that a sample of 10^7 B-decays brings, is a physics justification for a B-factory by itself. The machines discussed in Section 3 of this paper all can produce ~few times 10^6 B-decays in a reasonable running time; however, the SIN design (and CESR as well) which optimizes the machine for symmetric beams with E_{cm} at the $\Upsilon(4S)$ does not allow for measurements of B-lifetime, and so a crucial window on CP violation is lost. The SBF concept may be sufficient to achieve a measurement of CP violation in the B-system, but the development of such a machine and the measurements will probably require a staged effort over a decade. In addition, if an e^+e^- machine, a B-factory will yield more than 10^7 τ-lepton and C-meson decays while the B's are being produced. Thus many questions involving heavy flavor physics can be addressed at such a facility.

It is clear that much development work is needed in both the machine physics and detector design to achieve and CP violation measurement goals. It seems prudent to start in earnest soon, and to expect an extended effort.

6. Acknowledgements

Many of my colleagues have contributed to the content of this report. There are three major areas that I would like to separately achnowledge. First, my motivation to pursue this nascent field of CP violation in the B-system was sparked by extensive conversations with I. Bigi (SLAC), A. Fridman (CERN/SLAC/UCLA), F. Gilman (SLAC), H. Harari (Weizmann/SLAC), and P. Oddone (LBL). These colleagues have also suggested examples to clarify the physics goals, a number of which I have used in this report. Second, the section on "Where to B" was packed with the work of W. Hofmann (Berkeley) and G. Wormser (SLAC). Finally, the genesis of the SBF machine concepts have been strongly influenced through many discussions with M. Donald and D. Ritson of SLAC. In addition, important contributions to these ideas have been made by many members of the SLAC accelerator physics group, and H. Nesemann (DESY), D. Rubin (Cornell), R. Siemann (Cornell), R. Talman (Cornell), K. Wille (Dortmund), and H. Wiedemann (SSRL). Finally, I would like to thank G. Godfrey for a careful reading of the manuscript.

References

(1) H. Albrecht et al. (ARGUS), Phys. Lett. **192B**, 247 (1987).

(2) For example, see: I.I. Bigi and A. Soni, Phys. Rev. Lett. **53**, 1407(1984); I.I. Bigi and A.I. Sanda, Phys. Rev. **D29**, 1393 (1984).

(3) J.S. Hagelen, Phys. Rev. **D20**, 2893 (1979).

(4) For a recent review see the talks of: A. Montag, D. Muller, and R. Ong, Proceedings of the 2nd International Symposium on the Production and Decay of Heavy Flavors, Stanford University, Stanford, CA, Sept. 1-5, 1987, proceedings edited by E.D. Bloom and A. Fridman, (1988).

(5) I.I. Bigi and A.I. Sanda, SLAC-PUB-4299 (1987).

(6) I. Wingerter (UA-1), Proceedings of the 2nd International Symposium on the Production and Decay of Heavy Flavors, Stanford University, Stanford, CA, Sept. 1-5, 1987, proceedings edited by E.D. Bloom and A. Fridman, New York Academy of Science (1988).

(7) B. Winstein, Proceedings of the Fourteenth SLAC Summer Institute on Particle Physics, SLAC Report No. 312, 33(1987).

(8) H. Harari, Proceedings of the Twelfth SLAC Summer School on Particle Physics, SLAC Report No. 281, 264 (1985).

(9) R.N. Mohapatra and G. Senjanovic, Phys. Rev. Lett. **44**, 912 (1980); Phys. Rev. **D23**, 165 (181). See also, H. Harari, Proceedings of the Fourteenth SLAC Summer School on Particle Physics, SLAC Report No. 312, (1987).

(10) Much effort has gone into these questions at past conferences and workshops. Below is a partial list:
— Workshop on e^+e^- Physics at High Luminosities, SLAC Report No. 283, proceedings edited by H. Paar (1985);
— 1st International Symposium on the Production and Decay of Heavy Flavors, University of Heidelberg, Heidelberg, FRG, May 20–23, 1986, proceedings edited by K.R. Schubert and R. Waldi, DESY report (1986);
— Critical Issues in the Development of New Linear Colliders, University of Wisconson, Madison, WI, Aug. 27-29, 1986, AIP Proceedings **156**, 413–452 (1987).
— The Linear-Collider $B\underline{B}$-Factory Conceptual Design Workshop, University of California, Los Angeles, CA, Jan. 26-30, 1987, proceedings edited by Donald H. Stork, World Scientific (1988).
— 2nd International Symposium on the Production and Decay of Heavy Flavors, Stanford University, Stanford,

CA, Sept. 1-5, 1987, proceedings edited by E.D. Bloom and A. Fridman, New York Academy of Sciences (1988).

— B-Meson Factory Workshop, SLAC, Stanford University, September 7-8, 1987, proceedings edited by L. Friedsam, SLAC Report 324 (1988).

(11) B. Cox, Invited talk at this workshop.

(12) I.I. Bigi and A.I. Sanda, Nucl. Phys. **281**, 41 (1987); also, Ref. 5.

(13) Figure 6 is essentially from the talk of P. Oddone presented at The Linear-Collider B$\underline{B}$-Factory Conceptual Design Workshop, University of California, Los Angeles, CA, Jan. 26-30, 1987, proceedings edited by Donald H. Stork, World Scientific 423 (1988). Oddone discussed both symmeteric and asymmeteric colliders and their interaction with potential detectors.

(14) W. Hofmann et al., Workshop on e^+e^- Physics at High Luminosities, proceedings edited by H. Paar, SLAC Report No. 283, 35 (1985).

(15) T. Sjoestrand, Comm. Phys. Comm. **27**, 243 (1982); **28**, 229 (1983). This relatively early version of the Lund Monte Carlo was tuned by W. Hofmann to match the available data for heavy quark processes.

(16) W. Hofmann, private communication. This work used Lund V6.3 with the Peterson Fragmentation function and ϵ_b = 0.01. The accuracy of this model is discussed in, J. Chrin, Proceedings of the 2nd International Symposium on the Production and Decay of Heavy Flavors, Stanford University, Stanford, CA, Sept. 1-5, 1987, proceedings edited by E.D. Bloom and A. Fridman, New York Academy of Sciences (1988).

(17) H. Airara, et al. (TPC/2c), Phys. Lett. B **134**, 299(1987).

(18) G. Wormser, MarkII/SLC — Physics Working Group Note #9-15, (1987).

(19) E. Eichler, et al., Motivation and Design Study for a B-Meson Factory with High Luminosity, SIN-PR-86-13, (1986).

(20) K. Berkelman, talk at this workshop.

(21) J.M. Paterson et al., PEP Note 125, (1975).

(22) J.T. Seeman, SLAC-PUB-3825, (1985).

(23) R.H. Siemann and R. Talman, Private Communication.

(24) H. Wiedemann, Proceedings of the Workshop on PEP as a Synchrotron Radiation Source, SLAC, Stanford University, Oct. 20-21, 1987, SSRL Report, 18 (1987).

(25) K. Wille, Talk at this workshop, and Proceedings of the 2nd International Symposium on the Production and Decay of Heavy Flavors, Stanford University, Stanford, CA, Sept. 1-5, 1987, proceedings edited by E.D. Bloom and A. Fridman, New York Academy of Sciences (1988).

(26) M. Sands, SLAC-PUB-121 (1970). See Eq. 5.85.

B PHYSICS WITH pp COLLIDERS

A. FRIDMAN*

European Organization For Nuclear Research,
CERN, CH-1211 Geneva 23, Switzerland

Abstract

As the construction of *pp* colliders in the multi-TeV region (LHC, SSC or ELOISATRON) is under discussion, we briefly examine the possibility of investigating *B* physics in *pp* collisions. The rates and general features of $B\overline{B}$ production are discussed and the potentialities for tagging B's in very large multiplicity events are envisaged. Some physics points requiring large $B\overline{B}$ data samples (CP violation in the B–system and rare B–decays) as could be obtained with *pp* colliders are also presented. In the context of measuring CP violation effects, the implications of unequal B– and $\overline{B}$–production in *pp* collisions are addressed.

1. Introduction

In this report, we will briefly discuss the possibility of investigating B physics with *pp* colliders in the multi-TeV region. This possibility is of some interest as there are several *pp* collider projects under consideration: the Large Hadron Collider (LHC) (~15 TeV), the Superconducting Super Collider (SSC) (40 TeV) and the ELOISATRON (~100 TeV). These colliders would have the advantage of being an intense source of b–flavored hadrons (see below) but with the inconvenience that these hadrons are produced in final states with very large multiplicities. It will, thus, not be easy to extract a B–signal from such complicated final states. However, many fundamental features in B physics (CP violation effects, rare decays, etc.) can hardly be investigated with e^+e^- colliders because of the small cross sections involved. It is thus certainly worthwhile to explore closely the possibilities of using *pp* machines to study B physics.

We will first present some general features of $B\overline{B}$– production in *pp* collisions. In particular, the rates as predicted by the current models will be described and compared with those obtained with e^+e^- colliders (Section 2). Then, in Section 3, we will discuss some problems related to the tagging of B's in *pp* colliders. In Section 4, we will mention some physics points (CP violation in the B–system, rare B–decays) for which large $B\overline{B}$ data samples are required. Finally, we briefly examine the implication of unequal B and $\overline{B}$ production in *pp* collisions in the context of CP violation measurements.

2. $B\overline{B}$ Production in pp Collisions

The total *pp* cross section (σ_T) in the multi-TeV region is not known, although there exists some cosmic-ray estimates.[1] Based on the existing $\bar{p}p$ and *pp* data, several fits to σ_T have been proposed,[2,3] leading to predictions for σ_T in the 15–100 TeV region (see Fig. 1). Although there are many uncertainties in these predictions, one may conjecture that σ_T does not vary too much in the 15–100 TeV region (within 20 to 30%) and that σ_T is of the order of 100 mb. This cross section, together with the current luminosities envisaged for *pp* colliders, $\mathcal{L} = 10^{32} - 10^{33}\ \mathrm{cm}^{-2}\ \mathrm{s}^{-1}$, leads to the tremendous event production rate of 10^7–10^8 events per second. Clearly, to handle such an amount of information is not trivial. In particular, the triggering will be a major problem.[4]

*ELOISATRON Project and IN2P3.

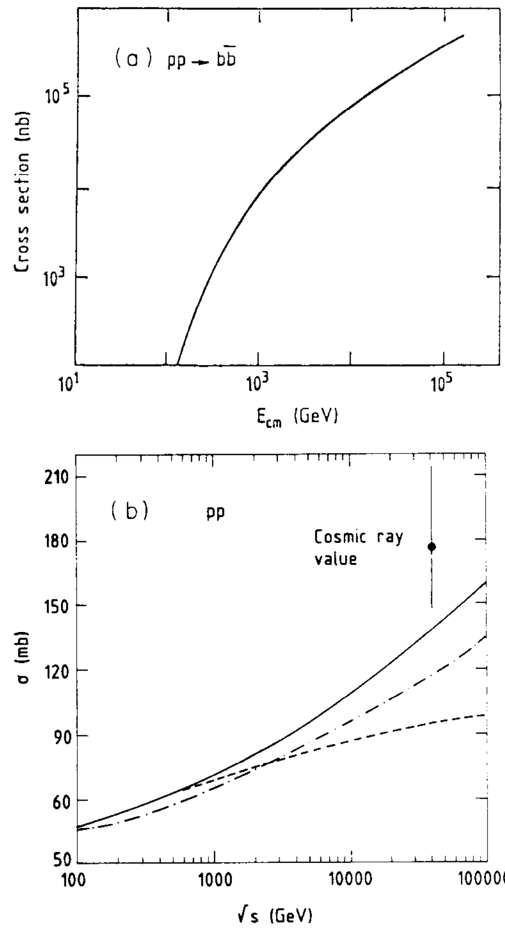

Fig. 1. The total *pp* (a) and $pp \to b\bar{b}$ (b) cross sections as a function of the c.m. energy $\sqrt{s} = E_{\mathrm{cm}}$. In (a) the full (dashed) line is obtained from a fit to *pp* and $p\bar{p}$ data assuming an asymptotic $\log^2$ (s/s$_0$) (constant) behavior (Ref. 3). The dash-dotted line is an extrapolation from a fit of Amos et al., Nucl. Phys. **B262**, 689 (1985). The curve in (b) is obtained from Ref. 6.

A further difficulty consists in the large multiplicity appearing in the multi-TeV region. At 15, 40 and 100 TeV, for instance, one expects a charged multiplicity of $\langle n_c \rangle = 80, 100$ and 120, respectively[5] (see Fig. 2). This will, of course, complicate the extraction of a B–signal from the final state.

For the $pp \to b\bar{b}X$ cross section $\sigma(b\bar{b})$ (X meaning anything) we will use the cross-section prediction given by the EUROJET Monte Carlo program.[6] This cross section is shown in Fig. 1 as a function of $\sqrt{s}$, the c.m. energy. The beauty production is believed to arise mainly from the $gg \to b\bar{b}$ subprocess (gluon fusion). This means that the $B\overline{B}$ mesons will tend to be collimated along the beam direction[7] (see below).

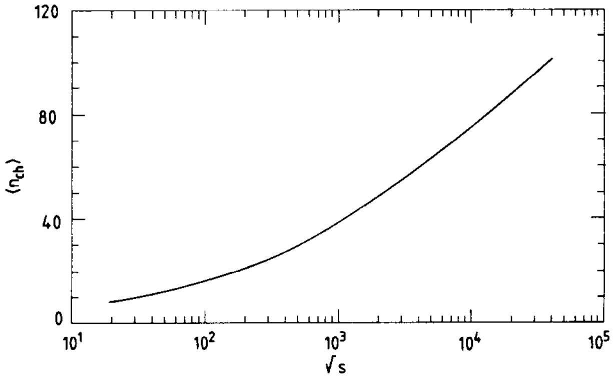

Fig. 2. The average charged multiplicity as a function of $\sqrt{s}$ (in GeV) as predicted by the PYTHIA Monte Carlo program (Ref. 5).

By requiring that the B–mesons be produced with an angle $\theta_{B\_} > 1°$ with respect to the beam line, one obtains the following $b\bar{b}$ production rates for one year of running (1 year = 10^7 s):

$$15 \text{ TeV} : \sim 7 \times 10^{10}\ b\bar{b} \text{ per year}$$

$$40 \text{ TeV} : \sim 2 \times 10^{11}\ b\bar{b} \text{ per year}$$

$$100 \text{ TeV} : \sim 3 \times 10^{11}\ b\bar{b} \text{ per year.}$$

These numbers are obtained with the help of the PYTHIA Monte Carlo program and their estimate should be considered as an order of magnitude. In any case these rates are much larger than those obtained with e^+e^- colliders (Table 1).

Table 1. Comparison of the number of $b\bar{b}$ events produced per year [$N(b\bar{b})/10^7$ s] with various e^+e^- colliders. At the Z^0 it was assumed that the $Z^0 \to b\bar{b}$ cross section is $\sim$ 6.6 nb, taking into account radiative corrections and a top-quark mass of $\sim$ 40 GeV/c^2 (a). For simplicity we considered a constant instantaneous luminosity $\mathcal{L}$ for all the colliders and we take into account the various inefficiencies by using 10^7 s as one year of running.

Accel.	L (cm^{-2} s^{-1})	L/day	$\sigma_{b\bar{b}}$ (nb)	$\sigma_b\bar{b}/\sigma_{\rm had}$	$N(b\bar{b})/10^7$s
CESR	$\sim 3.6 \times 10^{31}$	$\sim$ 3 pb^{-1}	$\sim$ 1	0.25	$\sim 3.5 \times 10^5$
B-factory	$\sim 10^{33}$	$\sim$ 86 pb^{-1}	$\sim$ 1	0.25	$\sim 1.0 \times 10^7$
PEP (25 GeV)	$\sim 5.8 \times 10^{31}$	$\sim$ 5 pb^{-1}	$\sim$ 0.046	0.09	$\sim 2.7 \times 10^4$
SLC	$\sim 5.0 \times 10^{29}$	$\sim$ 43 nb^{-1}	$\sim$ 6.6	$\sim$ 0.20	$\sim 3.3 \times 10^4$
LEP	$\sim 10^{31}$	$\sim$ 860 nb^{-1}	$\sim$ 6.6	$\sim$ 0.20	$\sim 6.6 \times 10^5$

(a) See, for instance, P. O. Kulth and K. Hullqvist, University of Stockholm Report USIP 85–019 (1985).

Still using the PYTHIA program to describe the gross features of $B\bar{B}$ production we find that 65% to 60% of all B's are produced in the $1 < \theta_B < 30°$ range for $\sqrt{s}$= 15–100 TeV. Moreover, the average B–momentum $\langle p_B \rangle$ is rather low, $\sim$ 60 GeV/c (15 TeV) to $\sim$ 70 GeV (100 TeV). These features indicate that as far as B–production is concerned, the exact c.m. energy of the pp collider is not really crucial (if one requires the $\theta_B > 1°$ condition). The $b\bar{b}$ production rate and the signal-to-background ratio ($\sigma_{b\bar{b}}/\sigma_T$) are not drastically changed when $\sqrt{s}$ varies from 15–100 TeV. However, the smaller multiplicity at lower $\sqrt{s}$ will certainly facilitate the identification of B–mesons among the final-state particles.

3. B Tagging

Because of the small $\langle p_B \rangle$ values, the B-decay particles will also be of low momentum. One may, therefore, hope that some B reconstruction will be possible, particularly for B's decaying into a small number of particles. Table 2 gives some examples of low-multiplicity, B–decay channels with their estimated branching ratios. One sees from this table that even with B–detection efficiencies of the order of 10^{-5} one will still be able to obtain an appreciable number of events per year. This implicitly assumes that one would be able to find solutions for extracting from 10^7–10^8 events per second of the desired B–decay processes.

Table 2. Number of B's decaying into a small number of particles and expected from one year of running with a pp collider producing 10^{11} $b\bar{b}$ per year.

Channel	Branching ratio (%)	Number per year
$B^0_d \to D^+\pi^-$ (a) $D^+ \to K^+\pi^+\pi^-$ (a)	0.6 ± 0.3 11.4 ± 1.1	$\sim 7 \times 10^7$
$B^- \to D^0\pi^-$ (a) $D^0 \to K^-\pi^+$ (a)	1.1 ± 0.6 5.4 ± 0.4	$\sim 6 \times 10^7$
$B \to F^+X \to \Phi\pi^+X$ (b) $\Phi \to K^+K^-$ (a)	0.38 ± 0.1 45.5 ± 1.5	$\sim 2 \times 10^8$
$B^0_s \to F^+\pi^-$ (c) $F^+ \to \Phi\pi^+$ (d) $\Phi \to K^+K^-$ (a)	0.6 ± 0.3 ~ 3.5 45.5 ± 1.5	$\sim 10^7$
$B^- \to \psi K^-$ (e) $\Psi \to \mu^+\mu^-$ (a)	~ 1 6.9 ± 0.9	$\sim 7 \times 10^7$

(a) Particle Data Table (1986).

(b) P. Hass et al., Phys. Rev. Lett. **56,** 2781 (1986).

(c) It is assumed that the BR($B^0_d \to D^+\pi^-$) and BR($B^0_s \to F^+\pi^-$) are equal.

(d) Value based on the theoretical estimate of D. Fadikov and B. Stech, Nucl. Phys. **B133,** 315 (1978), and on (b).

(e) The BR ($B \to \psi K$) value is overestimated since it corresponds in fact to the BR ($B \to \psi X$) value of M. S. Alam et al., Phys. Rev. **D34,** 3279 (1986).

In the attempts to reconstruct or tag B, the use of a vertex detector may help to reduce the important combinatorics due to the large multiplicities involved. With the help of the vertex detector one might identify some of the B-decay tracks and some other tracks which do not appear to arise from B-decays. This will clearly facilitate the B identification. In fact, because of the small σ_B involved, the vertex detector should allow the reconstruction of secondary vertices rather than the measurement of impact parameter values.

The drawback of small $\langle p_B \rangle$ is that the B–meson decay free path is also small (0.3–0.4 cm). Therefore, an efficient identification of B–mesons with the help of a vertex detector

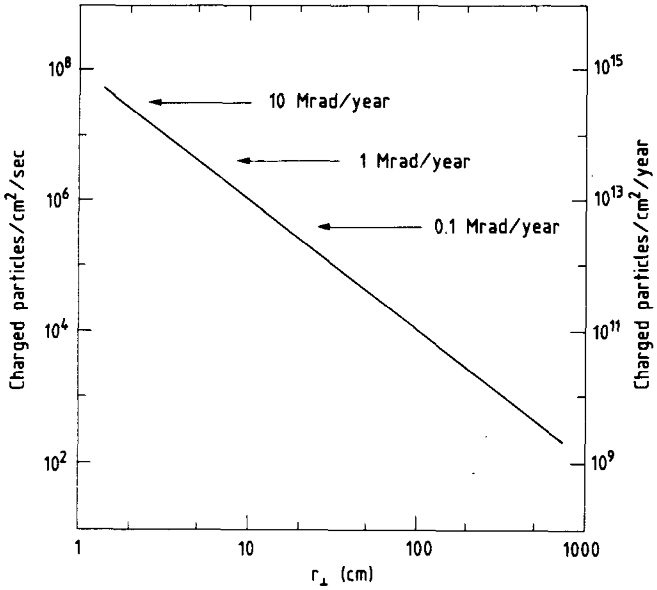

Fig. 3. Charged-particle rate per unit area perpendicular to the particle direction at $\mathcal{L} = 10^{33}$ cm^{-2} s^{-1} (Ref. 9). Note that 1 rad = 3×10^7 particles per cm^2.

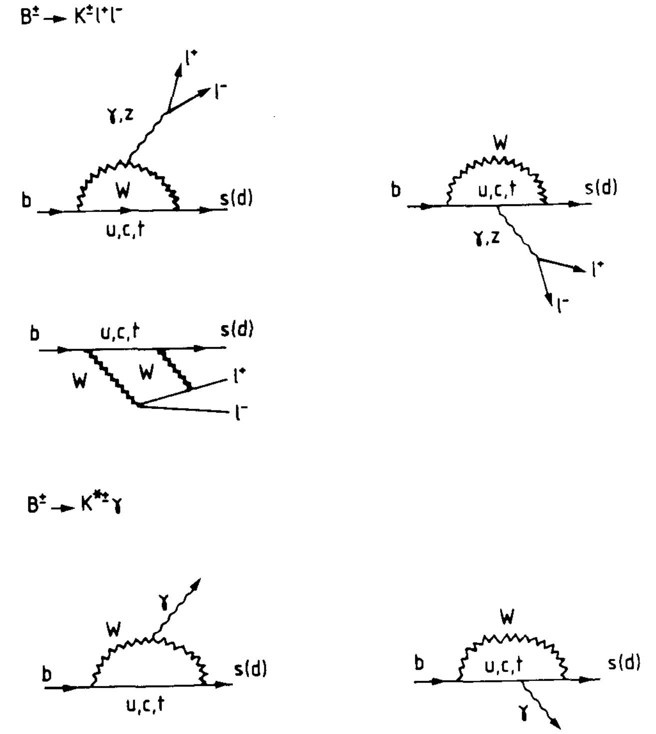

Fig. 4. Diagrams which may contribute to the rare decays $B^{\pm} \to K^{\pm}\ell^{+}\ell^{-}$, $K^{*}\gamma$.

will pose some problems. Indeed, it will be difficult to place the vertex detector close to the beam line where the radiation damage would be important. Figure 3 presents the estimated charged-particle flux as a function of the radial distance $r_{\perp}$ from the beam line.[9] This curve has been estimated for the SSC using $\mathcal{L} = 10^{33}$ cm^{-2} s^{-1}. The radiation doses accumulated in the vicinity of the beam line in one year of running are large when compared to the radiation currently accepted by actual devices, as for instance:

silicon strips : $\sim 10^6$ rad per year

current electronics : $\sim 10^4$ rad per year

plastic fibers : $\sim 10^5$ rad per year

glass fibers : $\sim 10^6$ rad per year.

For a tolerance of 10^5 rad per year the minimum distance $r_{\perp}$ min at which a vertex detector can be placed is $r_{\perp}$ (min) = 13, 5, 2 cm for $\mathcal{L} = 10^{33}$, 10^{32}, 10^{31} cm^{-2} s^{-1}. Thus, in order to tag B with the help of existing vertex detectors one has to run the pp colliders either with small luminosities (10^{31} cm^{-2} s^{-1}) or to develop devices which would be able to withstand high radiation doses. A value of 10^6 rad per year would permit having a vertex detector at $r_{\perp}$ (min) = 2 cm with $\mathcal{L} = 10^{32}$ cm^{-2} s^{-1}. This would certainly allow the tagging of some B's as their mean decay paths are 0.3–0.4 cm. The determination of the fraction of B's which could be detected (as well as the determination of the purity of the B-sample obtained) would require detailed Monte Carlo calculations using a realistic model for the detector.

What appears clear from this brief discussion is that one has to develop devices which would be able to accept high radiation doses. Vertex detectors withstanding radiation doses larger than 10^6 rad per year would certainly be useful for carrying out a B physics program with pp colliders. Finally, it should also be pointed out that the resistance of the equipment with regard to neutrons and photons still needs to be investigated.

4. B Physics Requiring Large B$\overline{\text{B}}$ Samples

As an illustration of the usefulness of large $B\overline{B}$ data samples, we will briefly discuss some problems related to rare B–decays. Then we will examine the possibility of detecting CP violation effects in the B-system. To this end we will use the predictions obtained in the framework of the Standard Model.

4.1 Rare B-Decays

Here we will consider the $B^{\pm} \to K^{\pm}\ell^{+}\ell^{-}$, $K^{*\pm}\gamma$ processes which have branching ratio values sensitive to the existence of a fourth generation. In addition, we will also examine the charmless B–decay from which one can obtain estimates for $|V_{bu}|$. Let us emphasize that in the framework of the Standard Model with three generations, $|V_{bu}|$ cannot vanish if CP violation (observed so far only for the K–system) has its origin in the phase present in the Kobayashi–Maskawa (KM) matrix.[10] A good measurement of $|V_{bu}|$ is thus of great importance. For the time being, there are the following estimates, $|V_{bu}/V_{cb}| < 0.14$ (Refs. 11 and 12), the recent ARGUS lower limit[13] of $|V_{bu}/V_{cb}| \geq 0.07$, and $0.037 < V_{cb} < 0.053$ (Ref. 13).

a) The $B^{\pm} \to K^{+}\ell^{+}\ell^{-}, K^{*\pm}\gamma$ Processes

Recently, several theoretical papers have dealt with the rare $B \to K\ell^{+}\ell^{-}$, $K^{*}\gamma$ decays[14–17] occurring through electroweak penguin diagrams (Fig. 4). Apart from the fact that the detection of these decays is important by itself as a further check of the Standard Model, the values of the decay branching ratios are sensitive to the existence of a fourth generation. First, let us note that the electroweak penguin diagram can best be studied within the B–system. Indeed, by assuming that the contribution of the heavy quark exchanged in the loop dominates,[15] one sees from Fig. 5 that the branching ratios for the penguin diagram will be larger for B– than for D– or K–mesons. Some of the theoretical estimates for the branching ratios[14–17] for typical masses of the t (top quark) and t' (top quark of the fourth generation) masses are given in Table 3. In fact, QCD enhancement factors can increase the BR($B \to K^{*}\gamma$) branching ratio by a factor of about 10 (Ref. 17).

It is, in any case, hoped that these decays are sufficiently peculiar to be recognized among the final-state particles. Detection efficiencies of the order of 10^{-3} will still allow the possibility of obtaining a few hundred (three generations) to a few

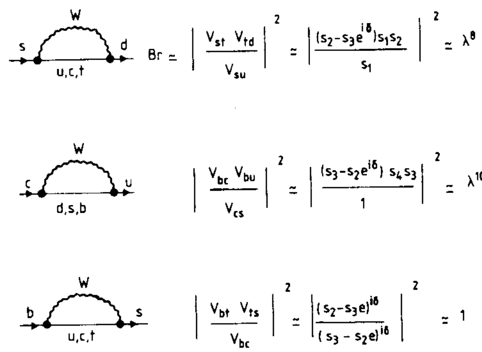

Fig. 5. The electroweak penguin diagrams leading to the decays of the s–, c–, and b–quarks. The Branching Ratios (BR) are proportional to the expressions given above.

Table 3. Estimates of branching ratios for some rare decays in the case of three and four generations. Here $m_t(m_{t'})$ denotes the $t(t')$ mass (in GeV/c^2) and V_{jk} is the $q_j \to q_k$ KM matrix element.

Decay channel	3 generations $m_t \approx 50$	4 generations $m_t = 50$ $m_{t'} \approx 200$ $\lvert V_{t's}V^*_{t'b}\rvert \approx 0.05$
$B^\pm \to K^\pm \ell^+\ell^-$	$\sim 3\times10^{-6}$	$\sim 2\times10^{-5}$
$B^\pm \to K^*\gamma$	$\sim 10^{-5}$	$\sim 10^{-4}$

thousand (four generations) events. For the $B^\pm \to K^{*\pm}\gamma$ decay the numbers can be larger because of the QCD enhancement factor just mentioned.

b) The $B^\pm \to F^\pm X_{c=0}$ Reactions

It has also been suggested[18] to carry out a systematic study of charmless decay of the B–meson in order to obtain information about V_{bu}. For instance, the observation of decays such as

$$B^\pm \to F^\pm X_{c=0}$$

would automatically imply $|V_{bu}| \neq 0$ (see Fig. 6). Note that $B \to \pi\pi$ would not necessarily indicate a $b \to u$ transition as $B \to \pi\pi$ can also arise from penguin diagrams[18] as shown in Fig. 6. To obtain quantitative estimates of $|V_{bu}/V_{bc}|$ one can measure the ratios of the partial widths (or branching ratios) of transitions involving $b \to u$ and $b \to c$ transitions, namely:

$$\frac{2\Gamma(B_u^+ \to F^+\pi^0)}{\Gamma(\overline{B}_d^0 \to D^-K^+)} = \frac{\Gamma(\overline{B}_d^0 \to D^0K^0)}{\Gamma(\overline{B}_d^0 \to \overline{D}^0K^0)} = \frac{\Gamma(\overline{B}_s^0 \to F^+K^-)}{\Gamma(\overline{B}_s^0 \to F^-K^+)} = \frac{2\Gamma(\overline{B}_s^0 \to D^0\pi^0)}{\Gamma(\overline{B}_s^0 \to D^-\pi^+)} = \left|\frac{V_{bu}}{V_{bc}}\right|^2 \left|\frac{V_{cs}}{V_{su}}\right|^2 .$$

In each ratio, the numerator (involving $b \to u$) and the denominator (involving $b \to c$) are partial widths of processes occurring via the same quark diagrams.[18] In this way, corrections due to QCD or final-state interactions are believed to be minimized. The branching ratios arising from the $b \to u$ transition are estimated in Ref. 18 to be of the order of 10^{-4}. One would thus hope to detect them in a pp collider experiment [remember that similarly to (a) one is dealing here with low-multiplicity B–decays].

4.2 CP Violation in the B–System

The detection of, or the possibility of setting limits on, CP violation in the B–system is certainly one of the key reasons for collecting large $B\overline{B}$ samples. There are essentially two ways in which CP violation can be detected.[19–22] One way consists of using the mixing properties of the $B^0_{d,s} - \overline{B}^0_{d,s}$, whereas in

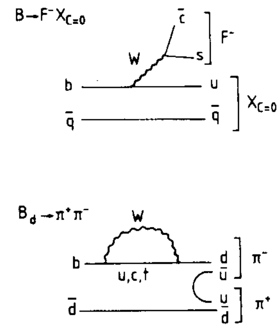

Fig. 6. Examples of charmless B–decays.

the second case CP violation will appear through final-state interaction. *4.2.1 CP Violation Involving Mixing*

a) Semileptonic Decays

The simplest case consists of searching for CP violation effects (in the mass matrix) by means of semileptonic decays. This can be done by evaluating the asymmetry parameter,

$$A_s = \frac{\Gamma(B^0 \to \overline{B}^0 \to \ell^+X) - \Gamma(\overline{B}^0 \to B^0 \to \ell^-X)}{\Gamma(B^0 \to \ell^-X) + \Gamma(\overline{B}^0 \to \ell^+X)}$$

where Γ denotes the corresponding width (X meaning anything). In practice, this is obtained by measuring the difference in the number of positive $N(\ell^+\ell^+)$ and negative $N(\ell^-\ell^-)$ dilepton pairs, i.e.,

$$A_u = \frac{N(\ell^+\ell^+) - N(\ell^-\ell^-)}{N(\ell^+\ell^-)} .$$

$N(\ell^+\ell^-)$ is the number of events with leptons of opposite charge. The A_u parameter is predicted to be small[22] as given in Table 4. This table also gives the number of $B\overline{B}$ events required to observe a signal with three standard deviations using the branching ratios and the CP asymmetries given in the same table. The ARGUS value for the $B^0 - \overline{B}^0$ mixing[13] has been taken into account to obtain the predicted branching ratio. In fact, for the dilepton case, the number of events must be increased since lepton momentum (p_ℓ) cuts must be applied to eliminate the background introduced by the $D \to l\nu X$ decays. This means that within the present estimates CP violation could not be detected in the $B^0 - \overline{B}^0$ mixing by measuring differences in the number of positive and negative dilepton pairs.

b) Exclusive Decays

When the B^0 and $\overline{B}^0$ can decay into the same final state f (hence necessarily also into its charged conjugated state $\bar{f}$), CP violation effects can appear as an interplay between mixing and decay amplitudes. In other words, the final state f (or $\bar{f}$) can be reached directly from the B^0 or $\overline{B}^0$ decays or through mixing and subsequent decay. It is the interference between the different routes leading to a given final state which can lead to CP violation. The time-integrated CP asymmetry is given by

$$A_s = \frac{\Gamma(B^0 \to f) - \Gamma(\overline{B}^0 \to \bar{f})}{\Gamma(B^0 \to f) + (\overline{B}^0 \to \bar{f})} .$$

Two cases can be considered; 1) where f is self conjugate ($f = \bar{f}$), for instance, $B^0\overline{B}^0 \to \Phi K_s$, $D\overline{D}K_s$, $D\overline{D}\ldots$ and 2) where $f \neq \bar{f}$ (for instance, $f = D^+\pi^-$). Table 4 gives predictions for the branching ratios and CP asymmetries for several channels[22] within the framework of the Standard Model with three generations. Note that the CP asymmetries have been calculated with the ARGUS mixing value (for the like-sign dilepton pairs, it is the branching ratio which is affected

Table 4. Number of $B\overline{B}$ events needed to observe CP violation effects with three standard deviations in some $B^0_{d,s}$ decays where mixing is present. The branching ratios and the CP asymmetries were taken from Ref. 17. The CP asymmetries for the case where $f = \overline{f}$ were increased in order to take into account the new $B^0_d - \overline{B}^0_d$ mixing value of Ref. 13. For the nondilepton case a tagging efficiency of 0.1 was taken for the other produced B. It was assumed that charged and neutral B are produced in the ratios $B^+ : B^0_d : B^0_s = 0.4 : 0.4 : 0.2$. At the $T(4S)$ the number of events has to be decreased by a factor of ~ 3 for the $B_d\overline{B}_d \to \ell^+ \ell^- X$ case.

Decay mode	Branching ratio	CP asymmetry	Number of events
$B_d\overline{B}_d \to \ell^\pm \ell^\pm X$	~ 0.01	$\sim 10^{-3}$	$\sim 3 \times 10^9$
$B_s\overline{B}_s \to \ell^\pm \ell^\pm X$	~ 0.05	$\sim 10^{-4}$	–
$B_d \to \Psi K_s$	$\sim 5 \times 10^{-4}$	0.05–0.3	3×10^6–9×10^7
$B_d \to \Psi K_s X$	$\sim 2 \times 10^{-3}$	0.05–0.3	6×10^5–2×10^7
$B_d \to D\overline{D}K_s$	$\sim (0.1\text{–}2) \times 10^{-2}$	0.05–0.3	6×10^4–2×10^6
$B_d \to D\overline{D}$	$\sim 5 \times 10^{-3}$	0.05–0.5	9×10^4–9×10^6
$B_d \to D^+\pi^-$	$\sim 10^{-2}$	10^{-3}–10^{-2}	10^8–10^{10}
$B_d \to D^0 K_s$	$\sim 10^{-3}$	10^{-3}–10^{-2}	–
$B_s \to F^+ K_s$	$\sim 10^{-3}$	0.1–0.5	9×10^5–10^7

by the new mixing value). In fact, in order to obtain A_s from experiment, one has to know if the observed final state f (or $\overline{f}$) is coming from a B^0 or a $\overline{B}^0$. Since in strong or electromagnetic interactions, beauty hadrons are produced in pairs, one measures, in fact, the cross sections $\sigma(\ell^\pm, f)$ and $\sigma(\ell^+, \overline{f})$. Here $\ell^\pm$ is the lepton coming from the other beauty hadron. Its charge indicates if we are dealing with a B or an $\overline{B}$. Thus, in practice, one measures the ratio:

$$A_s' = \frac{\sigma(\ell^- f) - \sigma(\ell^+ \overline{f})}{\sigma(\ell^- f) + \sigma(\ell^+ \overline{f})} \quad .$$

The number of events needed to observe a three-standard deviation effect were calculated in Table 4, assuming that in all cases the other B has to be tagged. In considering tagging by means of semileptonic $B \to e(\mu)X$ decays in which the lepton has a high momentum, we took a tagging efficiency of 0.1. From Table 4, one sees that one can hope to detect or to set limits for CP violation effects if B-decay channels could be identified with efficiencies in the range of 10^{-3}–10^{-4}.

The CP violation effects can also be detected in the absence of mixing. In this case, the effects will be observed with the help of interference phenomena via final-state interactions. This means that at least two different production mechanisms[21,22] (i.e., involving different sets of KM matrix elements) leading to the same final state must be present. With two production mechanisms, the production amplitudes can be written in the form:

$$\langle f|B^-\rangle = g_1 M_1 \, e^{i\alpha_1} + g_2 M_2 \, e^{i\alpha_2}$$

$$\langle \overline{f}|B^+\rangle = g_1^* M_1 \, e^{i\alpha_1} + g_2^* M_2 \, e^{i\alpha_2} \quad ,$$

yielding a CP asymmetry parameter

$$A_s \sim 4 \text{ Im } (g_1^* g_2) \sin (\alpha_1 - \alpha_2) \, M_1 M_2 \quad .$$

Here $g_{1,2}$ are the weak decay parameters, and $\alpha_{1,2}$ are the phases due to final-state interactions, while $M_{1,2}$ are (real) kinematical factors. Clearly $A_s \neq 0$ when $\alpha_1 \neq \alpha_2$ and when the product $(g_1^* g_2)$ has an imaginary part. Because of the rough estimates for the phases $\alpha_{1,2}$, there are large uncertainties on the asymmetry parameters as shown in Table 5 taken from Ref. 22. In the framework of these estimates CP violation will hardly be detectable for the decay channels given in Table 5.

Table 5. Number of $B\overline{B}$ events needed to observe a CP violation effect with three standard deviations in some $B^\pm$ decay cases. The branching ratios and the CP asymmetries were taken from Ref. 17. At the Υ(4S) the number of events has to be reduced by $\sim 23\%$.

Decay mode	Branching ratio	CP asymmetry	Number of events
$B^\pm \to \Sigma_{1,j}(K_s N_i) K M_j$	$\sim 10^{-3}$	10^{-3}–10^{-2}	10^8–10^{10}
$B^\pm \to D^{0*} D^\pm$	$\sim 10^{-3}$	10^{-3}–10^{-2}	10^8–10^{10}
$B^\pm \to K^\pm \varrho^0$	$\sim 10^{-4}$	10^{-2}–10^{-1}	10^7–10^9

5. Unequal $B\overline{B}$–Production

For pp collisions the $B-$ and $\overline{B}$–mesons are not produced in equal amounts.[23] The presence of valence $u-$ and d–quarks in the initial state leads to a preponderance of $B^+ \equiv (\overline{b}u)$ over B^-, and of $\overline{B}^0 \equiv (\overline{b}d)$ over B^0. There is another source of asymmetry in the $\overline{B}$– and B–production, namely that due to the subprocesses $qq \to qq$ and $qq \to qg$. The outgoing quark can radiate a gluon which then branches into a $b\overline{b}$ pair. For the same reasons as given above, this mechanism will tend to increase the preponderance of $\overline{B}$ over B–mesons. In searches for CP violation effects via mixing, the asymmetry in the B and $\overline{B}$ production will (in principle) not be important as long as we consider that one $B\overline{B}$ pair is produced per event (see below). Indeed, in these cases one detects the decay of one meson in an exclusive state while the other one has to be tagged. By detecting only events having a $B\overline{B}$ in the final state one loses some events. This loss has been estimated with PYTHIA. One obtains for $\theta_B > 1^\circ$ and $\sqrt{s}$ = 15–100 TeV, A_s losses of the order of 3%. As far as statistics are concerned, this effect is negligible. It has, however, an influence in the case of multi-B production. By this, we mean final states having B or/and $\overline{B}$ in addition to a $B\overline{B}$ pair. For the same reason as mentioned above, there will also be a tendency here to a preponderance of $\overline{B}$ over B. As the detection efficiency for B (or $\overline{B}$) is expected to be rather small, one may have cases where one associates two mesons which do not result from the same subprocess, the other B–mesons not being detected. This might stimulate a CP violation effect.

The multi-B production can arise from several sources:

i) a $gg \to \overline{b}b$ subprocess, in addition to others, leading to the production of $b\overline{b}$;

ii) the presence of several $gg \to b\overline{b}$ in one event.

The multi-B production due to point *i)* was estimated with the help of the PYTHIA Monte Carlo program. The fractions of these events at 15, 40 and 100 TeV are given in Table 6. The fractions due to point *ii)* cannot be estimated with PYTHIA as the feature of having several $gg \to b\overline{b}$ subprocesses in one event is not incorporated in the Monte Carlo program. We therefore estimated the number of $gg \to b\overline{b}$ subprocesses in a pp collision by assuming that this number is distributed according to a Poisson distribution with a mean (corresponding to one $gg \to b\overline{b}$ subprocess) given by the cross-section ratio $\sigma(b\overline{b})/\sigma_T$. Using the cross-section distributions shown in Fig. 1, we finally obtain the total fractions of multi-B events as given in Table 6 and which appear to be of the order of the percent. This value has to be considered as an order of magnitude, since in particular Higgs and $t(\overline{t})$ production were not taken into account. The exact background introduced by the multi-B production depends on the characteristics of the detector (and in particular on the B detection efficiency). Nevertheless, the numbers given in Table 6 indicate that multi-B production might pose a real problem for studying CP violation effects.

Table 6. Fraction of events having at least one B or $\overline{B}$ in the final state in addition to a $B\overline{B}$ pair at 15, 40 and 100 TeV ($\theta_B > 1$). The errors are statistical while no errors have been taken for the crude estimate of the number of $gg \to \bar{b}b$ subprocesses participating in a given collision.

c.m. energy (TeV)	$gg \to b\bar{b}$ + other subprocesses $\theta_B > 1$	multi $gg \to b\bar{b}$ processes	Total $\theta_B > 1°$
15	$(5.0 \pm 1.3) \times 10^{-3}$	$\sim 4.5 \times 10^{-4}$	$\sim 5.5 \times 10^{-3}$
40	$(6.8 \pm 1.7) \times 10^{-3}$	$\sim 1.1 \times 10^{-3}$	$\sim 7.9 \times 10^{-3}$
100	$(6.4 \pm 1.9) \times 10^{-3}$	$\sim 2.0 \times 10^{-3}$	$\sim 8.4 \times 10^{-3}$

A possible way to overcome these difficulties would consist in measuring the ratio $N(\overline{B})/N(B)$ by means of decays where CP violation is absent or at least negligible. To this end, one can use the decays $B^\pm \to K^\pm\ell^+\ell^-, K^{*\pm}\gamma, \ell^\pm v D^0(D^{*0})$. For the first two decays, the charge of the K tags the charge of the B, whereas in the last case it is the charge of the lepton which tags the $B^\pm$. Strictly speaking, the graphs shown in Fig. 4 for the $B^\pm \to K^\pm\ell^+\ell^-, K^{*\pm}\gamma$ decays can induce CP violation effects because there are various types of quarks exchanged in the loops. Nevertheless, in the leading order, where one considers only the exchange of the top quark, no CP violation will appear. For the $B^\pm \to \ell^\pm v D^0$ (D^{*0}) process one has the difficulty of reconstructing a B–meson having a neutrino among the decay products. The branching ratio is, however, higher than in the previous cases as it is expected to amount to a few percent (the $B \to \ell v X$ branching ratio is $\sim$ 12%). By measuring the above decays, one obtains $N(B^-)/N(B^+)$, which is assumed to be equal to $N(B^0_{s,d})/N(\overline{B}^0_{s,d})$.

Let us denote by $A_{\rm CP}$ the CP violation asymmetry parameter, i.e.,

$$A_{\rm CP} = \frac{\Gamma(B \to f) - \Gamma(\overline{B} \to \bar{f})}{\Gamma(B \to f) + \Gamma(\overline{B} \to \bar{f})}$$

and by $\mathrm{BR}^{\mathrm{CP}}$ the branching ratio of $B \to f$ or $\overline{B} \to \bar{f}$. A convenient situation would occur if the branching ratio BR^D of the channels serving to measure $N(\overline{B})/N(B)$ were larger than $\mathrm{BR}^{\mathrm{CP}}$. To illustrate this more precisely, we choose some typical values of $\mathrm{BR}^{\mathrm{CP}}$ and $A_{\rm CP}$ in Table 7. We first calculate the number of $B\overline{B}$ events required to observe $A_{\rm CP}$ with a three standard deviation effect. Then using $\mathrm{BR}^D = 10^{-3}$ and 10^{-4} we calculated the number of standard deviation actually observed when $N(\overline{B})/N(B)$ is determined from the experiment. As expected, the degradation occurs especially when $\mathrm{BR}^{\mathrm{CP}} > \mathrm{BR}^D$. Finally, we also give in Table 7 the number of standard deviations which would be observed with 5×10^8 $pp \to b\bar{b}$ events. The numbers are rather comfortable, but the possibility of accumulating 5×10^8 events with identified B in the final state in a reasonable period of time is still an experimental challenge.

Table 7. Number of events and statistical significance in standard deviations (s.d.) for typical values of branching ratios $\mathrm{BR}^{\mathrm{CP}}$ and CP asymmetries $A_{\rm CP}$. Here BR^D is the branching ratio of the channel serving to measure $N(\overline{B})/N(B)$.

CP violation		Number of events for 3 s.d.	BR^D	Number of s.d.	Number of s.d. with 5×10^8 events
$\mathrm{BR}^{\mathrm{CP}}$	$A_{\rm CP}$	$[N(\overline{B}) = N(B)]$		$[N(\overline{B}) \neq N(B)]$	$[N(\overline{B}) \neq N(B)]$
10^{-2}	10^{-2}	$\sim 5 \times 10^6$	10^{-3}	0.9	13
10^{-4}	10^{-2}	$\sim 5 \times 10^8$	10^{-3}	2.9	2.9
10^{-5}	10^{-1}	$\sim 5 \times 10^7$	10^{-4}	2.9	9.5
10^{-6}	10^{-1}	$\sim 5 \times 10^8$	10^{-4}	~ 3	2.9

6. Conclusions

We have briefly discussed the possibility of studying B physics with pp colliders in the multi-TeV region. Although, the $B\overline{B}$ production rate is expected to be very large ($\sim 10^{11} B\overline{B}$ per year for the envisaged colliders) the extraction of a B–signal among the large number of outgoing particles (at 40 TeV the charged multiplicity is $\sim$ 100) will certainly not be easy. The use of present vertex detectors in order to recognize B–decay tracks is handicapped by the presence of a large amount of radiation near the beam line. Moreover, further technical efforts are still needed in order to be able to trigger on the desired events when the total event production rate is expected to be 10^7–10^8 per second.

However, many fundamental aspects of B physics (CP violation and rare B–decays) cannot be studied with the statistics provided by the present colliders. It will thus certainly be useful to devote further efforts to using pp colliders also as a means of studying B physics. In any case, the triggering problems and the development of equipment able to withstand large radiation doses can be considered as technical challenges for the near future.

7. Acknowledgements

It is a pleasure to thank E. Bloom, A. Seiden and T. Sjöstran for useful discussions and Professor A. Zichichi for supporting this work.

References

1. T. K. Gaisser et al., *Hadron Cross Sections at Ultra-high Energies and Unitarity Bounds on Diffraction*, submitted to Phys. Rev., 1987.
2. G. J. Alner et al; Z. Phys. **C32**, 153 (1986).
3. M. M. Block and R. N. Cahn, report LBL 23472 (1987).
4. Proc. Workshop on Triggering, Data Acquisition and Offline Computing for High Energy/High Luminosity Hadron-Hadron Colliders, Fermilab, Batavia, Illinois, 1985.
5. T. Sjöstrand and M. van Zijl, *A Multiple Interaction Model for the Event Structures in Hadron Collisions*, Lund preprint LU TP 87–5 (1987).
6. A. Ali, B. Van Eijk and I. ten Have, *Heavy Flavor Production and Heavy Flavor Mixing at the CERN $p\bar{p}$ Collider*, preprint CERN–TH 4523/86 (1986); B. Van Eijk, Ph.D. Thesis, University of Amsterdam (1987).
7. B. Cox, F. J. Gilman and T. D. Gottschalk, SLAC–PUB–4144, CALT–68–1411, Fermilab Conf. 86/166, to appear in Proc. Summer Study on the Physics of the Superconducting Supercollider, Snowmass, Colorado, 1986; B. Cox and D. E. Wagoner in Proc. Summer Study on the Physics of the Superconducting Supercollider, Snowmass, Colorado, 1984.
8. H. –U. Bengtsson and T. Sjöstrand, LU–TP 87–3/ UCLA–87–001, to appear in Comput. Phys. Commun.; T. Sjöstrand and M. Bengtsson, Comput. Phys. Commun. **43**, 367 (1987); T. Sjöstrand, Comput. Phys. Commun. **39**, 347 (1986).
9. Report of Task Force on Detector R&D for the SSC (1986); G. H. Trilling, report LBL 22384 (1986).
10. If the nondiagonal $V_{ij} = 0$ one could redefine the quark fields in such a way that the phase in the KM matrix vanishes.
11. F. Gilman and K. Kleinknecht, Particle Data Table 1986, p. 74.

12. S. J. Behrends et al., Phys. Rev. Lett. **59**, 407 (1987).

13. W. Schmidt-Parzefall (ARGUS Collaboration), talk given at the 1987 International Symposium on Lepton and Photon Interactions at High Energies, Hamburg, 1987. The $|V_{bu}/V_{bc}|$ value has to be considered with some care as there appear to be some discrepancies between the ARGUS and CLEO results. See K. Berkelman, talk given at the Heavy Flavor Symposium, Stanford, California, 1987.

14. W.-Shu Hou, R. S. Wiley and A. Soni, Phys. Rev. Lett. **58**, 1608 (1987).

15. W.-Shu Hou and A. Soni, talk presented at the B–Factory Workshop at UCLA, 1987. W.-Shu Hou, A. Soni and H. Steger, report PITT 87-01, UCLA/87/TEP/1 (1987), B–Factory Workshop at UCLA, 1987, report PITT 87-05 (1987).

16. N. G. Deshpande et al., Phys. Rev. Lett. **57**, 1106 (1986).

17. S. Bertolini et al., report CMU–HEP 86–19, NYU/TR12/86 (1986).

18. L. L. Chau, Proc. Summer Study on the Physics of the Superconducting Supercollider, Snowmass, Colorado, 1986.

19. A. Ali and Z. Z. Aydin, Nucl. Phys. **B148**, 165 (1979); I. I. Bigi and A. I. Sanda, Nucl. Phys. **B193**, 85 (1981); J. Hagelin, Nucl. Phys. **B193**, 123 (1981); J. Bernabeu and C. Jarlskog, Z. Phys. **B281**, 42 (1987).

20. A. J. Buras, W. Slominski and H. Steger, Nucl. Phys. **B245**, 369 (1984); C. Wolfenstein, Nucl. Phys. **B246**, 45 (1986); L. L. Chau and W. Y. Keung, Phys. Lett. **165B**, 429 (1985). See also L. L. Chau, Phys. Rep. **95**, 1 (1983).

21. I. Dunietz and J. L. Rosner, Phys. Rev. **D34**, 1404 (1986).

22. I. I. Bigi and A. I. Sanda, Nucl. Phys. **B281**, 42 (1987).

23. This has been discussed in A. Fridman and T. Sjöstrand, Remarks about B–production in pp Collisions in the Multi-TeV Region, Note for the 1987 Berkeley SSC Workshop.

ASPECTS OF RARE B–DECAYS

A. Soni

Department of Physics,
University of California, Los Angeles, CA 90024

1. Introduction and Motivations

In the past several years intense kaon factories have become available, making it feasible to measure rare branching ratios down to the impressive level[1] of 10^{-11}. The need for a dedicated B–factory may therefore hardly appear necessary. What we wish to point out is that the B–system is extremely rich and its rare decays have a lot of potential for interesting physics.[2]

For one thing, B–decays are far cleaner from QCD corrections compared to K–decays. Indeed, there are two well-known tests of strong corrections to weak amplitudes; namely, the lifetime difference between charged and neutral mesons and the semileptonic branching ratio. Experimentally it is already known that $0.5 \lesssim \tau_{B^+}/\tau_{B^0} \lesssim 2$, which is a far cry from the factor of 450 for the kaon case. Furthermore, the semileptonic branching ratio for B's is also roughly in accord with naive quark counting. These are important indications that effects of QCD corrections are not that important on b–decays, at least in so far as tree graph decays are concerned. Presumably, the fact that $m_b^2 \gg m_s^2$ is at least in part responsible for the smallness of QCD corrections as a manifestation of the asymptotically free nature of QCD.

In the realm of loop decays, the u–quark in the flavor changing loop $b \to s$ transition essentially decouples because the u–quark has such a small mass (compare to c– and t–quarks) and also because the CKM angle $V_{ub} \gg V_{cb} \gg V_{tb}$. This decoupling of the light u–quark should make loop decays of b–quarks short (and not long) distance dominated, and therefore much more readily amenable to perturbative analysis.

Loop decays of b also have significantly larger BRs than the corresponding kaon decays. This happens as loop decays are often driven by the heaviest (virtual) quark in the loop, i.e., the top quark. Then the ratio of BR for $b \to s$ versus $s \to d$ transitions becomes:

$$\frac{\left|\dfrac{V_{ts}^* V_{tb}}{V_{cb}}\right|^2}{\left|\dfrac{V_{td}^* V_{ts}}{V_{us}}\right|^2} \simeq \lambda^{-8} \simeq 10^5 \quad .$$

Indeed,[3] $\mathrm{BR}(B \to K\nu\bar{\nu}) \sim$ (1–70) $\times 10^{-6}$, whereas for[4] $\mathrm{BR}(K \to \pi\nu\bar{\nu}) \simeq$ (1–3) $\times 10^{-10}$. Thus, loop decays of b may not be that rare and they provide an excellent probe for the short distance structure of the theory. These probes are the analogues of the precision tests, such as the (g-2) of the muon, except that in b–decays they are more powerful because they test the full non–Abelian gauge theory structure, including non–Abelian coupling and symmetry breaking mechanism of the SM.

Being a member of the third family b–quark is also likely to be much more sensitive to the parameters of the fourth generation than the s–quark.

2. Rare Decays via Electroweak Penguins

At the quark level, the interesting modes are $b \to s\ell^+\ell^-$ (Ref. 5), $b \to s\nu\bar{\nu}$ (Ref. 3), and $b \to s\gamma$ (Ref. 6). They materialize, for example, as $B \to Kee, KeeX$, $B_S \to \phi ee \ldots$; $B \to K\nu\bar{\nu} \ldots$; $B \to K^*\gamma \ldots$ etc.

Perhaps the cleanest and theoretically most interesting mode is $B \to Kee$, which has a well-defined and reconstructible final state. The decay is interesting because it provides a test of the full machinery of the SM at the one-loop level. If quarks with mass $> m_W$ exist, these decays ($b \to s\ell\ell, s\nu\bar{\nu}$) acquire special importance. In the limit of X_Q ($X_Q \equiv m_Q^2/m_W^2 \gg 1$) the formula for the rates takes a very simple form:

$$\sim \left|\frac{1}{4} X_Q + \frac{3}{4} \ln X_Q\right|^2 \quad ,$$

where (in the 't Hooft–Feynman gauge) the first contribution is due to Z exchange and the second one due to γ exchange. Presence of the first term due to Z exchange means that the rate grows as m_Q^4. Therefore, the process becomes an excellent way of monitoring mass scales and mixing angles of heavy quarks. The growth of the rate with virtual quark mass as m_Q^4 is very remarkable. This somewhat counter-intuitive behavior constitutes an evasion of the screening theorem of Appelquist and Carrazone and arises due to the fact that the underlying spontaneously broken gauge theory has Yukawa coupling constants which are proportional to fermion masses. A similar phenomenon in $K\overline{K}$ or $B\overline{B}$ mixing occurs. However, those mixing effects are governed by amplitudes which grow as m_Q^2. The rates for $b \to s\ell\ell$, $s\nu\bar{\nu}$ vary as $|\mathrm{Amplitude}|^2$ and consequently grow as m_Q^4. The presence of the m_Q^4 term is a consequence of the fermion mass generating Higgs mechanism of the underlying SM and therefore measurements of these decays constitute a very important test of the SM at its weakest sector, namely the symmetry breaking mechanism. The importance of these tests of the SM can therefore hardly be overemphasized.

The three-generation result is given in Fig. 1.[3] The current CLEO bound $\mathrm{BR}(B \to Kee) \lesssim 10^{-4}$ translates into $m_t \lesssim$ 500 GeV. So at the moment this bound on m_t does not compete favorably with that obtained from the ρ parameter and radiative corrections of $\sin^2\theta_W$ which now give $m_t \lesssim 200$ GeV.[7]

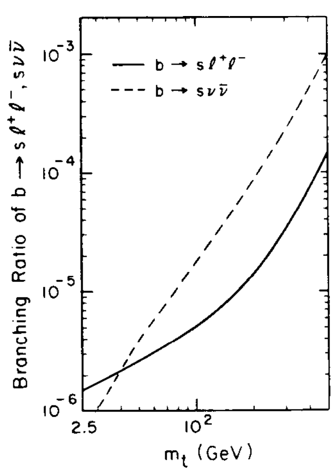

Fig. 1. BR's for the process $b \to s\ell^+\ell^-$, $s\nu\bar{\nu}$ in the three-generation case. For the $b \to s\nu\bar{\nu}$, the three-neutrino species have been summed over.

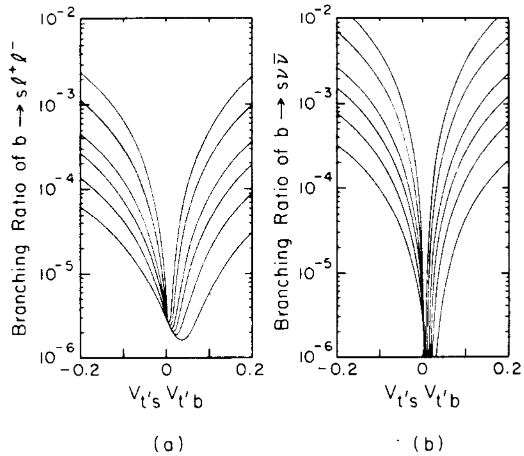

Fig. 2. The four-generation BR's versus $v_{t'} \equiv V_{t's}V^*_{t'b}$. We have used $V_{cb} = .05$, $m_t = m_L = 50$ GeV. Different curves from bottom to top are: $m_{t'} = 150$, 200, 250, 300, 400 and 500 GeV.

However, the latter bounds are a result of over five years of theoretical and experimental effort, whereas the bounds from B-decays are at a stage of pre-infancy. As improvements in measurements of B-decays become available, and certainly as a dedicated B-factory that we are advocating becomes available, these decays would start to compete very favorably with these other bounds.

The four-generation result for $b \to s\ell^+\ell^-$ and $b \to s\nu\bar{\nu}$ is shown in Fig. 2.[3] Here the controlling mixing angle is $v_{t'} \equiv V_{t'b}V^*_{t's}$. We have limited our considerations to $|v_{t'}| \leq .2$ and $150 \leq m_{t'} \leq 500$ GeV. We see that an order of magnitude enhancement over the three-generation result is quite possible.

Another interesting loop decay[6,8] is $b \to s\gamma$. A significant fraction of the time this should materialize into the exclusive mode $B \to K^*\gamma$. For the three-generation case the inclusive BR is $\sim 10^{-4}$ within a factor of two, and is quite insensitive to the top mass. In four-generation, the BR can be much larger or appreciably smaller (because of cancellation between t and t' contributions) than the three-generation case. This mode has the distinction of very likely becoming the first observable loop decay of the b-quark.

3. Loop Decays via QCD Penguins[9,10]

At the quark level these decays proceed through $b \to sg^*$ where g^* is a gluon on or off its mass shell. At the hadron (inclusive) level this materializes into $B \to K + X_{\not{c}}$ where again $X_{\not{c}}$ stands to emphasize that the hadronic final state must

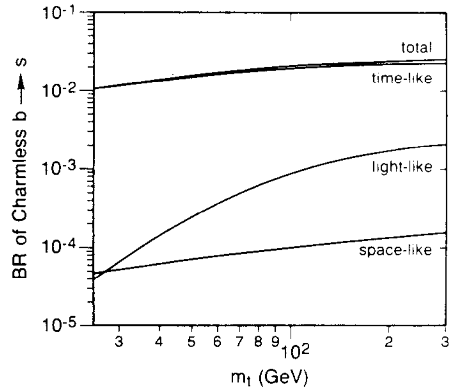

Fig. 3. The three-generation case.

be charmless. Denoting q as the four-momentum of the gluon, the contributing processes can be of three types:[11]

(*a*) $q^2 > 0$, i.e., time-like gluon which leads to $g \to q\bar{q}$ ($q = u, d, s$ for charmless final state) and $g^* \to gg$;

(*b*) $q^2 < 0$, i.e., the space-like case. At the quark level this leads to a two-body decay;

(*c*) $q^2 = 0$, which is the light-like case.

Although this last process is lowest order in α_s, it is driven by the magnetic form factor alone and contributes much less than the $O(\alpha_s^2)$ process (a) as the electric form factor is much larger than the magnetic. The contribution for these three cases as well as the total is shown in Fig. 3.[9] The total inclusive BR is fairly insensitive of the top quark mass and is 1–2% . For the four-generation case (see Fig. 4) the BR ranges from .5% to 15% .[9]

We thus see that at the inclusive level these loop decays have fairly large BR. However, they would materialize mostly into multibody final states such as $K + 2\pi$, $K + 3\pi$ ... and to a lesser extent multikaon states. Decays into two-body charmless modes such as $K\pi$ are going to be suppressed (BR $\sim 10^{-5}$). The experimental challenge in detection of QCD penguins lie in finding a good way to veto against the presence of charm in such final states. If that could be overcome, the interpretation is quite clear: BR($B \to K + X_{\not{c}}$) less than .5% or greater than 5% cannot be accommodated by three-generation SM, $5\% \lesssim$ BR $\lesssim 20\%$ would strongly suggest the existence of four families and BR $> 20\%$ cannot be accommodated even with four families and would imply a breakdown of the SM.

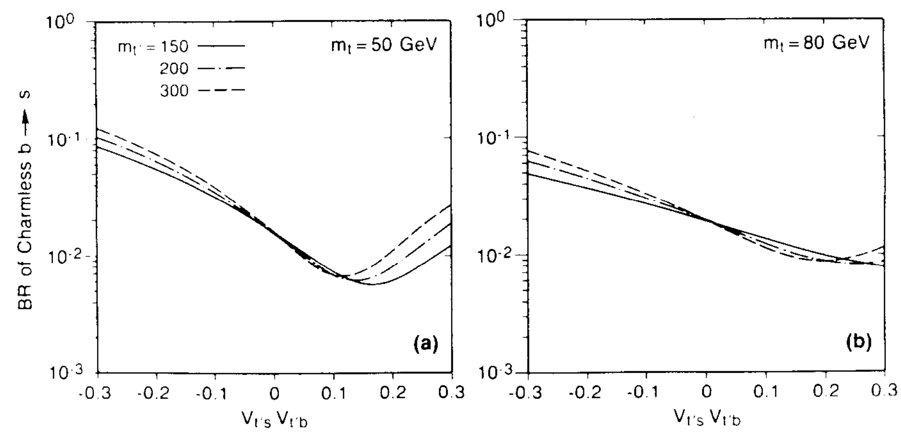

Fig. 4. The four-generation case.

Table 1 provides a summary of these rare loop decays (without CP): $b \to s\ell\ell$, $b \to s\nu\bar{\nu}$, and $b \to sg^*$ for three and four families, together with the current experimental bound.

Table 1. Some of the rare decays of the b-quark.

Mode	BR for Three-Generation[(a)]	BR for Four-Generation[(b)]	Current Experimental Limit[(c)]
$b \to s\ell^+\ell^-$	2×10^{-6}–2×10^{-5}	2×10^{-6}–4×10^{-4}	$\lesssim 2\times10^{-4}$
$b \to s\nu\bar{\nu}$	1×10^{-6}–7×10^{-5}	10^{-6}–3×10^{-3}	not available
$b \to s\gamma$	8×10^{-5}–2×10^{-4}	10^{-6}–2×10^{-3}	$\lesssim 2\times10^{-3}$
$b \to sg^*$	1–3%	.5–15%	not available

[(a)]For three-generation, ranges shown correspond to $m_t = 50$–200 GeV.
[(b)]For four-generation, ranges shown are obtained by taking 40 GeV $\lesssim m_t \lesssim m_W$, $|v_{t'}| \lesssim .3$ and $150 \lesssim m_{t'} \lesssim 500$ GeV.
[(c)]See Ref. 15.

4. B$\overline{\text{B}}$ Mixing[11]

Recently ARGUS has reported evidence for a large mixing in $B_d\overline{B}_d$ with the mixing parameter[12] $r_d = .21 \pm .08$. This has been translated by many authors as a lower bound[13,14] on m_t: $m_t \gtrsim 50$ GeV. The wide range in the values of the pseudoscalar decay constants given in the literature (50–600 MeV) do not allow a more restrictive bound on m_t. Some of the authors[13,14] have also noted that, due to various uncertainties, the ARGUS result does not necessarily mean that the SM with three-generation requires that r_s be maximal. While that may be true, one should note that the allowed parameter space will account for a sizable r_d, but a nonmaximal r_s is rather small.

In particular, we at UCLA have calculated f_B and the B-parameter, using lattice techniques, as part of our long-term program of calculating weak amplitudes on the lattice. We find:[16]

$$f_{cd} = 136 \pm 24 \pm 25 \text{ MeV} ,$$

$$f_{cs} = 196 \pm 17 \pm 36 \text{ MeV} ,$$

$$f_{bd} = 90 \pm 16 \pm 16 \text{ MeV} ,$$

$$f_{bd} = 162 \pm 14 \pm 28 \text{ MeV} ,$$

using the convention that $f_\pi = 132$ MeV. We also find[16] $B_{LL}^{latt} \simeq .80 \pm .17 \pm .22$. We note that B_{LL}^{latt} is the counterpart of the B-parameter whose departure from unity would be a measure of deviation from vacuum saturation. We thus find vacuum saturation to be a very good approximation for both $b\bar{s}$ and $b\bar{d}$ systems.

Taking $(Bf_B^2)_s > (Bf_B^2)_d$ as indicated by the lattice and for a given lower bound on $|V_{ub}/V_{cb}|$, we can deduce the SM (three-generation) constraint on the r_s-r_d plane, irrespective of m_t. We can now superimpose on this the ARGUS result. Even if we conservatively take $r_d = .08$, which is the 90% C.L. lower limit of the ARGUS result, the SM requires $r_s > .7$. For purposes of illustration, suppose we also include the MARK II bound in r_s–r_d plane deduced from data taken at PEP.[17] The MARK II curves are sensitive to a choice of s/u ratio. If we take $s/u = 0.2/0.4$, then even with $r_d = .08$, the overlap with the three-generation SM is very small indeed.[11] (See Fig. 5.)

On extension of the SM to include a fourth family, the situation changes drastically.[11] One can easily accommodate a large r_d with modest values of $m_t \sim 25$-100 GeV. A more significant impact of the fourth family is that r_s need not be maximal due to the unknown values of the new mixing angles,

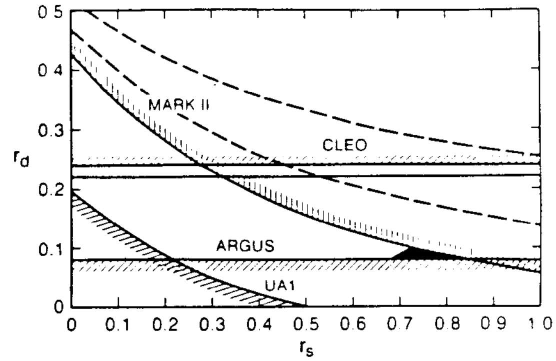

Fig. 5. Current experimental constraints on r_d and r_s. All results plotted are 90% C.L. limits. The ARGUS central value is just below the CLEO limit. The two dashed curves for MARK II are for values $(p_d, p_s) = (0.375, 0.15)$ and $(0.35, 0.1)$, respectively [and (0.4, 0.2) for the solid curve]. The shaded region represents the overlap between three-generation SM and the experimental constraints if you assume a solid curve for MARK II.

$V_{t'b}$, $V_{t'd}$, $V_{t's}$ .... One should note that this is nontrivial because other simple extensions of the three-generation SM, such as supersymmetry, L-R symmetry, ..., while alleviating the need for a heavy m_t, to not change the need[18] for a large r_s/r_d.

Concluding, then, while at the moment four generations are not required, reliable experimental information on $B_S\,\overline{B}_S$ mixing could be vital to settle the question. Such information is very difficult to obtain from continuum study of $B\,\overline{B}$ mixing as in the UAI[19] or MARK II[17] type of experiments as their interpretation sensitively depends on the assumed value for s/u. Thus, a direct measurement of $B_S\,\overline{B}_S$ mixing, by sitting on Υ (SS), would be very helpful for mixing, as well as for other B_S physics.

5. Summary

Rare (loop) decays of b's are very important as a test of the SM and as a probe of the mass scales and mixing angles of the heavy quarks. One difficulty in using the rare modes is that theoretical calculations involving BR of specific exclusive modes are not reliable. A more reliable calculational framework (such as the lattice) would be helpful.

We have given our preliminary results[16] of the decay constants and matrix element for the B's. Using these [specifically, $f_B^2\,B$], together with the ARGUS 90% C.L. lower bound on r_d, yields (independent of m_t) that the SM with three generations requires $r_s \sim 1$. That may be running in conflict with experiment, indicating the need for a fourth family. More reliable experimental information on r_s, e.g., via direct study of B_S mixing by sitting on Υ (SS) is urged.

References

1. See the talks by R. Cousins and W. Morse in the Proc. of the First Int. Symp. on the Fourth Family of Quarks and Leptons, D. Cline and A. Soni, eds.
2. Physics motivation for a B-factory has been emphasized in several papers. See, for example, D. Cline and A. Soni in Proc. of the Electroweak Session of Moriond (1987); A. Amaldi and G. Coignet, LAPP-EXP-86-71; R. Eichler, T. Nakada, K. R. Schubert and K. Willi, SIN-PR-86-13.
3. W.-S. Hou, A. Soni and R. S. Willey, Phys. Rev. Lett. 58, 1608 (1987).

4. J. Ellis and J. S. Hagelin, Nucl. Phys. **B217**, 189 (1983); U. Türke, Phys. Lett. **168B**, 296 (1986); see also the contributions of W. Marciano and E. Paschios in the Proc. of the Fourth Family Symposium, *ibid.*
5. N. G. Deshpande, G. Eilam, A. Soni and G. L. Kane, Phys. Rev. Lett. **57**, 1106 (1986); W.-S. Hou, R. S. Willey and A. Soni, see Ref. 3; J. O'Donnell, Phys. Lett. **175B**, 369 (1986).
6. S. Bertolini, F. Borzumati and A. Masiero, Phys. Rev. Lett. **59**, 180 (1987); N. G. Deshpande, P. Lo, J. Trampetic, G. Eilam and P. Singer, Phys. Rev. Lett. **59**, 184 (1987). W.-S. Hou, A. Soni and H. Steger, Phys. Lett. **192B**, 441 (1987); J. L. Hewett, Phys. Lett. **193B**, 327 (1987); B. Grinstein, R. Springer and M. Wise, to be published.
7. See the talk by Marciano in the Proc. of the Fourth Family Symposium, *ibid.*
8. The QCD corrections to this decay mode have been reexamined by Grinstein, Springer and Wise, see Ref. 6.
9. W.-S. Hou, A. Soni and H. Steger, Phys. Rev. Lett. **59**, 1521 (1987).
10. For earlier works, see M. Bander, D. Silverman and A. Soni, Phys. Rev. Lett. **43**, 242 (1979); B. Guberina, R. D. Peccei and R. Rückl, Phys. Lett. **90B**, 169 (1980); B. Guberina, Fizika **16**, 49 (1984); G. Eilam, Phys. Rev. Lett. **49**, 1478 (1982).
11. We follow the discussion of W.-S. Hou and A. Soni, Phys. Lett. **196B**, 92 (1987).
12. ARGUS Collaboration, H. Albrecht et al., Phys. Lett. **192B**, 245 (1987).
13. See, for example, J. Ellis, J. S. Hagelin and S. Rudaz, Phys. Lett. **192B**, 453 (1987); L. L. Chau and W. Y. Yeung, preprint (1987); I. I. Bigi and A. Sanda, Phys. Lett. **194B**, 307 (1987); V. Bayer, T. Nam, D. V. Nanopoulos and R. J. N. Phillips, Phys. Lett. **194B**, 312 (1987); A. Datta, E. A. Paschos and U. Turke, DO-TH-8719 (Dortmund preprint); H. Harari, Y. Nir, Phys. Lett. **195B**, 586 (1987). J. F. Donoghue, T. Nakada, E. A. Paschos and D. Wyler, Phys. Lett. **195B**, 285 (1987).
14. See the review talk by G. Altarelli, Int. Europhysics Conf., Uppsala, Sweden, 1987.
15. See the talks by N. Horowitz in the Proc. of the Fourth Family Sym., *ibid.;* see also, K. Berkelman, these Proceedings.
16. C. Bernard, T. Draper, G. Hockney and A. Soni, UCLA/87/TEP/28, in preparation.
17. MARK II Collaboration, T. Schaad et al., Phys. Lett. **B160**, 188 (1985).
18. A. Datta, E. A. Paschos and U. Turke, see Ref. 13.
19. UAI Collaboration, C. Albajar et al., Phys. Lett. **B186**, 247 (1987).

A SHORT VADEMECUM ON CP VIOLATION IN HEAVY FLAVOR DECAYS*

I. I. BIGI‡

Stanford Linear Accelerator Center, Stanford University, Stanford, California 94305

Abstract

A short introduction into the phenomenology of CP asymmetries in beauty (and D^0) decays is given. Different experimental environments are briefly compared and some semi-quantitative estimates listed.

1. Introduction

For more than 20 years now we have known CP invariance to be broken in nature; the profound importance of this discovery was immediately realized. However, no real understanding of this phenomenon has emerged yet; one cannot even claim to possess a unique parametrization. I believe that this embarrassing situation will not be overcome unless CP violation can be studied in a dynamical system that is quite different from neutral kaons.

When one relies on the minimal model for implementing CP violation, namely the KM ansatz, one is lead to a quite unequivocal answer to the question where to look for CP violation: the decays of beauty hadrons are the process of choice.

In the KM ansatz it is the interplay of three quark families that makes CP violation observable. Therefore, it is highly advantageous to study beauty decays: b-quarks belong to the third family, yet have to decay into members of the lower families.

This general result can easily be made more specific. The requirement that the KM matrix be unitary yields, among others, the following two relations:

$$V(ud)V^*(td) + V(us)V^*(ts) + V(ub)V^*(tb) = 0 \tag{1}$$

$$V(cd)V^*(td) + V(cs)V^*(ts) + V(cb)V^*(tb) = 0 \tag{2}$$

which simplify considerably when terms of higher order in the small KM angles are ignored ($\lambda = \sin\theta_c$):

$$V^*(td) + \lambda V^*(ts) + V(ub) \simeq 0 \tag{3}$$

$$-\lambda V^*(td) + V^*(ts) + V(cb) \simeq 0 \tag{4}$$

As first emphasized by Bjorken, Eqs. (3) and (4) are triangle relations that are accessible to intuitive arguments: Eq. (4) describes a "squashed" triangle with $V(td) = -V(cb) + \mathcal{O}(\lambda^2)$. Equation (3) can then be reexpressed as follows:

$$V^*(td) + V(ub) = A\,\lambda^3 \tag{5}$$

with $V(cb) \simeq A\,\lambda^2$ in the Wolfenstein notation. According to the data $-\ \tau_B$, $B^\circ - \overline{B}^\circ$ mixing and $B \to p\bar{p}\,\pi(\pi)$ $- |V(td)|, V(ub)| \sim \mathcal{O}(\lambda^3)$; the angles in this triangle are therefore not particularly small, i.e., $V(ub)$ and $V(td)$ carry sizeable complex phases. They can be probed in B–decays with high sensitivity: this is obviously true for $V(ub)$; it is also correct for $V(td)$ since it is a crucial element in $B_d - \overline{B}_d$ mixing. Accordingly, we can be confident that somewhere in B-decays large CP asymmetries, say $\sim \mathcal{O}(10\%)$, exist.

The next question is obvious: In which specific B–decays does one have the best chance to uncover such CP asymmetries? At present it would be quite premature to attempt a quantitative answer; after all, very few $B_{u,d}$ branching ratios are known, the lifetimes of neutral and charged B–mesons have not been determined separately and the actual value of the top mass is not known. Therefore, we will present semi-quantitative scenarios that can successively be refined when more data and a better theoretical understanding become available.

One basic classification should be made right from the start: one compares the evolution of decay rates in proper time

$$\text{rate}\big(B(t) \to f\big) = e^{-\Gamma t}\,G \leftrightarrow\ \text{rate}\big(\overline{B}(t) \to \bar{f}\big) = e^{-\Gamma t}\overline{G} \tag{6}$$

$G/\overline{G} \neq 1$ establishes CP violation. Such a difference can be realized in two quite distinct ways:

$$\frac{d}{dt}\,\frac{G}{\overline{G}} \equiv 0 \tag{7}$$

$$\frac{d}{dt}\,\frac{G}{\overline{G}} \neq 0 \quad . \tag{8}$$

When f is flavor-specific, i.e., $B(0) \to f \not\leftarrow \overline{B}(0)$, the first situation, Eq. (7), applies. This is always the case when final state interactions (hereafter referred to as FSI) are essential for making a CP asymmetry observable. When f is common to both B and $\overline{B}$–decays—possible only for neutral B–decays—then the second scenario, Eq. (8), applies which, as we will see, involves $B^\circ - \overline{B}^\circ$ mixing.

I will discuss these two cases where I will concentrate on the underlying concepts rather than on the technicalities and details; these can be found in the literature.[1]

II. $B^\circ - \overline{B}^\circ$ Mixing and CP Asymmetries

The Pais–Treiman formalism for mixing is applied in a straightforward way:

$$|\overline{B}^\circ(t)\rangle = g_+(t)|B^\circ\rangle_0 + \frac{q}{p}\,g_-(t)\,|\overline{B}^\circ\rangle_0 \tag{9}$$

$$|\overline{B}^\circ(t)\rangle = \frac{p}{q}\,g_-(t)|\overline{B}^\circ\rangle_0 + g_+(t)\,|\overline{B}^\circ\rangle_0 \tag{10}$$

$$\begin{gathered} g_\pm(t) = \frac{1}{2}\,e^{-\frac{1}{2}\Gamma_1 t}e^{im_1 t}\big(1 \pm e^{-\frac{1}{2}\Delta\Gamma t}e^{i\Delta m t}\big) \\ \Delta\Gamma = \Gamma_2 - \Gamma_1\,, \Delta m = m_2 - m_1 \quad . \end{gathered} \tag{11}$$

The phase of the quantity q/p depends on the phase convention adopted for $|\overline{B}^\circ\rangle_0$; yet $|q/p|$ does not and therefore represents an observable:

$$\begin{gathered} \left|\frac{q}{p}\right| = 1 + \frac{1}{2}\,F\,\sin\phi(\Delta S = 2) \ , \\ F \simeq \left|\frac{\Gamma_{12}}{M_{12}}\right| \qquad \phi(\Delta B = 2) = \arg\frac{M_{12}}{\Gamma_{12}} \quad . \end{gathered} \tag{12}$$

A deviation of $|q/p|$ from unity represents a violation of CP invariance.

Semi-leptonic B°–decays which are flavor-specific allow in principle to search for the corresponding CP asymmetry: the notation

$$r = \frac{\Gamma(B^\circ \to \ell^- X)}{\Gamma(\overline{B}^\circ \to \ell^+ X)} \quad , \quad \bar{r} = \frac{\Gamma(\overline{B}^\circ \to \ell^+ X)}{\Gamma(B^\circ \to \ell^- X)} \tag{13}$$

refers to time-integrated rates where $r, \bar{r} \neq 0$ signals the occurrence of mixing. One then finds

$$a_{SL} = \frac{r - \bar{r}}{r + \bar{r}} = \frac{1 - |\frac{p}{q}|^4}{1 + |\frac{p}{q}|^4} \quad . \tag{14}$$

*Work supported by the Department of Energy, contract DE–AC03–76SF00515.

‡Heisenberg Fellow.

Unfortunately one predicts tiny asymmetries in the KM ansatz (with three families):

$$a_{SL}(B_d) \lesssim 10^{-3} \tag{15}$$

$$a_{SL}(B_s) \lesssim 10^{-4} \quad . \tag{16}$$

The smallness of these asymmetries is readily understood: One estimates

$$F \simeq \frac{\Delta\Gamma}{\Delta m} \sim \mathcal{O}\left(\frac{m_b^2}{m_t^2}\right) \ll 1 \tag{17}$$

in contrast to the K° case where $F(K^\circ) \simeq 1$ holds and

$$\phi(\Delta B = 2) \sim \mathcal{O}\left(\frac{m_c^2}{m_b^2}\right) \ll 1 \tag{18}$$

not dissimilar from the K° case.

To observe the kind of CP asymmetry as expressed by $\phi(\Delta B = 2)$, Eq. (12), appears therefore to be a rather hopeless enterprise.

This should, however, not drive us into despair about ever observing CP violation in B–decays: there is a second scenario for observable CP violation as characterized by Eq. (8). It applies when a final state f can be reached in both B° and $\overline{B}^\circ$–decays. There are two types of final states than can satisfy this requirement, namely

(i) CP eigenstates like $B^\circ \to \psi K_s, D_s\overline{D}_s, D\overline{D}, \pi\pi \leftarrow \overline{B}^\circ$.

(ii) Non-CP eigenstates like $B^\circ \to D^\pm\pi^\mp \leftarrow \overline{B}^\circ$.

The same basic formalism applies in both cases. For this reason, I will restrict myself to discussing CP eigenstates only: our predictions are more reliable there and the physics involved more transparent.

A little theorem can help to illustrate the situation: Let B_{neut} denote any combination of B° and $\overline{B}^\circ$–mesons and f a CP eigenstate of definite CP parity. Finding the (proper) time dependence of the decay rate $B_{neut} \to f$ to be different from a *single, pure* exponential, i.e.,

$$\frac{d}{dt} e^{\Gamma t}\, \text{rate}\big(B_{neut}(t) \to f\big) \neq 0 \text{ for all } \Gamma \tag{19}$$

amounts to an *observation of CP violation*. The proof is very elementary and can be found elsewhere.

One can be even more specific and show that the most general time evolution is given by four terms:

$$\begin{aligned}\text{rate}\big(B_{neut}(t) \to f\big) \alpha e^{-\Gamma t}\Big(1 + Ae^{-\Delta\Gamma t} \\ + Be^{-\frac{1}{2}\Delta\Gamma t}\cos(\Delta m t) + Ce^{-\frac{1}{2}\Delta\Gamma t}\sin(\Delta m t)\Big) \quad .\end{aligned} \tag{20}$$

Since one estimates $\Delta\Gamma \ll \Gamma$, $|q/p| \simeq 1$ one can simplify Eq. (20) considerably

$$\text{rate}\big(B_{neut}(t) \to f\big) \alpha\, e^{-\Gamma t}\left(1 + \frac{N - \overline{N}}{N + \overline{N}}\, Im\, \frac{q}{p}\, \bar{\rho}_f \sin\Delta m t\right) \tag{21}$$

where $\bar{\rho}_f = \text{Ampl.}(\overline{B} \to f)/\text{Ampl.}(B \to f); N[\overline{N}]$ denotes the number of $B^\circ[\overline{B}^\circ]$–mesons present at $t = 0$.

Equation (21) contains three crucial elements:

(i) Im $\frac{q}{p}\, \bar{\rho}_f$: It is this quantity that is intrinsically connected with CP violation which suggests the following notation:

$$\frac{q}{p}\, \bar{\rho}_f \equiv \left|\frac{q}{p}\, \bar{\rho}_f\right| e^{i\phi(\Delta B = 1\&2)} \quad . \tag{22}$$

The phase $\phi(\Delta B = 1\&2)$ represents the strength of CP violation and combines the effects of the $\Delta B = 2$ mixing process—q/p—and the $\Delta B = 1$ decay $-\bar{\rho}_f$.

(ii) sin$\Delta m t$: This factor explicitly exhibits the need for mixing to occur—$\Delta m \neq 0$—to have an observable CP asymmetry. Yet it should be noted that its dependence on Δm is quite different from the time-integrated quantity r usually employed to express mixing:

$$r = \frac{\Gamma(B^\circ \to \ell^- X)}{\Gamma(B^\circ \to \ell^+ X)} \simeq \frac{x^2}{2 + x^2}\ , \ x = \frac{\Delta m}{\Gamma} \quad . \tag{23}$$

(iii) $N - \overline{N}$: If one starts from an equal population of B° and $\overline{B}^\circ$ in the sample under study (and if as expected $\Delta\Gamma \ll \Gamma$) no asymmetry can emerge. The reason for that is quite obvious: since these final states are common to B° as well as $\overline{B}^\circ$–decays, they can by themselves not reveal whether they came from a B° or a $\overline{B}^\circ$; thus no CP asymmetry can be defined.

These quantities will now be discussed in more detail:

ad(iii) The required flavor tagging can be provided by Nature, i.e., through a production asymmetry like the forward-backward asymmetry in $e^+e^- \to b\bar{b}$ or through associated production or leading particle effects in hadronic collisions; or it can be imposed by human intervention, i.e., by identifying the flavor of the hadron that was produced in conjunction with the neutral B–meson whose decay one is studying.

ad(ii) The time dependence of the signal is quite unique and striking. Therefore, one has to place a high premium on the ability to resolve the time evolution. If that cannot be achieved, i.e., if one can observe only time-integrated rates, one has to keep three complications in mind:

- Since

$$\int_0^\infty dt\ \text{rate}\big(B(t) \to f\big) \alpha \frac{x}{1 + x^2}\ \text{Im}\frac{q}{p}\bar{\rho}_f \tag{24}$$

one encounters large suppression for large mixing, i.e., $x \gg 1$.

- The reaction

$$e^+e^- \to \Upsilon(4s) \to B\overline{B}$$

produces the $B\overline{B}$ pair in a configuration that is *odd* under charge conjugation. Then one obtains

$$\begin{aligned}\int\!\!\int dt d\bar{t} \Big\{ \text{rate}\big(B^\circ(t)\overline{B}^\circ(\bar{t}) \to (\ell^+X)f\big) \\ - \text{rate}\big(B^\circ(t)\overline{B}^\circ(\bar{t}) \to (\ell^-X)f\big)\Big\} \alpha \\ \int\!\!\int dt d\bar{t}\ e^{-\Gamma(t+\bar{t})} \sin\Delta m(t - \bar{t}) \text{Im}\,\frac{q}{p}\,\bar{\rho}_f = 0 \quad ,\end{aligned} \tag{25}$$

i.e., no asymmetry can be observed.

- In

$$e^+e^- \to B^\circ\overline{B}^{\circ *} + h.c. \to B^\circ\overline{B}^\circ\gamma \tag{26}$$

one finds after complete time integration a factor $2x/(1 + x^2)^2$ in the asymmetry which acts like a $1/x^3$ suppression for $x \gg 1$.

A value $x = \Delta m/\Gamma \sim 1$—similar to the ARGUS findings on $B_d - \overline{B}_d$ mixing—is quite optimal for these studies.

ad(i) As already mentioned one predicts $|q/p| \simeq 1$ with a high degree of confidence. For decays like $B \to \psi K_s$ where only one isospin amplitude contributes $|\bar{\rho}_f| = 1$ holds. In those cases $q/p\ \bar{\rho}_f$ represents a unit vector in the complex plane whose phase — $\phi(\Delta B = 1\&2)$ — is given in terms of KM parameters.

Decays like $B_s \to \psi\phi\, , D_s\overline{D}_s$ which involve $(\bar{b}s) \to \bar{c}c\bar{s}s$ transitions on the quark level are expected to exhibit relatively small CP asymmetries:

$$\text{Im}\ \frac{q}{p}\ \bar{\rho}_f(\bar{b}s \to \bar{c}c\bar{s}s) \sim \mathcal{O}(\lambda^2) \lesssim \text{few}\ \% \quad . \tag{27}$$

This is not surprising at all, since on the leading level only quarks of the second and third families contribute. More specifically, this situation is described by the triangle of Eq. (4).

The quark level transitions $(\bar{b}d) \to \bar{c}c\bar{s}d, (\bar{b}d) \to \bar{u}u\bar{d}d$ and $(\bar{b}s) \to \bar{s}u\bar{u}s$, on the other hand, probe the Bjorken triangle, Eq. (5). More precisely, for the decays

$$B_d \to \psi K_s \, , B_d \to \pi^+\pi^- \, , B_s \to K^+K^-$$

one finds

$$Im \, \frac{q}{p} \, \bar{\rho}_f \sim \sin 2\varphi_1 \quad , \sim -\sin 2\varphi_2 \quad , \quad \sim \sin 2\varphi_3 \tag{28}$$

where

$$-V(td) = |V(td)| e^{i\varphi_1} \quad , \; V(ub) = |V(ub)| e^{i\varphi_3} \quad . \tag{29}$$

Any violation of Eq. (27) or (28)—like Im $q/p\bar{\rho}_f(\bar{b}s \to \bar{c}c\bar{s}s) \gtrsim 0.1$ or $\varphi_1 + \varphi_2 + \varphi_3 \neq 180°$, i.e., a "nonplanar geometry"—would show the existence of New Physics, most likely a fourth family.

None of the angles $\varphi_i = 1, 2, 3$, has a particular propensity to have a value close to 0° or 90°. Overall one can say (details can be found in the literature):

$$\text{Im} \, \frac{q}{p} \, \bar{\rho}_f \simeq \mathcal{O}(0.1) \tag{30}$$

is quite realistic and even values like

$$\text{Im} \, \frac{q}{p} \, \bar{\rho} \simeq 0.5 \tag{31}$$

though being optimistic are attainable.

Since the branching ratios for the most promising modes are nothing to brag about—for instance,

$$BR(B_d \to \psi K_s) \sim 5 \times 10^{-4}$$

$$BR(B_d \to \pi^+\pi^-) \sim \mathcal{O}(10^{-5})$$

is expected theoretically—the question arises quite naturally whether one can gain in statistics by analyzing inclusive decays without jeopardizing the signal, i.e., the CP asymmetry. The answer is yes—but only under certain carefully maintained circumstances. For the sign of the asymmetry depends—among other things—on the CP parity of the final state. Therefore,

$$\text{Asymm.}(B \to \psi K_s) = -\text{Asymm.}(B \to \psi K_L) \quad . \tag{32}$$

Accordingly

$$\text{Asymm.}(B_d \to \psi X) = 0 \quad . \tag{33}$$

A similar concern has to be addressed in $B^\circ \to p\bar{p}$-decays. For $p\bar{p}$ can form a p- or an s-wave and

$$\text{Asymm.}(B \to [p\bar{p}]_p) = -\text{Asymm.}(B \to [p\bar{p}]_s) \quad . \tag{34}$$

For the same reason one can state quite generally that adding a π to a final state will flip the sign of the CP asymmetry since CP $|\pi^\circ\rangle = -|\pi^\circ\rangle$.

There is one meaningful test of CP invariance that can be performed in $e^+e^- \to \Upsilon(4s) \to B\overline{B}$ even without any capability to resolve decay vertices: one searches for the reaction

$$e^+e^- \to \Upsilon(4s) \to B^\circ \overline{B}^\circ \to f_1 f_2$$

where f_1, f_2 denote two CP eigenstates of the *same* CP parity. A single event of this type (in principle) establishes CP violation. For the initial state is CP even, the final state CP odd:

$$\text{CP}[\Upsilon(4s)] = +1 \quad ; \quad \text{CP}[f_1 f_2] = \text{CP}[f_1]\text{CP}[f_2](-1)^\ell = -1 \tag{35}$$

since $B\overline{B}$ are produced in a p-wave.

Quantitatively one finds

$$\begin{aligned} &BR(B^\circ \overline{B}^\circ \, |_{\Upsilon(4s)} \to f_1 f_2) \sim F \; BR(B \to f_1) BR(B \to f_2) \\ &F = \frac{x^2}{1+x^2} \left(2 \, \text{Im} \, \frac{q}{p} \, \bar{\rho}_{f_1} \right) \left(2 \, \text{Im} \, \frac{q}{p} \, \bar{\rho}_{f_2} \right) \sim \frac{1}{4} - 1 \quad . \end{aligned} \tag{36}$$

As a final remark: The same phenomenology can be applied to D°-decays like $D^\circ \to K^+K^-$:

$$\text{rate}(D^\circ(t) \to K^+K^-) \alpha \, e^{-\Gamma t} \left(1 - \sin \Delta m t \; \text{Im} \, \frac{q}{p} \, \bar{\rho}_f \right) \quad , \tag{37}$$

$$\text{rate}(\overline{D}^\circ(t) \to K^+K^-) \alpha \, e^{-\Gamma t} \left(1 + \sin \Delta m t \; \text{Im} \, \frac{q}{p} \, \bar{\rho}_f \right) \quad . \tag{38}$$

Such a study is greatly helped by two very beneficial circumstances:

- The branching ratio is quite decent:

$$BR(D^\circ \to K^+K^-) \sim 0.5\% \quad .$$

- Flavor tagging can effectively be achieved via $D^{*\pm} \to \overset{(-)}{D}\pi^\pm$ decays.

There is of course a double caveat:

(*i*) The Standard Model predicts very little $D^\circ - \overline{D}^\circ$ mixing and no observable CP violation. This makes it a unique hunting ground for New Physics.

(*ii*) The E691 collaboration has placed a very stringent upper bound on $D^\circ - \overline{D}^\circ$ mixing

$$r_D \equiv \frac{\Gamma(D^\circ \to \overline{D}^\circ \to \bar{f})}{\Gamma(D^\circ \to f)} < 0.5\% \quad . \tag{39}$$

Yet one has to keep in mind that

$$r_D \sim \frac{x^2}{2+x^2} \quad . \tag{40}$$

Therefore, $r_D = 0.5\%$ corresponds to $x = \Delta m/\Gamma = 0.1$ and accordingly in this case

$$\text{rate}(D^\circ(t) \to K^+K^-) \alpha \, e^{-\Gamma t} \left(1 - 0.1 \times \frac{t}{\tau_D} \text{Im} \frac{q}{p} \bar{\rho}_f \right) , \tag{41}$$

i.e., *CP asymmetries of order 5–10% are still allowed in principle and should be searched for.*

III. Final State Interactions and CP Violation

When two different amplitudes contribute to the decay of a bottom hadron B into a final state f, one writes for the matrix element

$$\begin{aligned} M_f &= \langle f | \mathcal{L}(\Delta B = 1) | \rangle \\ &= \langle f | \mathcal{L}_1 | B \rangle + \langle f | \mathcal{L}_2 | B \rangle \\ &= g_1 M_1 e^{i\alpha_1} + g_{2,2} \, e^{i\alpha_2} \end{aligned} \tag{42}$$

where M_1, M_2 denote the matrix elements for the weak transition operators $\mathcal{L}_1, \mathcal{L}_2$ with the KM parameters g_1, g_2 and the strong (or electromagnetic) phase shifts α_1, α_2 factored out. For the CP conjugate decay $\overline{B} \to \bar{f}$ one then finds

$$\begin{aligned} \overline{M}_f &= \langle \bar{f} \mid \mathcal{L}(\Delta B = 1) \mid \overline{B} \rangle \\ &= g_1^* M_1 e^{i\alpha_1} + g_2^* M_2 e^{i\alpha_2} \quad . \end{aligned} \tag{43}$$

The same phase shifts α_1, α_2 (instead of $-\alpha_1, -\alpha_2$) have been written down in Eq. 43 since CP invariance is obeyed by the strong and electromagnetic forces. Comparing Eq. 42 with Eq. 43 one obtains

$$\Gamma(B \to f) - \Gamma(\overline{B} \to \bar{f}) \propto \; \text{Im} \; g_1^* g_2 \sin(a_1 - a_2) M_1 M_2 \quad . \tag{44}$$

Thus two conditions have to be met simultaneously for such an asymmetry to show up:

(α) The weak couplings g_1 and g_2 have to possess a relative complex phase; therefore small KM angles have to be involved.

(β) Nontrivial phase shifts $\alpha_1 \neq \alpha_2$ have to be generated from the strong (or electromagnetic) forces.

Condition (β) does not, in principle, pose a severe restriction; in practice it introduces considerable uncertainties into numerical predictions. An interesting scenario—in my judgment—is provided by invoking Penguin contributions.[2] The phase shift $\alpha_1 - \alpha_2 \neq 0$ is produced by the loop diagram with charm as the internal quark—which does *not* yield a local, though maybe a short-distance operator. Doing detailed calculation one finds

$$BR(B \to K^{\pm}\pi^{\mp}) \sim \mathcal{O}(10^{-5})$$

$$\frac{\Gamma(B^{\circ} \to K^{+}\pi^{-}) - \Gamma(B^{\circ} \to K^{-}\pi^{+})}{\Gamma(B^{\circ} \to K^{+}\pi^{-}) + \Gamma(B^{\circ} \to K^{-}\pi^{+})} \sim 1 - 10\% \quad . \tag{45}$$

The nice feature of this decay mode is that it is flavor-specific: $K^{+}\pi^{-}$ can come only from a B° whereas $K^{-}\pi^{+}$ is necessarily produced in a $\overline{B}^{\circ}$-decay.

IV. Conclusions

There is one basic unequivocal statement: The KM scheme of implementing CP violation leads to relatively large CP asymmetries in beauty decays. Theoretical uncertainties enter only into questions on the exact size of such asymmetries and on the best modes to search for them.

Improved experimental information on branching ratios, the top mass and on $V(ub)$ will help in an essential way to refine our predictions or expectations.

When CP violation becomes observable due to $B^{\circ} - \overline{B}^{\circ}$ mixing, the following rather general statements can be made:

(+) Large asymmetries of order 10% or more are expected.

(+) The predictions are relatively reliable.

(+) The very special dependence on proper time that is introduced by mixing should provide a striking signature in searches for asymmetries.

(−) Typically one has to identify exclusive modes; otherwise substantial cancellations can occur as far as the CP asymmetries are concerned. In particular, one does not want to lose π°-mesons.

(−) Flavor tagging is essential.

(−) The reaction

$$e^{+}e^{-} \to \Upsilon(4s) \to B\overline{B}$$

is quite ill-suited for any such analysis as long as no information on the B-decay vertices is available.

The scorecard looks quite different when it is the final state interactions that make CP violation observable:

(+) No flavor tagging is required.

(+) One can study it also in $\Upsilon(4s) \to B\overline{B}$.

(−) One has to rely on number counting since no special time dependence is introduced.

(−) The branching ratios are quite low and it is very hard to see how such a CP asymmetry could ever reach or exceed the 10% level.

(−) The predictions are less than compelling or reliable.

References

1. For an up-to-date review see, I. I. Bigi, V. A. Khoze, N. G. Uraltsev and A. I. Sanda, *The Question of CP Noninvariance—as seen through the Eyes of Neutral Beauty,* SLAC-PUB-4476.

2. M. Bander, S. Silverman and A. Soni, Phys. Rev. Lett. 43 (1979), 242; Ref. 1.

THE UCLA e^+e^- LINEAR COLLIDER $\overline{\text{B}}$B FACTORY PROJECT

DAVID B. CLINE

Department of Physics, University of California, Los Angeles, CA 90024

Abstract

We describe the conceptual design of a linear collider $\overline{B}B$-factory being designed to reach a luminosity of 10^{34} cm^{-2} sec^{-1}. The major uncertainties and the proposed R&D program are described. Recent progress in the development of cold e^+ sources and plasma lens focusing is described.

1. Introduction

The study of the b-quark system promises to provide new insights into fundamental aspects of fundamental particle physics. This includes the origin of CP violation, flavor changing weak neutral current and deviations from the standard model. In order to accomplish these goals, very large numbers of clean $\overline{B}B$ events are required. It is now assumed that 10^8 $\overline{B}B$ pairs are the minimal number required.

Circular colliders can reach a luminosity of $\sim 10^{33}$ cm^{-2} sec^{-1} at the γ(4s) resonance providing $\sim 5\times10^6$ $\overline{B}B$/year. It is possible that e^+e^- linear colliders can reach luminosity in excess of 10^{34} cm^{-2} sec^{-1} and may provide 10^8 $\overline{B}B$/year in a very clean environment. There are advantages of linear colliders over circular colliders, such as the possibility of a very small beam pipe to use vertex detectors.

For this reason, a study of a high luminosity e^+e^- $\overline{B}B$-factory using a linear collider has been underway at UCLA for some time.[1] The design presented here is in contrast to the superconducting linear collider by Amaldi and Coignet.[2] A progress report on this design study.

2. Physics Goals for a $\overline{\text{B}}$B Factory

Following the report of Cline and Soni, we give an introduction to the need for a $\overline{B}B$-factory.[3] In the past several years intense kaon factories have become available, making it feasible to measure rare branching ratios down to the impressive level of 10^{-11}. The need for a dedicated B-factory may therefore hardly appear necessary, but we wish to point out that the B-system is extremely rich and its rare decays have a lot of potential for excellent physics.

For one thing, B-decays are far cleaner from QCD corrections compared to K-decays. Indeed, there are two well-known tests of strong corrections to weak amplitudes; namely, the lifetime difference between charged and neutral mesons and the semileptonic branching ratio. Experimentally, it is already known that $0.5 \lesssim \tau_{B^+}/\tau_{B^0} \lesssim 2$, which is a far cry from the factor of 450 for the kaon case. Furthermore, the semileptonic branching ratio for B's is also roughly in accord with naive quark counting. These are important indications that effects of QCD corrections are not that important on b-decays, at least in so far as tree graph decays are concerned. Presumably, the fact the $m_b^2 \gg m_s^2$ is at least in part responsible for the smallness of QCD corrections as a manifestation of the asymptotically free nature of QCD.

In the realm of loop decays, the u-quark in the flavor changing loop $b \to s$ transition essentially decouples because the u-quark has such a small mass (compared to c- and t-quarks) and also because the CKM angle $V_{ub} \ll V_{cb} \ll V_{tb}$. This decoupling of the light u-quark should make loop decays of b-quarks short (and not long) distance dominated, and therefore much more readily amenable to perturbative analysis.

Freedom from QCD corrections can be a very important consideration for electroweak experiments as the computational ability of the theoretical community in the realm of small momentum transfers is at such an abysmal state. A case in point is the situation regarding the CP violating parameter ϵ'/ϵ in neutral kaon decays. As of now, there is no theoretical calculational scheme that can reliably calculate this quantity. As a result, the heroic experimental efforts which are now on the verge of measuring this quantity with an impressive accuracy of one part in a thousand *may* tragically fail to have an impact on the SM unless the calculational situation improves.

Loop decays of b also have significantly larger BR's than the corresponding kaon decays. This happens as loop decays are often driven by the heaviest (virtual) quark in the loop, i.e., the top quark. Then the ratio of BR for $b \to s$ versus $s \to d$ transitions becomes:

$$|V_{ts}^*V_{tb}/V_{cb}|^2/|V_{td}^*V_{ts}/V_{us}|^2 \simeq \lambda^{-8} \simeq 10^5 \quad .$$

Indeed BF $(B \to K\nu\overline{\nu}) \sim (1-70)\times10^{-6}$ whereas for BR $(K \to \pi\nu\overline{\nu}) \simeq (1-3)\times10^{-10}$. Thus, loop decays of b may not be that rare and they provide an excellent probe for the short-distance structure of the theory. These probes are the analogues of the precision tests such as the $(g-2)$ of the muon, except that in b-decays they are more powerful as they test the full non-Abelian gauge theory structure, including non-Abelian coupling and the symmetry breaking mechanism of the SM.

Being a member of the third family, the b-quark is also likely to be much more sensitive to the parameters of the fourth generation than the s-quark.

As $m_B^2 \gg m_K^2$, B has a lot more final states available to it than the K. This has the important effect that restrictions imposed by the CPT theorem get watered down compared to the case in kaons in so far as tests of CP invariance are concerned. Thus, CPT plus strong interactions selection rules require $\text{BR}(K^+ \to \pi^+\pi^\circ) = \text{BR}(K^- \to \pi^-\pi^\circ)$ so that two-body decays of $K^\pm$ cannot be used for testing CP nonconservation. The large mass of the B makes it available to many more final states so that in contrast, e.g.,

$$\text{BR}(B \to K\pi) - \text{BR}(\overline{B} \to \overline{K}\overline{\pi})$$

is a perfectly viable and indeed an interesting test of CP invariance.

Finally, we take the opportunity to reiterate what has been repeatedly emphasized in the literature: b-decays offer the only hope for observable CP violating effects outside of the neutral kaon system, at least if the SM with three generations is the correct explanation for the observed CP violation. Analysis of the potential signatures strongly suggest that successful tests of CP would require $\gtrsim 10^8$ clean $B\overline{B}$ pairs in an e^+e^- environment. Such fluxes seem difficult, if not impossible, to attain at circular machines and, therefore, a dedicated linear collider B-factory would be very highly desirable.

3. The Maximum Luminosity: Limits

There are three major constraints to the maximum luminosity for a $\overline{B}B$-factory:

1. The Beam Disruption
2. The Energy Spread in the Collision due to Radiation from the Beam-Beam Interaction

1. The Bunch Length of the e^+e^- Beams

Of course, there are many practical limitations such as the high frequency driver, positron source and final focus, but these are problems that might be cured! In order to understand these limitations we first give the basic formulas.

For linear colliders the luminosity is given by

$$L = \frac{N_e + N_e - fH(D)}{\sigma_\perp^2} \quad ,$$

and the disruption parameter

$$D = \frac{14.4\ N_e \pm \sigma_z}{E\sigma_\perp^2} \quad ,$$

where $N_{e\pm}$ = number of particles/event, H = enhancement factor due to pinch, $\sigma_\perp$ = transverse beam size (round beam) and σ_Z is the longitudinal beam size.

For working on the γ(4s), the following limitations on the machine energy spread are:

$$\delta_c \approx \frac{0.12\ E_0 L}{\sigma_z f_b} \cdot \left(\frac{4}{R}\right) ; \qquad R \sim \frac{\sigma_z}{\sigma_y}$$

$$\frac{\sigma_\omega}{\omega} = 0.32 \left[1 + \frac{10}{\langle N_p \rangle}\right]^{1/2} \delta_c \quad .$$

These formulas can be used to determine the limits on the luminosity: we identify four specific limits to reach $L > 10^{34}$ cm^{-2} sec^{-1} below.

(1) Disruption Limit

$$L \propto \frac{1}{\sigma_\perp^2} \quad ;$$

work with small beams. Note, however, that $D \propto \sigma_z/\sigma_\perp^2$ and to keep disruption small, we must reduce σ_z (i.e., $\sigma_z \sim 30\ \mu$m).

(2) $\frac{\sigma_\omega}{\omega}$ Limit

Note that:

$$\left(\frac{\sigma_\omega}{\omega}\right) \propto \delta_{ce} \propto \frac{1}{\sigma_z f_b R} \quad .$$

Therefore, we can increase σ_z, f_b or R. For the High Resolution Mode we can keep σ_z large and increase R as well; $\sigma_z > (0.2\text{–}0.4)$ mm.

(3) f_b Limit

New, High Frequency Drivers may have limited repetition rate: $f \sim 1$ kHz.

(4) Positron Source Limit

Note that $L > 10^{34}$ cm^{-2} sec^{-1} requires $fN_e < 10^{15}$ sec^{-1}. The design of a $\overline{B}B$-factory must include an R&D program to address these limits.

One solution to a high luminosity e^+e^- $\overline{B}B$-factory is given in Table 1. This solution has the general characteristics given in Table 2.

A sketch of the UCLA e^+e^- $\overline{B}B$-factory collider is shown in Fig. 1.

It is possible to envision a very high luminosity mode of operation of this linear collider if we relax the σ_ω/ω requirement giving $> 10^8$ $\overline{B}B$/year off the γ (4s) resonance.

$$L = 4 \times 10^{34}\ \text{cm}^{-2}\ \text{sec}^{-1}$$
$$\sigma_z \simeq 20\ \mu\text{m}$$
$$\sigma_\perp \simeq 0.05\ \mu\text{m}$$
$$D = 22 \quad .$$

These parameters are similar (except for D) to the parameters envisioned for the TLC and CLIC e^+e^- linear collider designs.

Table 1. Parameters of a submicron spot $\overline{B}B$-factory collider.

$$E_0 = (5\text{–}7)\ \text{GeV per beam}$$
$$L = 10^{33}\text{–}4 \times 10^{34}\ \text{cm}^{-2}\ \text{sec}^{-1}$$
$$L = 50\text{–}75\ \text{m}$$
$$b = 4$$
$$\sigma_p/p = 3 \times 10^{-3}$$
$$\sigma_z = (0.4\text{–}0.2)\ \text{mm}$$
$$\eta_b = 0.03$$
$$N = 3 \times 10^{10}$$
$$\sigma_\perp = (0.1\text{–}0.05)\ \mu\text{m}$$
$$D = 36, N_D \simeq 6$$
$$\gamma = 5 \times 10^{-3}$$
$$\delta = 8 \times 10^{-3}$$
$$f_r = 1\ \text{kHz}$$
$$f_b = 4\ \text{kHz}$$
$$P_b = 0.2\ \text{MW}$$
$$\epsilon_\eta = 3 \times 10^{-6}\ \text{m-RAD}$$
$$\beta* = 0.7\ \text{mm}$$
$$\sigma_\omega/\omega = 4 \times 10^{-3}$$

Table 2. General characteristics of possible solution for UCLA $\overline{B}B$-factory.

1. Submicron Beam Spot Size
2. Low Beam Power
3. Low Repetition Rate (1 kHz)
4. e^+ Production by Nonconventional Technique
   e^- Using New Guns or FEL Techniques
5. High Gradient Room Temperature Accelerator
6. Large Disruption Parameter
   (Little is known of the beam
   dynamics behavior in this region)
7. Modest σ_ω/ω (4×10^{-3})

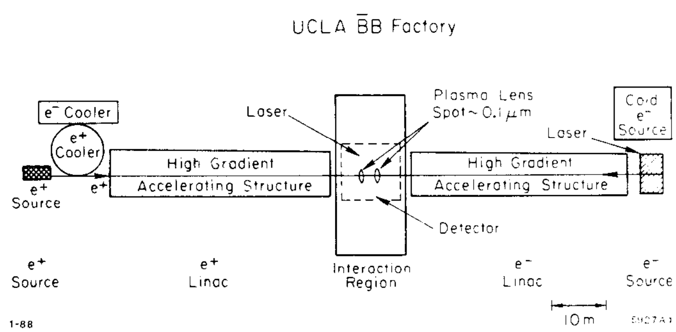

Fig. 1.

4. The e^+ Source

It is generally considered that the e^+ source for a $\overline{B}B$-factory is the most severe limitation. U. Amaldi and collaborators are in the process of designing an e^+ source using a high energy linac, rotating target and GeV damping rings.[4] We are studying a different technique—low energy e^+ production and collection (radioactive source or linac) and beam cooling of the positrons to reduce the emittance to 10^{-6} m-r. For a description of this technique, see D. Larson's report, "Cold Intense Positron Sources Using Electron Cooling," a UCLA preprint.

5. The e^- Source

The development of bright low emittance sources for FEL work can be directly applied to the e^- source for the $\overline{B}B$-factory. In addition, the short bunch length of the e^- source can be either obtained from this source or by using two preaccelerators and phase space rotation techniques as recently described by P. Wilson (private communication). Another technique has been developed by Los Alamos.[5] A high gain in a single pass FEL requires a very high electron density in the bunches. Very high density bunches are being developed at Los Alamos by Frazer, Sheffield and others[5] using laser-driven photocathodes in rf guns. To date, these devices have produced the brightest electron bunches. We expect advances in this area to make it possible to obtain bunches with the required properties for a $\overline{B}B$-factory when subpicosecond lasers are used and higher gradients in the rf gun are employed.

6. Possible High Gradient Accelerator Structure

A number of new techniques are being studied to provide high gradient drivers for linear colliders. The Relativistic Klystron is very promising and is the one we will study for the UCLA design. In addition, the use of semiconventional Klystrons with rf pulse compression looks promising.

6.1 The High Gradient Linear Accelerator

In order to produce a unique compact source of visible or UV light or X-rays (the Linear Light Source) or to collide e^+e^- beams at the highest luminosity and/or energy it will be necessary to develop new higher gradient acceleration techniques that are an extension of the present linear acceleration techniques such as that used at the Stanford Linear Accelerator Center (SLAC). The next generation of linear colliders likely will need a gradient of 200 MeV/m. Devices to produce this gradient are under study at SLAC. For the program proposed here a gradient of 100 MeV/m will be adequate and several techniques are expected to be tested in the next year or so that would be appropriate. We will describe two such techniques here: (1) the Relativistic Klystron and (2) the rf Klystron with bunch compression. In both cases it will be necessary to work with driver frequencies in the 9–11 GHz range to obtain the high gradient. The power requirements from these systems will be in the 100 MW range for the present use.

In a more general sense, the design and development of a high gradient linear accelerator must be carried out such that the shortest possible bunches can be accelerated in the future. Thus, if even shorter bunches in the 1–10 μm range become available using new sources such as the laser photocathode or plasma generated electron bunching, the accelerator must be capable of accelerating these bunches. Therefore, the development of these new sources can lead to even shorter time resolved X-ray light sources in the 10 Femtosecond range. Attention to the wake fields generated in the structure must be made. In addition, the injector complex for the system must be modular allowing for different sources. These features will help make the R&D program on the development of the ultra-short radiation source viable.

In order to reach high gradients using Cu structures it is likely necessary to use drivers of higher frequency than is presently being used at linacs such as SLAC. This is because the breakdown fields for the surface of Cu increases with driver frequency as shown in Fig. 2. Thus it may be possible, in principle, to reach gradients above 200 MeV/m.

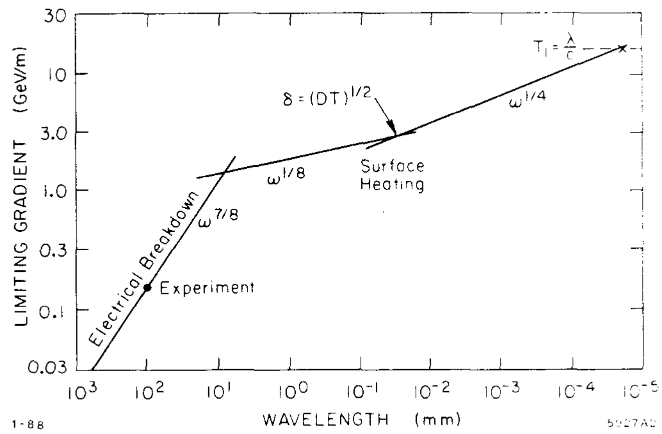

Fig. 2

6.2 The Accelerating Structure

The most logical candidate for a next generation, high gradient, compact accelerator will likely use copper cavities operated at high frequency (10–30 GHz). In addition, the requirements of high average brightness for a light source or high luminosity for an e^+e^- collider dictate that the repetition rate of the beam pulses be high (> kHz). These conditions then help define a class of structures that can be used. Superconducting cavities operate at a small gradient at present (less than 10 MeV/m) and may not be useful for compact high energy light sources.

We first turn to the possibility of reaching high gradients with copper structures. J. Wang and G. Loew have measured the ultimate accelerating gradients in the SLAC disc-loaded structure.[6] They find the upper limit of

$$\begin{bmatrix}\text{Accelerating}\\ \text{Axial Field}\end{bmatrix} \qquad E_{Z,TW} = \sqrt{\frac{\text{Pin}}{17}} \times 100 \text{ MeV/m}$$

where Pin is the power input in MW. Thus it appears possible to reach gradients in excess of 100 MeV/m. In addition, the maximum gradient is found to scale with the frequency of the driver in a manner as shown in Fig. 2.

The maximum gradients for the cu cavities likely scale as $\omega^{1/2}$ and $T_p^{-1/4}$ where ω is the driver frequency and T_p is the pulse length.

If the filling time varies as $\omega^{-3/2}$, the net scaling is $\omega^{7/8}$ for the maximum gradient. Thus, higher frequency drivers confine higher gradients. We may, thus, consider that a high frequency driver could give 200 MeV/m gradient for a linear accelerator. However, high frequency and high power will likely be required to reach this gradient. Very roughly, the energy gain per meter is proportional to the square of the driver frequency and the volume of the structure.

P. Wilson has described a special structure (disc-loaded structure) that would give 107 MeV/m gradient.[7] The parameters of this structure are given in Table 3.

This example shows that it is possible to design a structure to provide a high gradient, provided the peak power of the driver is high enough and that the frequency of the driver is in the range of 10–30 GHz. Thus, the key to obtaining a high gradients acceleration is the development of a high power/high frequency driver. Two possible examples of such drivers are near to the stage of being tested and are described below.

Table 3.

Parameters	Value (disc aperture radius = 0.37 cm)	Explanation of Parameters
V_g	0.03	V_g = group velocity
T_f (ns)	112	Filling time ($T_f = Ls/V_g$)
S (Ω/ps–m)	1025	The elasticity
T_0 (ns)	195	Structure time constant $T_0 = 2\phi_0/w$
c	0.58	$\tau = T_f/T_0$
η_s	0.58	Structure efficiency
$\hat{p}$/L (mw/m)	420	Peak power/omit length
$\hat{E}_{surface}/G$	2.2	Peak surface gradient to accelerating gradient

$G \equiv$ unloaded gradient of the structure

$= 167$ MeV/m for this example

$s \equiv G^2/u$; u is the stored energy per unit length

$L_s \equiv$ structure length

$Q_0 \equiv$ quality factor of the cavity

Clearly, a careful simulation of the high gradient structure, including beam loading, must be carried out in order to determine the quality of the accelerated beam. In such a study, structures other than the disc and washer type might be studied, and increasing the aperture over that in Table 3 to reduce wakefield effects would be considered as well.

6.3 The Relativistic Klystron

The Relativistic Klystron is a varient of the two-beam accelerator of A. Sessler. It uses an induction linac as a high current driving beam at relatively low energy. The driving beam is bunched at the rf wavelength and energy is extracted by an interaction with the longitudinal field in a cavity. The induction accelerator technology has been developed at LLNL and has recently been applied to the Relativistic Klystron (a SLAC/LBL/LLNL collaboration). During the past few months a successful operation of the Relativistic Klystron has been achieved. In order to achieve a gradient of 100 MeV/m it is necessary to provide a peak power of 150 MW/m. It is expected that the next tests of the Relativistic Klystron in the Spring of 1988 will reach this level, thus making this driver a strong candidate for the program outlined here!

Figure 3 shows a conceptual drawing of the Relativistic Klystron as envisioned by the LLNL, LBL and SLAC group. The LIA (Linear Induction Accelerator) is a monolithic relativistic klystron that runs the length of the high frequency rf accelerator. The injector and accelerator cells of the induction linac consist of nonresonant, axisymmetric gap structures that enclose toroidal cores of ferromagnetic material such as ferrite. A drive voltage is applied across the gap by the powerdrive, changing the flux in the core, thus inducing an axial electric field that accelerates the electrons. The fundamental limits of the LIA are set by beam transport physics, material properties and the primary commutator recovery times. W. Barletta of LLNL has carried out extensive modeling of the LIA, including cost optimization and studying the scaling principles and costs of the Relativistic Klystron.

Schematic of a relativistic klystron

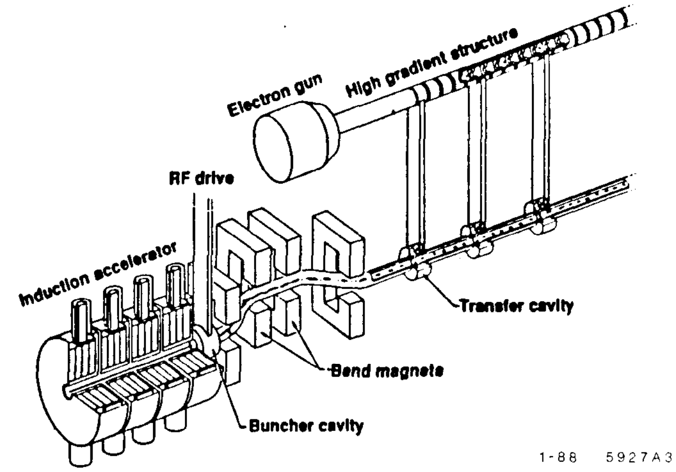

Fig. 3

6.4 RF Klystron with Bunch Compression

P. Wilson has recently reviewed the progress on such systems. M. Allen and J. M. Paterson are designing these systems at SLAC. A peak power of about 150 MW/m would be needed to give a practical gradient of 100 MeV/m. One technique to achieve this power at 10 GHz frequency is to use tubes with a lower peak power and a longer pulse length and then use rf pulse compression. Using two stages of pulse compression with a tube with a pulse length of 0.5 μ and a peak power of 150 MW could drive 4 m of accelerating structure. In order to reach 5 GeV/c^2 energy we would need about 12 tubes. P. Wilson has estimated the cost of this system to be $\sim$ 0.40 M\$/GeV of final energy. Additional information on rf pulse compression techniques can be found in Z. D. Farkes, IEEE Trans. Microwave Theory and Techniques **MIT–34**, 1036 (1986). The initial goal of the program proposed here is to choose one of the most promising rf drivers and to construct a prototype for the applications described later. The UCLA group will be joined by the TRW accelerator physics group, consulting with SLAC and LLNL on the developments in the field. We would expect to make a preliminary decision during 1988 and start the construction of the driver in 1989.

7. Final Focus

The basic design concept of the UCLA $\overline{B}B$ factory is the use of a very short focal length lens to reduce the spot size, and hence the power requirement and e^+ intensity.[8] We now give a brief discussion of the plasma lens concept that can be applied to the $\overline{B}B$-factory. Figure 4 shows a layout.

Dense particle beams traveling in plasmas can produce very high electric and magnetic fields, and these fields, described by Chen and others, can be used to accelerate and focus particles. The effects on trailing beams and self-focusing can be strong and nonlinear. This paper discusses a short focal length lens which uses linear electrostatic plasma oscillations to produce self-pinching. The dynamics of this focusing are similar to pinching produced by currents in plasmas and pinching by other beams (in disruptions). As an example, we consider a final focus system for the Stanford Linear Collider (SLC), considering methods of plasma production, vacuum system and backgrounds, and show how the luminosity could be increased using this system.

We have considered a number of possible applications for a plasma lens using self-pinching, including the first element in a positron or antiproton production system; however, the most obvious use seems to be as a short focal length lens to be used

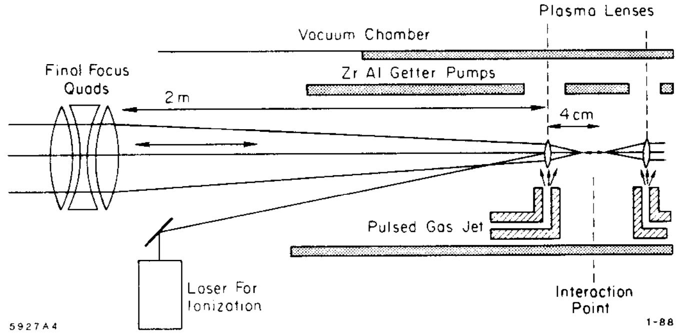

Fig. 4

as the final focusing element in a linear collider. For this application, the plasma lens must provide very high focusing gradients; however, additional constraints include compatibility with experiments, ability to cope with a disrupted beam leaving the Interaction Point (IP), and compatibility with other elements in the beam lines.

Since plasma lens performance is ultimately limited by aberrations, optimizing the luminosity gain implies comparatively short focal lengths. The length of the plasma; however, also rises for short focal lengths, producing increased beam gas event rates. An additional constraint considered was the ability to discriminate between tracks originating at the IP and those originating in the plasma lenses, which seems to require a few centimeters between the lenses and the IP.

The focusing strength of a self-pinch calculated by Chen for parabolic bunches of width a and length b is given by

$$K = \frac{4Nr_e}{\gamma a^2 b} \approx 20 \text{ cm}^{-2}$$

for B–factory parameters, assuming a slightly defocused beam: $E = 5$ GeV, $a = 5$ μm, $b = 1000$ μm, r_e is the electron radius and $N = 5 \times 10^{10}$ e/bunch. The thickness of a lens capable of producing a 2 cm focal length with a 5 GeV beam can be calculated from the relation

$$t = \frac{1}{Kf} \approx .02 \text{ cm} \quad .$$

The plasma density required is determined by two constraints: (1) the plasma density must be higher than the beam density, so the plasma oscillations will be approximately linear, (2) and the plasma wavelength must be shorter than the bunch length to insure that the focusing force varies smoothly with the bunch length. Both constraints are satisfied if the plasma density is 10^{17} to 10^{18}, corresponding to a complete ionization of a gas at 1–10 torr.

8. Layout and a Possible Site at UCLA

The $\overline{B}B$ linear collider factory discussed here makes use of a high gradient accelerator (G $\geq$ 150 MeV/m). Since the center-of-mass energy should exceed 14 GeV above threshold for the $B_c\overline{B}_c$ states formation, and 30 m are required for the collision hall and $e^{\pm}$ sources. The total layout need not exceed 110 m. Thus, it could be placed on a relatively small area adjacent to a university. There are many advantages to this arrangement, as can be seen from the style of operation of the Cornell collider. We have, therefore, explored the possibility of siting the $\overline{B}B$–factory at UCLA. Figures 5 and 6 show a possible layout of a $\overline{B}B$–factory on the West Campus of UCLA in Westwood, Los Angeles.

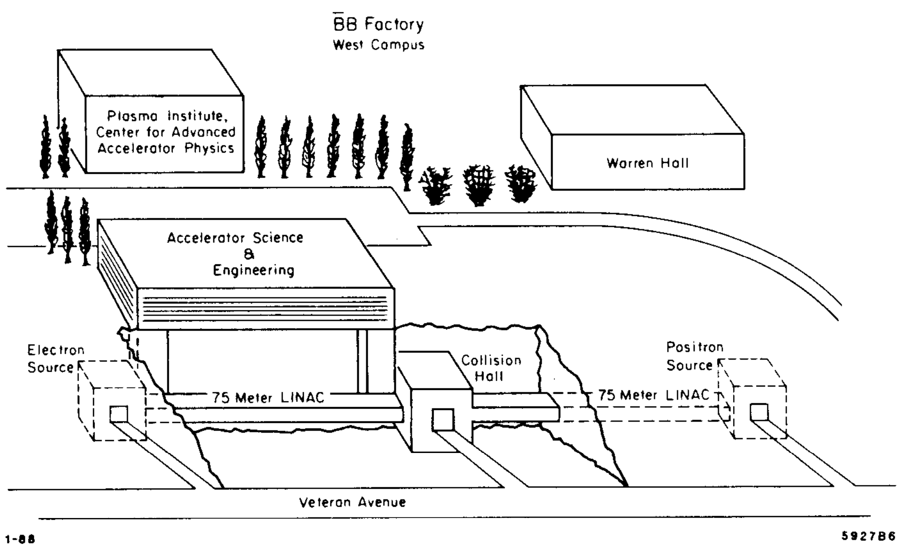

Fig. 5

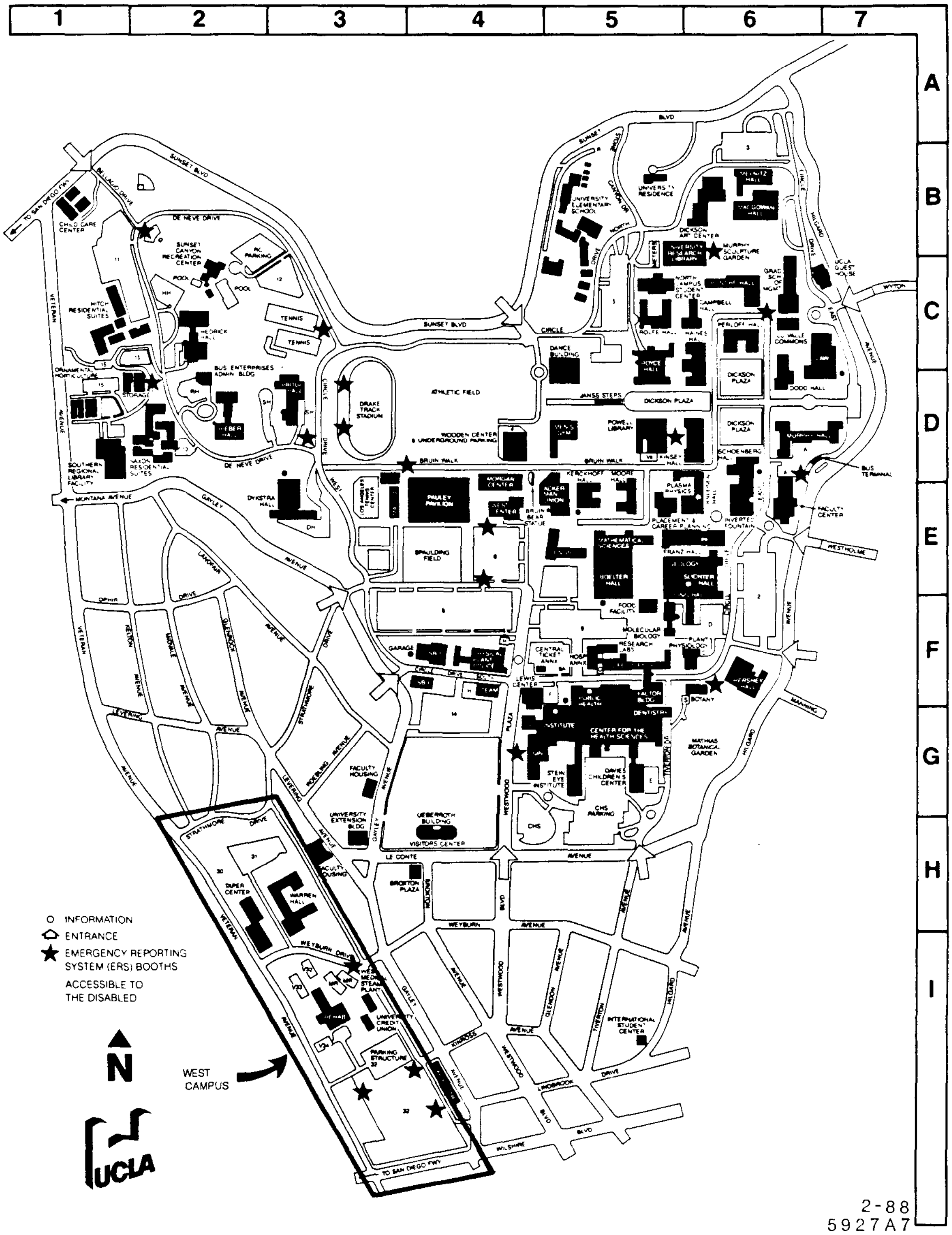
1
2
3
4
5
6
7
A
B
C
D
E
F
G
H
I
O INFORMATION
ENTRANCE
EMERGENCY REPORTING SYSTEM (ERS) BOOTHS
ACCESSIBLE TO THE DISABLED
N
WEST CAMPUS
UCLA
2-88
5927A7

Fig. 6

9. Possible Applications of the Technology for a $\overline{B}B$ Factory

The acceleration of intense, bright pulses of electrons and positrons to several GeV and focus to submicron spots will solve many, if not all, the problems to be encountered in the CLIC (CERN), TLC (SLAC), VLLC (USSR) or Japan high energy linear colliders. In this sense, the development of a $\overline{B}B$-factory is a test model for a TeV linear collider. In addition the ultra-short bunches, bright source and high energy of the electron beam could lead to a new type of light source. We call this a Linear Light Source (LLS) and it is capable of producing 10–100 femtosecond visible, UV and X-ray light bursts. There seems to be a great need for such light sources in many other fields.

10. An R&D Program to Define the $\overline{B}B$ Factory Parameters: The Estimated Cost of the $\overline{B}B$ Factory

As a first stage of the $\overline{B}B$-factory, we are proposing to construct a 5 GeV LLS. If this machine is constructed in a timely fashion, it will provide extremely valuable information about the next generation of linear colliders.

We have attempted to estimate the cost of a $\overline{B}B$-factory driven by a Relativistic Klystron (with the help of W. Barletta, LLNL, private communication) in Table 4.

Table 4. Cost of an e^+e^- linear collider $\overline{B}B$-factory driven by a Relativistic Klystron.

		Kilo $	
Linac:			
	Building	3,000	
	Utilities	1,000	
	Waveguides	2,100	
	Induction Drive	11,000	
	Sundries	1,600	
		18,700	$\times 2 = 37,400$
Collider:			
	Final Focus	2,000	
	Collider Hall	5,000	
	I&C	5,000	
	Utilities	500	
		12,500	12,500
e^+ Source		$\sim$ 6,000	6,000
e^- Source		$\sim$ 5,000	5,000
			60,900
35% for EDIA			21,000
Total			$81,900,000

11. Acknowledgements

I wish to thank the many people who have provided information on novel acceleration and collider techniques, including P. Wilson, W. Barletta, K. Brown, P. Chen, U. Amaldi, B. Richter and J. Rees.

References

1. D. Cline, *A Small Test Linear Collider and $\overline{B}B$-Factory*, Proceedings of the Madison Workshop, *Advanced Accelerator Concepts*, ed. by Fred Mills, AIP **156**, 1987, p. 12.
2. U. Amaldi and G. Coignet, Nucl. Inst. & Methods (in print) and CERN EP/86–211 (1986).
3. D. Cline and A. Soni, in *Proceedings of the 1987 Moriond Conference.*
4. U. Amaldi (private communication).
5. W. Frazer et al., IEEE Trans. on Nucl. Sci. **NS–32**, Vol. 5, 1791 (1985).
6. IEEE Trans. on Nucl. Sci. **NS–32**, Vol. 5, 2915 (1985).
7. P. B. Wilson, SLAC–PUB–4310 (1987).
8. This work was done in conjunction with J. Norem, J. Simpson and J. Rosenzweig.

CRITICAL ISSUES IN LINEAR BEAUTY FACTORIES

UGO AMALDI
CERN, Geneva, Switzerland

1. Review of the Limiting Factors

I have reviewed all the available designs of linear beauty factories in Ref. 1. In this contribution I want to discuss the critical issues which are relevant to all the proposed schemes.[2–8]

In my definition a linear *beauty factory* is an electron-positron accelerator which produces on the order of one pair of beauty quarks per second, or more. This implies luminosities $L \geq 10^{33}$ cm^{-2} s^{-1} and $L \geq 10^{34}$ cm^{-2} s^{-1} at $W = 2\ E_0 \simeq 10$ GeV (on the narrow Υ resonances) and at $W \simeq 15$ GeV (in the continuum), respectively. The list of requirements and the main limitations to its performances is quite long.

1. The rms energy spread at $W \simeq 10$ GeV has to be small ($\Delta W \leq$ 10–15 MeV) since the resonances are narrow. As shown in Ref. 1, the two main limiting factors are (a) the *longitudinal emittance* $\epsilon_L = \sigma_z \Delta E_L/\mathrm{mc}^2$ and (b) the *beamstrahlung fractional energy loss* $\langle\epsilon\rangle$. When a bunch of $N \geq 2 \times 10^{10}$ positrons is extracted from a damping ring (DR) having a short damping time ($\tau \simeq 1$ ms), its longitudinal emittance is $\epsilon_L \geq$ (3–4)10^{-2} m and the corresponding energy spread in the center-of-mass has the lower limit

$$\Delta W_L \geq 2^{1/2}\ \epsilon_L\ \mathrm{mc}^2/\sigma_Z \simeq 25\ \mathrm{MeV\ mm}/\sigma_Z \quad . \tag{1}$$

2. As it was shown in Ref. 1, the beamstrahlung energy spread ΔW_b can be expressed as a function of the bunch length σ_Z and of the average collision repetition rate f_r in the form:

$$\Delta W_b/\mathrm{MeV} \simeq 1.2(E_0/\mathrm{GeV})^2(L/10^{33}\mathrm{cm}^{-2}\ \mathrm{s}^{-1})\\ (\mathrm{mm}/\sigma_Z)(\mathrm{kHz}/f_r) \quad . \tag{2}$$

In a machine designed for the largest luminosity with the minimum energy spread the natural choice is $\Delta W_L \simeq \Delta W_b$ so that, by combining Eqs. (1) and (2), one gets

$$f_r/\mathrm{kHz} \geq (E_0/4.5\ \mathrm{GeV})^2(L/10^{33}\ \mathrm{cm}^{-2}\ \mathrm{s}^{-1})\\ [\Delta W_L \simeq \Delta W_b] \quad , \tag{3}$$

which shows that for $W \simeq 10$ GeV ($E_0 = 5$ GeV) and $L \simeq 10^{33}$ cm^{-2} s^{-1} the repetition rate has to be larger than 1 kHz. At the same time, from Eq. (1), one gets $\sigma_z \geq 2.5$ mm for $\Delta W_L \leq 10$ MeV and $\Delta W \simeq (\Delta W_L^2 + \Delta W_b^2)^{1/2} \leq 15$ MeV.

3. It is well known that in a linear collider the luminosity is proportional to beam power:[1]

$$L/10^{33}\ \mathrm{cm}^{-2}\ \mathrm{s}^{-1} \simeq (DH_D/30)(\mathrm{mm}/\sigma_Z)(P/\mathrm{MW}) \quad , \tag{4}$$

where $P = NE_0\ f_r$ and D is the *disruption parameter*. All linear beauty factories considered in the literature[2–8] are chosen to run with large values of the disruption parameter D (let us say $D \simeq$ 20–30), and make use of the advantages of a large pinch enhancement factor: $H_D \geq 6$. According to Eq. (4) this provides larger luminosities. At the same time, σ_Z should be chosen as small as possible, but this is incompatible with Eqs. (1) and (2). Combining Eqs. (1) and (4) one gets

$$P/\mathrm{MW} \geq (750/DH_D)(L/10^{33}\ \mathrm{cm}^{-2}\ \mathrm{s}^{-1})(\mathrm{MeV}/\Delta W_L) \quad . \tag{5}$$

This relation is plotted in Fig. 1 as dashed and dashed-dotted lines for $L = 10^{33}$ cm^{-2} s^{-1} and $L = 10^{34}$ cm^{-1} s^{-1}, respectively. For $\Delta W_L \leq 10$ MeV the beam power has to be $P \geq 0.5$ MW if one wants to get $L \geq 10^{33}$ cm^{-2} s^{-1}.

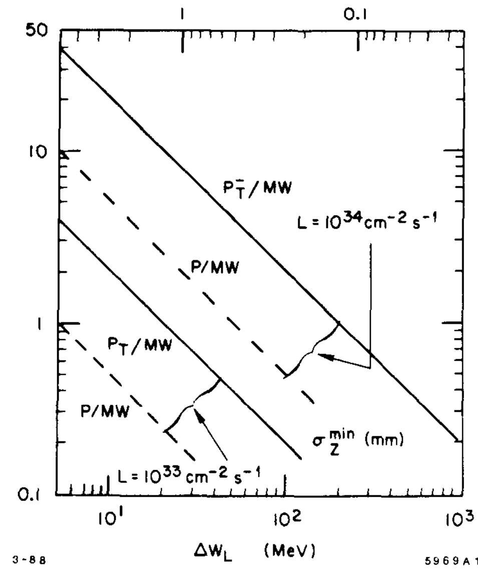

Fig. 1. The power/beam P and the power of a 2.2 GeV electron beam needed to produce the positrons are plotted versus the energy spread ΔW_L with a longitudinal emittance $\epsilon_L \simeq 3.5 \times 10^{-2}$ m. The second horizontal scale gives the minimum value of the bunch length σ_Z [Eq. (1)].

4. Since in a conventional positron target one has to dump an electron energy $E_T \sim 20$ GeV in order to collect on average one positron. The beam power P determines the electron power P_T^- to be sent on the target to get N^+ positrons: $P_T^-/P = E_T/E_0$. More explicitly from Eq. (5)

$$P_T^-/\mathrm{MW} \simeq (1500/D\ H_D)(E_T/W)(L/10^{33}\ \mathrm{cm}^{-2}\ \mathrm{s}^{-1})\\ (\mathrm{MeV}/\Delta W_L) \quad . \tag{6}$$

This equation, plotted as continuous lines in Fig. 1, expressed quantitatively the *main* problem posed by high-luminosity low energy linear colliders: *the positrons have to be produced by a MW electron beam* hitting a converter if ΔW_L is to be of the order of 10 MeV *and* the DR limitation of Eq. (1) is valid for the longitudinal emittance. (Note that this conclusion does *not* depend on either the invariant transverse emittance ϵ_n of the bunches or the repetition rate f_r chosen.)

5. The number of particles per bunch N can be obtained by combining the following expression for the power

$$P/\mathrm{MW} = 0.016\ (E_0/\mathrm{GeV})\ (f_r/\mathrm{kHz})\ (N/10^{11}) \quad , \tag{7}$$

with Eq. (5):

$$N/10^{11} \geq \frac{4.7\ 10^4}{DH_D}\ \frac{(L/10^{33}\mathrm{cm}^{-2}\ \mathrm{s}^{-1})}{(E_0/\mathrm{GeV})}\ \frac{\mathrm{kHz}}{f_r}\ \frac{\mathrm{MeV}}{\Delta W_L} \quad . \tag{8}$$

For $f_r \simeq 1$ kHz (point 2) and $\sigma_z \simeq 2.5$ mm (point 1), so that $\Delta W_L \simeq \Delta W_b \simeq 10$ MeV at $E_0 \simeq 5$ GeV, N has to be at least equal to 5×10^{11} to have $L = 10^{33}$ cm^{-2} s^{-1}, even if D is chosen to be as large as 30. Such a high population of bunches causes problems both in the DR's and during the acceleration, because of wakefields. To avoid this effect, the repetition rate has to be made larger than 5 kHz, i.e., much larger than the lower limit imposed by Eq. (3).

6. The required luminosities and the above arguments almost fix the invariant transverse emittance ϵ_n of the electron and positron bunches. For $\Delta W_L \leq 10$ MeV, as needed at $W \simeq 10$ GeV, Fig. 1 says that the beam power is $P \simeq 0.5$ MW, which implies $(N/10^{11})(f_r/\mathrm{kHz}) \simeq 6$. The disruption parameter, defined as $D = r_e\, N\sigma_z/(\gamma\sigma_z^2)$, can be written in the form

$$D \simeq 28(N/10^{11})(10^{-5}\mathrm{m}/\epsilon_n)(\sigma_z/\beta^*) \quad , \qquad (9)$$

which shows that to have $D \simeq$ 20–30, since β^*/σ_Z has to be larger than about 1.5 in order to not lose luminosity, $(N/10^{11}) \geq 1.5(\epsilon_n/10^{-5}\ \mathrm{m})$. Since the argument under point 5 gives $N \leq 10^{11}$, we conclude that $\epsilon_n \leq 7 \times 10^{-6}$ m.

Figure 2 helps in understanding the situation. To have a collider running in a *high-resolution mode* with a luminosity $L = 10^{33}\ \mathrm{cm}^{-2}\ \mathrm{s}^{-1}$ one has to roughly follow the continuous line; for each choice of N the maximum value of the transverse emittance is given. Note that the best synchrotron light sources can today give $\epsilon_n \simeq 10^{-6}$ m, but also that their damping times τ are much longer than the few milliseconds needed in this application (see point 8).

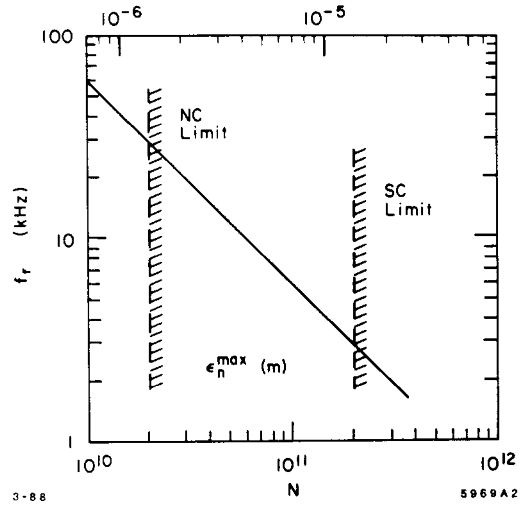

Fig. 2. The repetition rate f_r is determine by the number of particles N if one wants $\Delta W_L \simeq 10$ MeV and $L \simeq 10^{33}\ \mathrm{cm}^{-2}\ s^{-1}$ at $W = 10$ GeV with $\epsilon_L \simeq 3.5 \times 10^{-2}$. In this case $\sigma_Z \simeq 2.5$ mm. The scale of $\epsilon_n^{\mathrm{max}}$ corresponds to the choice $\beta^*/\sigma_Z = 1.5$ [Eq. (9)].

7. As already mentioned under point 5, the number of particles per bunch N is limited by the wakefields in the accelerating structure. It has been shown by Wilson[7] that longitudinal wakefields introduce a momentum spread larger than $\Delta W/W \simeq 10^{-3}$ for $N \geq$ (2–3) $\times\ 10^{10}$ in a copper normal conducting (NC) structure running at a rf frequency $f \geq 10$ GHz. The limit is *at least* ten times higher for a superconducting (SC) structure running at a much lower frequency (let us say 0.5 GHz); such a limit is indicated in Fig. 2. Note, however, that effects in the DR's may limit N to less than about 10^{11}, if one wants to avoid deterioration of ϵ_n by intrabeam scattering and increase of ϵ_L by the anomalous lengthening of the bunches. From the combination of points 5, 6 and 7 we conclude that NC linear beauty factories for $\Upsilon(4)$ physics, if they are limited by ϵ_L (as indicated in point 1) have to run at much higher repetition rate than SC beauty factories. Wilson's choice, for instance is $f_r = 44.4$ kHz, $N = 2.2 \times 10^{10}$ and $\epsilon_n = 3 \times 10^{-6}$ m. For an SC factory of Ref. 1, I have chosen $f_r = 10$ kHz, with $N = 8 \times 10^{10}$, a number of electrons per bunch which is equal to the maximum one foreseen for SLC.

8. The repetition rate fixes the length of the DR system, which can be made either by one long or many short storage rings. By indicating with the symbol ℓ_b the *average* distance between two consecutive bunches in the ring, the *total* length ℓ_d of the (positron) DR system is

$$\ell_d = (T/\tau)\ f_r\ \tau\ \ell_b \simeq 5\ f_r\ \tau\ \ell_b \quad , \qquad (10)$$

were τ is the (transverse) damping time and T is the waiting time of each bunch in the ring (typically $T \simeq 5\tau$). For $\tau = 3$ ms (as at SLC) and $\ell_b = 8$ m[9], with $f_r = 44.4$ kHz (as in Wilson's design) one would have to build ~ 5 km of DR's! A remedy is to have many bunches following each other at shorter distances, so that a *train* of b bunches is extracted from the ring and accelerated. This, however, has problems with the wakefields in an NC copper structure. In his parameter list Wilson has $b = 4$, so that the length of the DR is[1] only ~ 1.6 km, but this may not be possible with bunches containing $N = 2.2 \times 10^{10}$ particles. Another possibility, to be discussed in the next section, is to reduce the damping time τ to about 1 ms.

The above list shows that there is not much freedom in the choice of the parameters of a beauty factory which aims at running *both* on the narrow resonances Υ(4S) and Υ(5S) *and* in the continuum. Clearly, the main limitations come from the longitudinal emittance of DR's and from the positron target. These points are further discussed in the next section.

2. Positron Production

A target which can produce bunches with $N^+ \sim 5 \times 10^{10}$ positrons at a rate f_r = 12 kHZ has been described by Peter Sievers[10] in connection with the SC factory of Ref. 2. Figure 3 shows the target and Fig. 4 indicates the computed temperature cycle of the various components.

Damping rings have been looked at by many authors in connection with TeV linear colliders. However, most of this work is *not* relevant here because

i) the longitudinal emittance plays no role in fixing the final energy spread in a TeV accelerator, while it is very important for running on the resonance Υ (4S) (point 1 of Section 2);

ii) at TeV colliders, the number of particles per bunch is on the order of 5×10^9, and *not* 5×10^{10}, so that the anomalous lengthening in the DR plays practically no role.

The only dedicated study known to me is due to Mario Bassetti and collaborators,[11] who have designed a racetrack DR with long wigglers which at $E_0 \simeq 2.2$ GeV can give $\tau \simeq 1$ ms with $\epsilon_L \simeq 4 \times 10^{-2}, \epsilon_n \simeq 3 \times 10^{-6}$ m and $N^+ \simeq 5 \times 10^{10}$. Unfortunately, the phenomenon of bunch lengthening (which contributes to ϵ_L) is not well understood and experiments on existing rings are needed to draw final conclusions on the longitudinal (and transverse) emittances which can be achieved in a real storage ring.

Since positron production is the main difficulty on the way to linear beauty factories, the R&D project that D. Cline and collaborators have started at UCLA on new types of sources is very important. The possible lines of development the UCLA group is looking into are:[5]

i) cold positron sources which would not need DR's;[12]

ii) neutron activation in nuclear reactors of positron-emitting radioisotopes;[13]

iii) positron production by ~ 10 MeV protons produced in fusion plasmas;[14]

iv) the use of electron cooling to damp the transverse emittance of a few MeV positrons.[5]

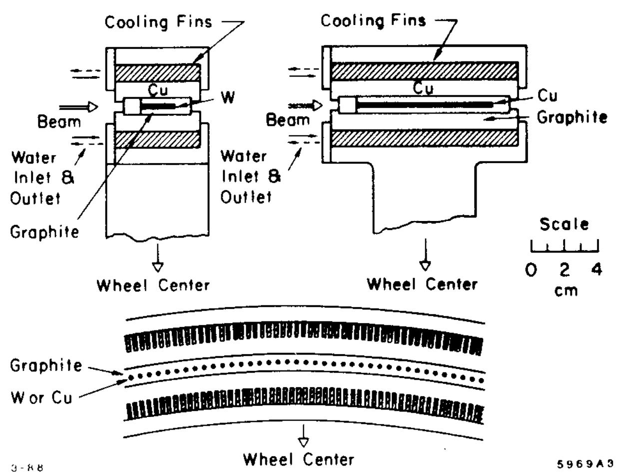

Fig. 3. Rotating positron targets proposed by P. Sievers.

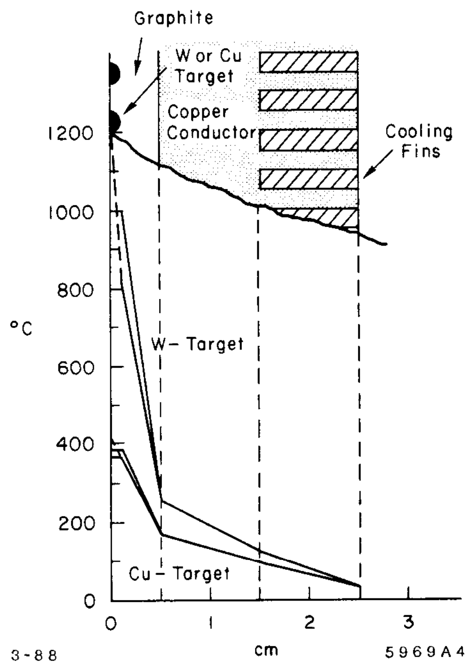

Fig. 4. Temperature cycles of the targets of Fig. 3.[10]

If any one of these ideas come to fruition, the cost of positron production may be greatly reduced.

In conclusion, the good energy resolution method to run on the Υ (4S) puts severe constraints on the choice of the parameters, so that no freedom is left. The main problem is posed by the production and the longitudinal emittance of the positron bunches and *not* by the transverse emittance. New methods would be extremely useful here. In the continuum, the longitudinal emittance and the energy spread are not a problem, but the power on the positron target is still large if one requires luminosities of the order of 10^{34} cm^{-2} s^{-1}.

A way of simplifying the problem of positron production has been proposed by Wurtele and Sessler:[6] have the number of positron per bunch N^+ smaller than the number of electrons per bunch N^-. A further step is to combine this with the fact that, to have a small energy spread ΔW_L, the positron bunch extracted from a conventional DR has to be relatively long due to Eq. (1). Since $D \propto N\sigma_z$, I have chosen in Ref. 1 not only $N^+ < N^-$ but also $\sigma_z^+ > \sigma_z^-$ *so that* $N^+\sigma_z^+ \simeq N^-\sigma_z^-$.

Table 1. A possible set of parameters for a low-repetition rate SC beauty factory.

Symbol	High-resolution mode	Low-resolution mode
E_0(GeV)	5.3	7.5
L(cm^{-2} s^{-1})	10^{33}	1.5×10^{34}
P^+(MW)	0.25	0.35
P^-(MW)	0.75	0.7
P_T^-(MW)	1.0	1.5
f_r(kHz)	6.0	6.0
ϵ_n(m)	5×10^{-6}	2.5×10^{-6}
D^+	17	32
D^-	17	32
H_D [a]	6.5	10
N^+	5×10^{10}	7×10^{10}
N^-	1.5×10^{11}	1.4×10^{11}
σ_z^+(mm)	3.0	0.8
σ_z^-(mm)	1.0	0.4
β^*(mm)	5.0	2.0
σ_x(μm)	1.55	0.58
W (GeV)	10.6	15.0
ΔW_b (MeV)	3	250
ΔW_L (MeV)	8	30

a) Computed using the expression given in Ref. 17.

This choice goes in the direction of solving two of the main problems:

i) the large power P_T^- on the positron target,

ii) the large value of the longitudinal emittance ϵ_L.

By pushing all the arguments given in the previous section to the extreme, as an example I have collected in Table 1 the parameters of a SC factory running on the Υ(4S), which uses long positron bunches ($\sigma_z^+ \simeq 3$) mm. Due to the low repetition rate, in this case the damping ring can be short if $\tau \simeq 1$ ms and $\ell_b = 8$ m: $\ell_d \simeq 240$ m from Eq. (10). Table 1 also gives the parameters for running in the continuum with the same repetition rate. I underline that in both cases the transverse emittance is relatively large and the β^*-value is very easy to obtain with conventional magnets and a small chromaticity correction.

Let me remark that electron production has not been discussed here because, following Refs. 1 and 2, the electrons of the needed invariant emittance ($\epsilon_n \simeq 2 - 5 \times 10^{-6}$ m) are supposed to be directly produced by a source without the need for DR's. Along these lines, recent developments at Stanford University and Los Alamos are very encouraging. At Stanford[15] a scheme based on magnetic bunching and harmonic compensation has been developed which should provide, from a conventional thermionic source, bunches containing $N \simeq 10^{10}$ electrons with $\epsilon_n \simeq 2 \times 10^{-6}$ m. At Los Alamos an rf source has run at 1.3 GHz with a Cs_3 Sb photocathode which was illuminated by a neodymium laser. After a first series of runs, the production of more than 100 A of peak current with an invariant emittance $\epsilon_n \simeq 10^{-5}$ m and a bunch length $\sigma_z \simeq 30$ mm has been reported.[16] Further tests are going on with a postaccelerating cavity, which should produce directly 2 MeV electrons. The first source is already satisfying the requirements of X-UV FEL's. At Los Alamos one thinks that the new source will give $\epsilon_n \simeq 2 \times 10^{-6}$ m at lower peak currents, corresponding to $N \simeq 10^{10}$ electrons per bunch.

References

1. U. Amaldi, *Linear Colliders as Beauty Factories,* Proc. of the Int. Symp. on the Production and Decay of Heavy Flavors, Stanford, California, Sept. 1–5, 1987, E. Bloom and A. Fridman, eds., Annals N. Y. Acad. Sciences, in print (1988).
2. U. Amaldi and G. Coignet, Nucl. Instr. and Meth. **A260**, 7 (1987), U. Amaldi, *A Superconducting Radiofrequency Complex for Molecular, Nuclear and Particle Physics,* preprint CERN EP/87, **104** (1987), Proc. Topical Seminar on Heavy Flavors, S. Miniato, 1987, ed. F. Navarria, Nucl. Phys. Conf. Suppl., in print.
3. Proc. Symp. on Advanced Accelerator Concepts, Madison, Wisconsin, 1986, F. E. Mills, ed., (AIP Conf. Proc. **156**, New York, 1987), p. 435.
4. D. Cline, Proc. UCLA Workshop on Linear Collider $B\overline{B}$ Factory Conceptual Design (World Scientific, Singapore, 1987), p. 386.
5. D. Cline, *The UCLA e^+e^- Linear Collider $B\overline{B}$ Factory Project,* to be published in these Proceedings.
6. J. S. Wuertele and A. M. Sessler in Ref. 3, p. 322.
7. P. B. Wilson in Ref. 4, p. 373.
8. S. S. Yu, see Ref. 7.
9. D. Fiander has shown that kicker magnets having rise- and fall-times of 10–20 ns can be built (private communication).
10. P. Sievers, *A Megawatt Electron Positron Conversion Target — A Conceptual Design,* CERN–ST–TE/87–1 and CLIC Note 55 (1987).
11. M. Bassetti, S. Guiducci and L. Palumbo, private communication.
12. P. Schoessow and J. Simpson, Ref. 5, p. 403.
13. E. H. Ottewitte, Ref. 5. p. 407.
14. J. M. Dawson, Ref. 5, p. 417.
15. T. I. Smith, Nucl. Instrum. and Meth. **A250**, 64 (1986).
16. J. S. Fraser, *Photocathodes in Accelerator Applications,* Los Alamos Internal Note LA–UR 87–863 and in Proc. Particle Accelerator Conf., Washington, D.C., 1987.
17. P. Chen, *An Introduction to Beamstrahlung and Disruption,* SLAC–PUB–4379, (1987) to be published in Proc. US–CERN Joint Topical Course on *Frontiers of Particle Beams,* South Padre Island, Texas, 1986.

THE FUTURE CORNELL PROGRAM OR CESR AS A B FACTORY

KARL BERKELMAN

Cornell University, Ithaca, New York 14853

1. History and Motivations

Since 1979 the Cornell Electron Storage Ring (CESR) has been colliding electrons and positrons at an energy near the threshold for producing b–quarks. During these past eight years we at Cornell and our collaborators from other universities have been using the CLEO and CUSB detectors to explore the physics of the $b\bar{b}$ bound state spectroscopy, B–meson weak decays, and charm and τ production and decay, and we have searched for glueballs, axions, Higgs bosons, gluinos, squarks, free quarks, monopoles, and the ς. We and our friends at DORIS have measured the masses of many b–hadrons, mapped out the space and spin dependence of the interquark potential, tested quantum chromodynamics by measurement of the strong coupling α_s in quarkonium annihilation processes, established the dominance of the $b \to c \to s$ decay chain in b weak interactions, set stringent limits on flavor changing neutral currents, and measured mixing in the $B^\circ\overline{B}^\circ$ system.

In spite of these accomplishments, we are still far from a satisfactory understanding of the physics of the b–quark. The big questions today in elementary particle physics are:

- Is the Standard Model right?
- What are the parameters of the Standard Model?
- What is beyond the Standard Model?

Although the experimental results on the spectroscopy of the heavy quarkonium bound states have convinced most of us that quantum chromodynamics is the correct theory of the strong interactions, we have almost no information on the singlet states, which can tell us about the spin-spin interaction between quarks. D–states, vibrational levels, and other expected $b\bar{b}$ states have yet to be seen. In contrast to the situation in ψ–decay, we still have yet to measure a single hadronic decay mode of the Υ. And nothing is known of the spectroscopy of baryon states containing a b–quark.

The Standard Model contains many parameters whose values are not predicted, but must come from some kind of grand unification beyond the Standard Model. It is important to measure these parameters accurately in order to complete our knowledge of the model, and more importantly, to take us to a formulation of what is beyond. In the quark sector there are ten parameters, the six quark masses and the three angles and one phase of the Cabibbo–Kobayashi–Maskawa matrix. The u, d, s and c masses and the Cabibbo angle θ_{12} can be inferred from experimental data available before the discovery of the b–quark. Of the remaining five parameters, four have to be inferred from b–quark data. Our knowledge of m_b comes from the masses of the Υs and B–mesons. The CKM angle θ_{23} governs the $b \to c$ weak transition and is determined to be about 0.05 from the b–quark lifetime measurements at PEP and PETRA along with the B–semileptonic branching ratio data from CESR. Our knowledge of the angle θ_{13}, which governs the $b \to u$ transition, is in the form of crude experimental bounds (0.003 to 0.008) from the relative probability of charmless B–decays as determined at CESR and DORIS. Even a bound on the t–quark mass ($m_t > 50$ GeV) has been obtained from b–quark decays, combining the ARGUS lower bound on $B^\circ\overline{B}^\circ$ mixing with the bounds on the CKM angles.

In the Standard Model with three generations, it is the phase parameter in the CKM matrix (say in the V_{ub} matrix element, $\sin\theta_{13}\, e^{-i\phi}$) which is responsible for CP nonconservation. Its value is completely unknown, except that the observation of CP violation in K°–decay constrains ϕ to be nonzero and non–π. If the Standard Model with six quarks is correct, we can expect that CP will also be violated in B–decays, that is, that there will be modes $B \to f$ in which the rate for the CP conjugate decay $\overline{B} \to \bar{f}$ will be different, either as a function of lifetime or integrated over all lifetimes. The expected asymmetry is proportional to the product of the sines of the CKM angles and phase. It depends on an interference between decay amplitudes, and its size varies with decay mode. The CP asymmetry could be as large as 20% for the rarer modes which have branching ratios already suppressed by CKM angle factors (for details, see Bigi's talk at this workshop).

What is required to make further progress in b physics? Reviewing the limits to the accuracy of existing measurements and the obstacles to new measurements both in Υ–decays and in B–meson decays, one finds several common threads.

1) Relative to the e^+e^- production of charm in the ψ region, the b–quark production cross section in the Υ region suffers from a factor of 1/40 in the QED cross section, coming from a factor of 1/4 in the q^{-2}–quark charge dependence and a factor of 1/10 in the E^{-2} energy dependence.
2) The high masses of the decaying states make many decay modes kinematically accessible, so that any single exclusive hadronic final state has a very low branching ratio, the largest being less than 1% and many of the more interesting ones being less than 10^{-4}.
3) Also, because of the high available energies, the average multiplicities in the final states are high. That makes the easily reconstructible all-charged, low-multiplicity modes especially rare, and places serious demands on detector efficiency and resolution for the more plentiful modes.

Presently, operating detectors at CESR and DORIS are becoming inadequate for future requirements. They have emphasized either charged particle resolution (CLEO and ARGUS) or photon resolution (the Crystal Ball and CUSB), but are incapable of efficiently reconstructing final states involving both charged and neutral particles in the presence of high backgrounds. Out of the 200,000 $B\overline{B}$ events that ARGUS and CLEO have detected so far at the Υ (4S) resonance, less than 100 clean B–decays have been reconstructed with low background. We, therefore, need a real improvement in detector capabilities.

Production rates for $b\bar{b}$ states in existing rings are inadequate. The bulk of the DORIS and CESR data sample has been obtained with peak luminosity near 2×10^{31} cm^{-2} s^{-1}. The present analyzed sample of $B\overline{B}$ events totals about 2×10^5, but it is estimated that one can see CP violation in B–decay only with 10^7 B–decays and perhaps only with 10^8. So we need really large gains in e^+e^- luminosities before we can hope to make progress.

2. Detector Improvements

At CESR, we are now in the third year of a four-year capital improvement program which includes a rebuilding of the CLEO detector, an upgrading of the CESR machine to provide higher luminosity, and a new computing facility for the laboratory. The original CLEO detector is being replaced in phases.

A new main tracking chamber has already been installed and has been operating for a year. It is a one-meter diameter cylindrical drift chamber with 51 layers of single-sense-wire rectangular cells, 40 axial layers in half-cell staggered sets of three, alternating with 11 stereo layers, with 12,240 cells in all.

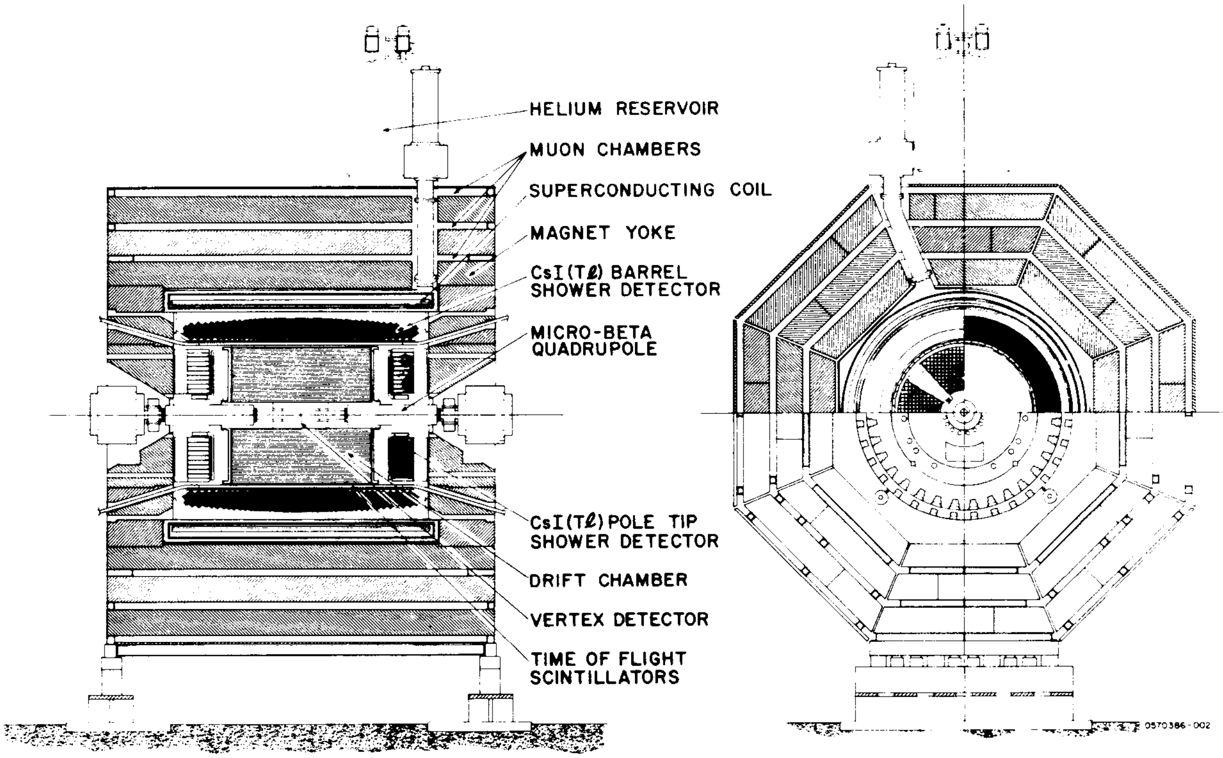

Fig. 1. Side and end views of the CLEO II detector.

In the present 1.0 Tesla solenoid we achieve an rms momentum resolution

$$\left(\frac{\delta p}{p}\right)^2 = 0.008^2 + (0.0028 \times p)^2 \qquad (p \text{ in GeV/c}) \ .$$

This should improve with the 1.5 Tesla field of the eventual solenoid and with better understanding of the drift time corrections. Along with the 13 layers in the vertex detector, we now have 64 layers of dE/dx for particle identification inside the solenoid. We have so far achieved better than 7% rms; we hope for better than 6%.

The most expensive component of the new CLEO II detector (Fig. 1) will be the electromagnetic calorimeter, an array of about 8000 cesium iodide scintillation crystals viewed by four photodiodes each. The rms energy resolution for photon showers will be better than 2% for energies above 150 MeV (Fig. 2), comparable to that of the Crystal Ball and CUSB detectors. The CsI procurement is on schedule; over two-thirds of the crystals have been delivered. In front of the electromagnetic shower detector array in the barrel section and on the end caps will be an array of time of flight scintillation counters.

Outside the calorimeter will be the new superconducting solenoid coil, 3.1 m diameter by 3.5 m long, giving a 1.5 Tesla field. It has been wound and factory tested, and will be delivered by October 1987. The 1000 tons of iron for the flux return and muon filter is now being delivered. The Iarocci tube wire chambers for muon detection are under construction. Before mid-1988 we expect to shut down CESR operations for installation of the new CLEO II components outside of the main tracking chamber.

The present vertex chamber of 13 drift cell layers has an inner radius of 6 cm and achieves a hit resolution of about 90 μm rms on Bhabhas. This has been sufficient for measurements of charmed and τ-lifetimes competitive with other e^+e^- experiments. However, to make a significant improvement in B-decay reconstruction efficiency we want to be able to recognize D-vertices reliably, and this requires better spatial resolution closer to the interaction point. We are exploring the possibility

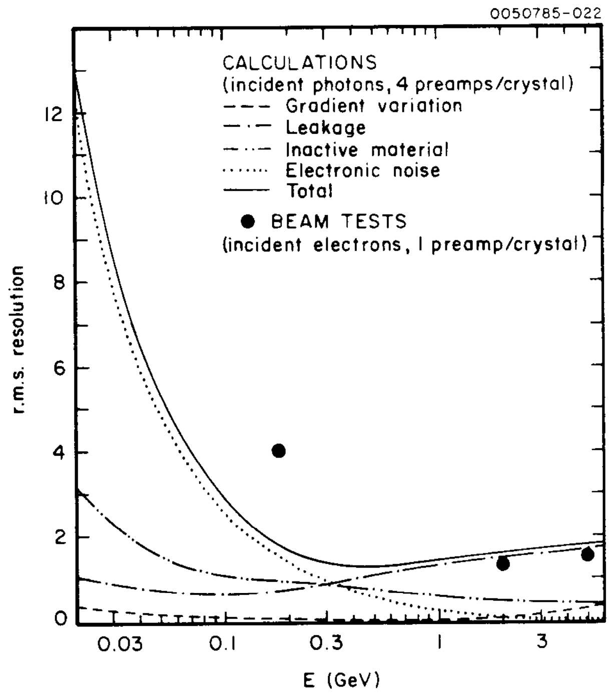

Fig. 2. Calculated rms energy resolution for the CLEO II cesium iodide electromagnetic calorimeter (continuous curve). Also shown are the various contributions to the resolution (broken curves), and test beam measurements (points). The resolution in the test run at 180 MeV was limited by electronic noise, because only one of the eventual four preamps/crystal was installed.

of either a high resolution drift chamber using dimethyl ether or a silicon detector, at a radius of about 2.5 cm.

The CLEO II detector will be the first to combine the advantages of the classic solenoidal magnet detector—(good momentum resolution and identification for charged particles) with the advantages of the crystal calorimeter detector—good energy resolution for photons and electrons. Monte Carlo simulations have convinced us that, very conservatively, this should guarantee us at least a tenfold improvement in B-decay reconstruction efficiency over the existing CLEO and ARGUS detectors. The further gain to be expected from the vertex detector improvement will depend on the minimum radius and spatial resolution we are able to achieve, but is potentially just as great. The CsI shower energy resolution combined with dE/dx in the tracking chambers will make electron identification much more reliable, and the more compact muon detector should do the same for muons, so that lepton tagging and especially dilepton measurements should be greatly improved in CLEO II.

We are convinced that for a B-factory, nothing less than the CLEO II detector is sufficient to do the physics.

3. Storage Ring Improvements

In recent months many have come to realize the potential for important new discoveries in electron-positron collisions in the b threshold region. I know of six different suggestions for high luminosity B-factories, either storage rings or colliding linacs. In any discussion of the merits of one or more of these proposals the question naturally arises, what luminosities can we expect from CESR?

CESR was designed for a peak luminosity per interaction region of 10^{32} cm^{-2} s^{-1} at an energy of 8-on-8 GeV. With an E^2 energy dependence, this means 4.4×10^{31} at 5.29 GeV, the energy of the Υ (4S) resonance where CESR usually runs. CESR is now running at the Υ (4S) with a peak luminosity of over 8×10^{31}, and is the only e^+e^- ring that runs above its design luminosity, as far as I know. But it is not the same machine we designed. Instead of being a single-bunch machine with a β_v^* of 10 cm, it now circulates seven bunches in each beam and collides at $\beta_v^* = 1.5$ cm. Figure 3 is a plot of the maximum luminosity in each week since 1981. The major milestones in the transformation from the original design to the present configuration of CESR are the following:

1981 Quadrupoles moved closer to the IR,
1983 Increased positron source intensity,
Conversion to 3 bunches each beam,
1985 Positron injection in topping-off mode,
1986 Permanent magnet quadrupoles installed closer to the IR,
1987 Conversion to 7 bunches each beam,
Doubled RF cavity installation.

The improvements fall in three categories: (a) multibunch, (b) microbeta, and (c) injection.

In the original single-bunch CESR machine the e^+ bunch collided with the e^- bunch in the two diametrically opposite interaction regions. When there are N bunches in each beam, each e^+ bunch (say $\#1_+$) collides with a particular e^- bunch (say $\#1_-$) at two diametrically opposite points and collides with each of the other e^- bunches ($\#2_-, \ldots, \#N_-$) at $N-1$ other pairs of opposite points. For the same number of particles per bunch, one gains a factor of N in the number of collisions at the two interaction regions occupied by the experiments, but one has to avoid somehow the collisions at the other $2N-2$ points. The right way to do this would be to have the two beams circulate in two independent rings everywhere except at the desired interaction regions, as in the SIN double-ring proposal (see Wille's talk at this workshop). Alternatively, we can separate the two beam orbits vertically or radially at the undesired collision points. In CESR we do this by creating a charge dependent horizontal betatron oscillation with an electrostatic field at the entrance to each 180° arc and cancel it with another field at the exit. The two beams therefore travel the same orbit only in the interaction straights, and oscillate out of phase with each other everywhere else (see Fig. 4). With either 3 or 7

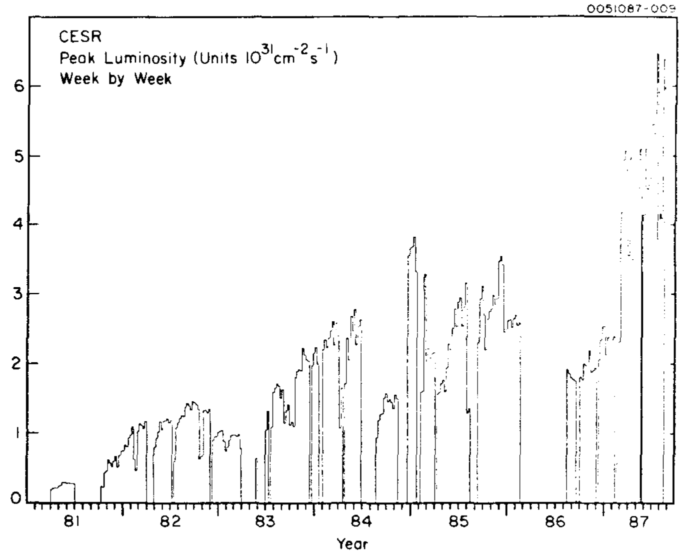

Fig. 3. Maximum CESR luminosity in units of 10^{31} cm^{-2} s^{-1} for each week since 1981.

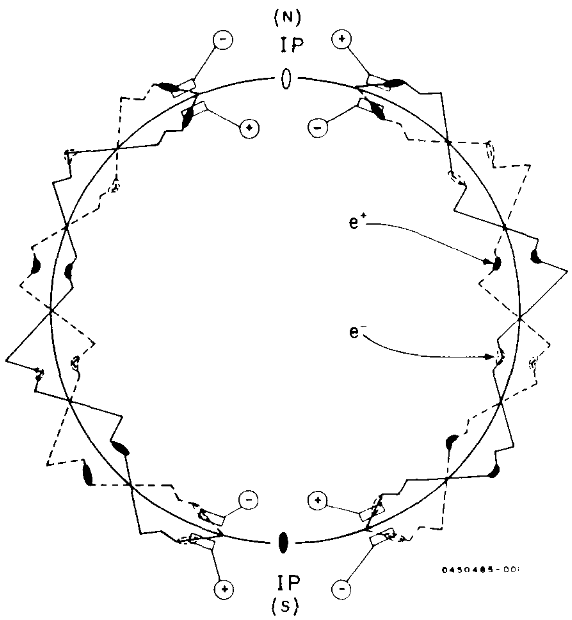

Fig. 4. CESR pretzel orbits for multibunch operation.

equally spaced bunches per beam, the bunches pass each other at antinodes of the *"pretzel"* orbits. We have the equivalent of a two-ring collider with only one ring. The disadvantages are: (a) the expense of having four more electrostatic beam separators, (b) the complexity of injecting into and running with pretzel orbits, and (c) the loss in beam aperture and consequent limitation of beam emittance. The change from one to three bunches per beam brought us only a factor of about 1.5 in luminosity; the later increase to seven bunches gave us the full 7/3 factor, however.

The final focusing element in the interaction regions has been brought closer to interaction point in two stages, first (*"minibeta"*) by moving the last quadrupole into the space formally occupied by the compensation solenoids (compensation is now accomplished by skew quadrupoles elsewhere),

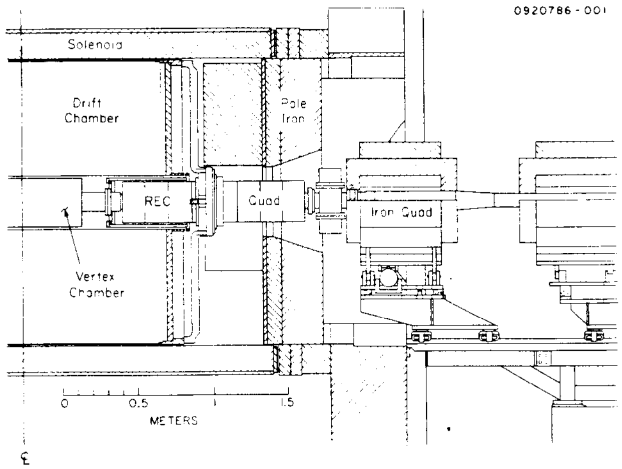

Fig. 5. The CLEO interaction region at CESR, showing the location of the a rare-earth-cobalt quadrupole magnet inside the detector.

and more recently ("*microbeta*") by installing rare-earth-cobalt permanent quadrupoles inside the detectors. Figure 5 shows the geometry inside the CLEO detector, with ± 60 cm free space around the interaction point. The vertical β^* was brought down from its initial value of 10 cm, first to 3 cm and now to 1.5 cm. The luminosity should be proportional to $1/\beta^*$, but is limited by the "*hourglass*" effect, due to the length of the bunch and the variation of β away from the interaction point. In practice also, the maximum bunch current can depend on the β^*. In order to shorten the beam bunch from 2.2 cm to 1.75 cm rms we have raised the peak RF voltage from 4 to 7 MeV/turn. There is still luminosity to be gained shortening the bunch further, with more RF and by raising the horizontal tune from $\nu_h = 9.3$ to 11.3.

Improvements in injection can shorten the time required to refill the ring after the 1 to 2 hour running cycle, and thus tend to improve the average rather than the peak luminosity. The following is a list of some of the improvements already made and contemplated for the future:

- higher current e^+ injection (installed mid-1983),
- improve e^+ injection septum (installed mid-1985),
- topping-off mode for e^+ injection (implemented late-1985),
- improve e^- injection septum (installed mid-1987),
- stabilize linac (in progress),
- reduce wakefield effects between bunches,
- increase linac energy,
- shield CLEO to permit tune up of synchrotron during HEP,
- separate e^+ and e^- linacs,
- damping ring,
- alternate cycle acceleration of e^+ and e^-,
- increased automation in filling.

As of October 1987, the record integrated luminosity per interaction region in CESR is 3.5 pb^{-1} per day. Even with no further changes in equipment, the peak luminosity continues to improve as we optimize the running conditions, and more important, improvements in reliability and reproduceability increase the average luminosity. The cross section on the Υ (4S) resonance is such that we produce 1150 $B\overline{B}$ events per pb^{-1} of integrated luminosity; at 3.3 pb^{-1} per day it takes only 124 days to produce 10^6 B-mesons.

There are more improvements we can make to CESR, however. I list them below in order of priority, with an estimate of the expected average luminosity gain from each:

increase current/bunch from 9 mA to 11 mA	$\times 1.2$
reduce time to fill ring (see list above)	$\times 1.5$
emittance-control wiggler	$\times 1.2$
more aperture & control of beam tails	$\times 1.5$
single IR operation	$\times 1.3$

It may take us several years to accomplish all of these changes, and it may take us even longer (if ever) to achieve the promised luminosity gains. But if we simply multiply the listed factors, we get a net increase of $\times 4.2$. That would imply more than 2×10^{32} cm^{-2} s^{-1}, 15 pb^{-1} per day, or 300 days to produce 10^7 B-mesons. By the time the next B-factory is operating there is a good chance that CESR will have produced 10^8 B-mesons. If we are lucky, that may be enough to make a good measurement of CP violation in B-decays, as well as a host of other rare processes. It is not unreasonable to expect some luck. Nature has been kind in giving us the Υ (4S) resonance so close to $B\overline{B}$ threshold, a B-lifetime long enough to measure, and a healthy $B^\circ\overline{B}^\circ$ mixing rate, all in spite of gloomy theoretical expectations. Maybe CP violation will not be as hard as the theorists now predict.

4. The Future

We are committed to exploiting CESR and CLEO to the fullest. That will certainly occupy most of our energies for some years to come. It does not preclude preparing for future B-factory initiatives, however. It makes no sense for us to propose building a successor to CESR unless it can guarantee much more luminosity, say well above 10^{33} cm^{-2} s^{-1}. With our practical experience in storage ring construction and operation, we are studying the feasibility of a double ring machine for very high luminosity. In parallel, we are also considering the possibility of a linear collider using superconducting cavities, where we also have a lot of experience. I expect that b-quark physics will remain vital for a good time to come, and as long as that is true, we at Cornell intend to remain leaders in the field.

ASPECTS OF B PHYSICS*

MARY K. GAILLARD†

Lawrence Berkeley Laboratory
and
Department of Physics, University of California,
Berkeley, California 94720

1. Probing the Standard Model

As is well-known, the study of B–decays plays an essential role in the determination[1] of the elements of the Cabibbo–Kobayashi-Maskawa (CKM) matrix[2] of charged-current weak couplings, including the CP violating phase δ. In addition, it can shed new light on nonleptonic decay dynamics;[3] here the buzz words are factorization, annihilation and penguins. I will comment in more detail below on various aspects of weak decays.

Perturbative QCD can be further probed by, for example, measurements of inclusive $b\bar{b}$ production in hadron colliders. These measurements are of considerable intrinsic interest, particularly the effects of mass dependence on the approach to scaling. They are also important for extrapolating the $b\bar{b}$ content of structure functions to very high energy machines like the SSC or the LHC. They are in any case an essential prerequisite for meaningful decay studies, in particular for CP violating searches, at hadron colliders.

Somewhere on the borderline between perturbative and non-perturbative QCD, there is the possibility for studying the spectroscopy and static properties of a heavy/light bound state system. Interpolation from the presumably relativistic $b\bar{u}, b\bar{d}$ and $b\bar{s}$ systems to the approximately nonrelativistic $b\bar{c}$ system could provide new insight on quark bound states in QCD.

In the realm of nonperturbative QCD, lattice calculations are a growing industry with an ever widening range of applications. Measurements of f_B, the leptonic B decay constant, and the infamous "bag factor" B_B, to be defined below, can be confronted with the results of lattice calculations,[4] as well as of other calculational techniques such as QCD sum rules[5] and the $1/N$ expansion.[6] These parameters play an important role in the analysis of CP violation and the CKM matrix, so reliable information is needed.

Lattice calculations are now also being applied to the determination of structure functions. One could imagine that experimental measurements of the heavy quark content of structure functions or heavy quark fragmentation functions would eventually be able to further test these calculational techniques.

2. Probing Beyond the Standard Model

One tool for probing new physics is the CKM analysis itself. An inconsistency among data could be interpreted as a signal for a nonstandard effect. An obvious possibility is the existence of one or more additional generations of quarks and leptons. Couplings of known quarks to those of heavier generations destroy the unitarity of the 3×3 CKM submatrix for couplings of the first three generations. Thus at some level a discrepancy should show up.

In addition, new particles could mediate additional contributions to decay matrix elements, either at tree level or at the one loop level that determines $B - \overline{B}$ mixing. Candidate particles include additional Higgs bosons, which are expected, in particular, in supersymmetric extensions of the standard models that also predict superpartners for all known particles. Superstring-inspired models suggest even more exotic new scalars as well as fermions. New gauge bosons can be present in left-right symmetric extensions of the standard electroweak gauge theory and in some superstring-inspired versions.

Another probe of new physics is the study of rare decays.[7] These might involve emission of a new pseudoscalar particle

$$B \to a + X \text{ or } f + X \tag{1}$$

where a is an axion first suggested[8] in the context of a Peccei–Quinn $U(1)$ symmetry invoked[9] to suppress strong CP violation. Axions tend to turn up naturally in supersymmetric models, especially superstring-inspired ones.

In a different vein, some theorists attempt to understand the observed patterns of fermion masses and mixing in terms of a "horizontal symmetry," i.e., a symmetry that interchanges particles of different generations with the same $SU(3)_c \times SU(2)_L \times U(1)$ quantum numbers.[10] This symmetry is obviously broken since these states are not degenerate. If it is a spontaneously broken global symmetry there are necessarily associated goldstone bosons that can be emitted[11] in flavor changing neutral transitions; these are the "familons" f of Eq. (1).

If the horizontal symmetry is gauged, there are neutral gauge bosons that directly mediate lepton and quark flavor-changing interactions, so one expects[10] decays like

$$B \to \left\{ \begin{array}{c} \tau\mu \\ \tau e \\ \mu e \end{array} \right\} + X \quad . \tag{2}$$

Such decays are also predicted in extended technicolor models[12] that have been constructed in attempts to solve the gauge hierarchy problem. They can also be induced by some of the exotic particles of superstring-inspired models.

3. Why B's? (Theory)

Theorists view B–mesons as heavier replicas of K–mesons. The point is that D–decay, as will be T–decay, is dominated by fast CKM allowed transitions: $c \to s$ and $t \to b$. On the other hand, K and B decays can proceed only through first forbidden transitions: $s \to u$ and $b \to c$. This means that rare processes have enhanced branching ratios. B–decay of course provides an additional probe of the CKM matrix through its second forbidden $b \to u$ transition.

CKM suppression of decay rates also enhances flavor changing $|\Delta F| = 2$ transitions that induce meson–anti–meson mixing and superweak CP violation, since these necessarily entail at least first CKM forbidden couplings. The loop diagrams of Fig. 1 induce mass mixing via a mass difference Δm between eigenstates.[13] The GIM mechanism,[14] i.e., unitarity of the CKM matrix, assures that these diagrams cancel exactly in the limit that the internal quark masses are degenerate. The

*This work was supported in part by the Director, Office of Energy Research, Office of High Energy and Nuclear Physics, Division of High Energy Physics of the U.S. Department of Energy under Contract DE-AC03-76SF00098 and in part by the National Science Foundation under grant PHY85-15857.

†On appointment as a Miller Research Professor of the Miller Institute for Basic Research in Science.

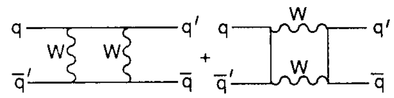

Figure 1: One-loop quark diagrams that contribute to neutral meson–anti–meson mass mixing.

relatively long B lifetime tells us that the first two generations couple rather weakly to the third. This means that Δm_K nearly vanishes for $m_u = m_c$, obviously a bad approximation relative to the scale m_K, but $\Delta m_D \simeq 0$ for $m_s = m_d$, which is an excellent approximation relative to the scale m_D. For Δm_B, t–exchange is comparable to c, u exchange so the GIM cancellation is again badly broken, but it will be quasi-exact for Δm_T.

The width difference $\Delta\Gamma$ can be schematically represented[15] by the cut diagrams of Fig. 2, i.e., the absorptive parts of Fig. 1. For K and B the GIM cancellation is *a fortiori* broken by the fact that the decay energy is below the threshold for charm and top emission, respectively. There is, however, here an essential difference between neutral kaons and B–mesons. K–decay has very limited phase space. As a consequence, approximate CP invariance implies that K_S decays almost exclusively into two pions while K_L has only phase space suppressed 3–body final states: $\Gamma_L \ll \Gamma_S$. In this case "width mixing" is maximal: $\Delta\Gamma_K/\Gamma_K \sim 1$. In contrast, B–decays have a large energy release, so that many channels are open for both CP modes and one expects $\Gamma_1 \simeq \Gamma_2$ for the decay eigenstates. Another difference is that nonleptonic decays of K^0 and $\overline{K}^0$ are into the same (first forbidden) $(n\pi)^0$ channels. Decay channels can be common to B^0 and $\overline{B}^0$ only through an additional Cabibbo suppression factor except for $B_s^0 \leftrightarrow c\bar{c} + X \leftrightarrow \overline{B}_s^0$ which is phase-space inhibited. The net result of these effects is that one expects $\Delta\Gamma_B/\Gamma_B \ll 1$.

The situation is somewhat different when one considers mass mixing and superweak CP violation. In the standard model, observable CP violation can occur only to the extent that a process probes the existence of all three quark generations. To the extent that the third generation decouples from the first two, the loop diagrams, Fig. 1, that determine $K^0 - \overline{K}^0$ mass mixing are dominated by c and u exchange, so one gets[13]

$$\Delta m_K^2 \propto f(m_c^2) G_F^2 \theta_c^2 \tag{3}$$

where the function[16] $f(m_c^2) \simeq m_c^2$ for $m_c^2 \ll m_W^2$, so

$$\Delta m_K/\Gamma_K \propto m_c^2/m_K^2 \sim 1 \quad . \tag{4}$$

On the other hand, CP violation, which determines[17] the imaginary part of Δm_K, requires t–exchange. The smallness of the observed CP violation in the kaon system can be understood in terms of the small $s - t$, and very small $d - t$, couplings.

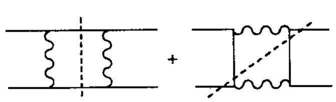

Figure 2: The absorptive parts of the diagrams of Fig. 1 that contribute to width differences in neutral $(q\bar{q}')$ meson systems.

For $B_d - \overline{B}_d$ mixing the presence of the first and third generations in the $(b\bar{d})$ and $(\bar{b}d)$ external states means that the existence of three generations is implicit in the process. More precisely if I denote by $\theta \ll 1$ the degree of forbiddeness of a transition, and by θ_{ij} the CKM matrix element for $i \leftrightarrow j$, the observed CKM pattern

$$\left.\begin{array}{llllll} \theta_{us} & \equiv \theta_c & \sim \theta_{cd} & \sim \theta_{cb} & \sim \theta_{ts} & \sim \theta \\ \theta_{ub} & \sim \theta_{td} & \sim \theta\ 2 & & & \end{array}\right\} \tag{5}$$

implies that u, c and t exchange are of roughly comparable importance for $B_d \leftrightarrow \overline{B}_d$. One finds in fact that the imaginary part of Δm_{B_d} is simply determined by the CP violating phase parameter in the CKM matrix:[18]

$$\arg(\Delta m_{B_d}) \simeq \tan\delta \quad . \tag{6}$$

On the other hand, $B_d - \overline{B}_d$ mixing itself is doubly CKM forbidden

$$\Delta m_{B_d}/\Gamma_{B_d} \propto \theta^2 f(m_t^2) \tag{7}$$

and therefore small[19] unless the top quark mass m_t is large.

In contrast, Δm_{B_s} is dominated by c and t exchange and suffers no CKM suppression relative to the decay width

$$\Delta m_{B_s}/\Gamma_{B_s} \propto f(m_t^2) \quad , \tag{8}$$

but since the first generation is now relatively unimportant, CP violation is expected to be small.

Note that for large m_t, $B - \overline{B}$ mass mixing grows roughly linearly with m_t^2, whereas $\Delta\Gamma_B$ remains fixed (except for the mild, logarithmic dependence of Penguin diagrams — see below — on m_t). Observable "superweak" CP violation arises through a clash of CP violating phases[20] of the contributions of Figs. 1 and 2 and is measurable only if they give comparable contributions to meson–anti–meson mixing. For example, in the standard model the charge asymmetry in same sign dilepton events, $B \to \ell^\pm\ell^\pm + X$:

$$A \equiv \frac{\ell^+\ell^+ - \ell^-\ell^-}{\ell^+\ell^+ + \ell^-\ell^-} \tag{9}$$

is, for small $|\Delta\Gamma/\Delta m|$, given by[20]

$$A \simeq \sin\delta |\Delta\Gamma/\Delta m| \quad . \tag{10}$$

This is expected to be negligibly small for values of m_t as large as those suggested by the data to be analyzed in the next section. This means that one will have to look for CP violating signals by studying particular decay channels, each of which will have a small branching ratio.

B–decay should also provide an interesting new probe of weak decay dynamics.[3] The collective wisdom is that since B–mesons involve a heavier quark, with a higher energy release in their decays, QCD corrections to weak amplitudes should be smaller and better understood than for the lighter K– and D–mesons.

This wisdom is almost certainly well-founded for some applications, notably for penguin diagrams,[21] depicted in Fig. 3. For B–decay, the loop momentum is effectively cut off at the scale $\mu \simeq m_t$. At this scale the effective QCD fine structure constant α_S is small, so the penguin contribution should be well-approximated by the leading single gluon exchange diagram which gives an amplitude

$$A_{Penguin} \propto \theta \frac{\alpha_S(m_t^2)}{4\pi} \ln(m_t^2/m_c^2) \quad . \tag{11}$$

In contrast, for K–decay the loop momentum is cut off at the much lower scale $\mu \simeq m_c$.

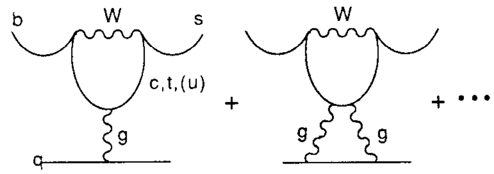

Figure 3: Penguin diagrams for nonleptonic B–decays.

Penguin diagrams in B–decay are particularly interesting because they yield a distinctive final state: $B \to K + \cdots$ at the first CKM forbidden level. Therefore, selecting final states with strange particles that are not charm decay products should enhance the penguin contribution. The competing decay mechanism is a third CKM forbidden transition:

$$b \to u + W^- \quad \hookrightarrow s\bar{u} \quad . \tag{12}$$

Since the matrix elements for (11) and (12) have different phases in the standard model,[2] these final states may also be a good laboratory for studying CP violation. Bjorken[22] has estimated that the two contributions should be of comparable magnitude with the $\alpha_S(m_t^2)$ suppression of the penguin diagrams approximately compensating the extra θ^2 suppression of the decay (12).

QCD corrections also govern the value of the "bag parameter," so named because it was first estimated[23] in the context of the MIT bag model. Specifically, for a neutral pseudoscalar P, $P - \overline{P}$ mass mixing is determined at the quark level by the diagrams of Fig. 1. After loop integration the resulting effective quark-field operator is a $V - A$ current-current operator, shown schematically in Fig. 4a. The matrix element of this effective operator between P and $\overline{P}$ states, which determines Δm_P, is parameterized as

$$\Delta m_P \propto m_P^2 f_P^2 B_P \quad . \tag{13}$$

For $B_P = 1$ this is just determined[13] by the squared P–to–vacuum matrix element

$$\langle P | J_\mu | 0 \rangle = p_\mu f_P \tag{14}$$

evaluated on the P mass shell: $p^2 = m_P^2$. In the context of QCD, after corrections for hard gluon exchange,[24,25] the parameter $B_P \neq 1$ takes into account soft gluon exchange between the two $V - A$ quark currents, Fig. 4b. Conventional wisdom (which seems to be supported by lattice gauge calculations[4,7]) holds that QCD corrections should be small, so that $B_P \simeq 1$, for heavy quark bound states. The physical grounds for this assumption are questionable because a heavy/light bound state

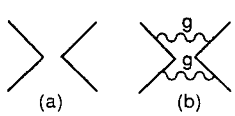

Figure 4: Schematic representations of a) the factorization approximation to the meson–anti–meson matrix element of the effective $\Delta S = 2$ quark operator generated by the diagrams of Fig. 1 and b) QCD corrections to factorization that generate a "bag factor" $B_P \neq 1$.

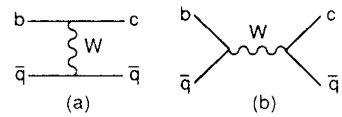

Figure 5: Annihilation diagrams for nonleptonic B–decays in the free quark approximation.

is not really a short-distance system. To tighten the analysis of mass mixing and CP violation, as well as to measure (via Δm) the bag parameter B_B, it is important to have independent measurements of f_P for each pseudoscalar. These measurements also provide tests of nonperturbative QCD calculational techniques.[4–6] Thus one would like to know the partial widths for

$$\left.\begin{matrix} D \\ F \\ B \end{matrix}\right\} \to \tau\nu_\tau \quad . \tag{15}$$

In the important B–decay case, this means measuring very small branching ratios. Bjorken has estimated[26] the branching ratio for $B_c(b\bar{c}) \to \tau\nu_\tau$ at about 1.5%; the decay $B_u(b\bar{u})$ is further suppressed by a double CKM factor θ^2.

Another issue in nonleptonic decay dynamics is the importance of "annihililation" diagrams,[18] Fig. 5, relative to the presumably dominant "spectator" diagram,[27–29] Fig. 6.

For free quarks the annihilation processes of Fig. 5 are helicity suppressed for a $J = 0$ final state with quasi-massless quarks. The argument is identical to that which explains the suppression of $K \to e\nu_e$ relative to $K \to \mu\nu_\mu$. Specifically, the B–decay amplitudes arising from the diagrams of Fig. 5 are determined[18] as

$$A_5 \propto G_F f_B m_q \tag{16}$$

where in Eq. (16) m_q is the mass of the heaviest final state quark. In QCD, gluon emission, Fig. 7, can modify this result, since the final state $q\bar{q}$ pair no longer has to be in a $J = 0$ configuration.[30] The fact that the $D^+(c\bar{d})$ decays more slowly than the $D^0(c\bar{u})$ or the $F^+(c\bar{s})$ is generally attributed to the presence of the annihilation mechanism. The diagrams in Figs. 7a and 7b contribute, respectively, to CKM allowed transitions for D^0 and $F^\pm$. No CKM allowed annihilation process can contribute to $D^\pm$–decay. In contrast, the spectator decay of Fig. 6 is independent of the flavor of the quark bound to the decaying charmed quark. If only this process is important one expects[27–29] equal lifetimes for D^0, D^+ and F^+, up to interference effects[31] that may occur in $D^\pm$–decays, due to the fact that the spectator quark is the same as one of the decay products in the CKM allowed transition. In fact, the difference in lifetimes is much less dramatic than indicated by early experiments and could possibly be attributed[32] solely to destructive interference of spectator diagrams in $D^\pm$–decay.

In any case, the common wisdom[33] is that the annihilation process of Fig. 7 should be less important in B–decay because of the higher mass scalar and thus the smaller effective QCD

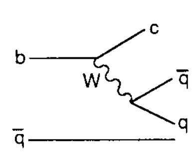

Figure 6: Spectator diagram for nonleptonic B–decays.

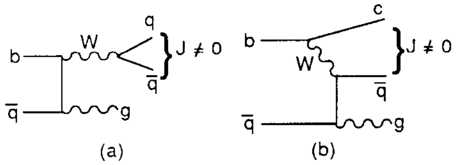

Figure 7: QCD corrections to the diagrams of Fig. 5.

coupling constant. As I noted above, however, a heavy (Q)–light (q) bound quark system is not really a short-distance system. Its inverse size is determined by the reduced mass, which is simply m_q if $m_q \ll m_Q$. Put another way, the distance over which the annihilation processes of Fig. 7 take place is the requisite "off-mass-shellness" of the virtual quark which, for emission of a massless gluon, is of the order of the mass of the quark from which the gluon is emitted. This suggests that the relevant QCD fine structure constant is $\alpha_S(m_q)$ rather than (the much smaller) $\alpha_S(m_Q)$. Within this perspective the $B_c(b\bar{c})$ system is really "small," in that the relevant distance scale is m_c^{-1}. It would therefore be extremely interesting to study the annihilation process in B–decay as a function of the mass of the lighter bound quark. For the $B_s(b\bar{s})$ system CKM allowed annihilation (Fig. 6a or 7b) is signed by a $c\bar{c}$ final state, for example,

$$B_s \to \begin{cases} D\overline{D} & + \quad \pi's \\ \psi & + \quad \pi's \\ \eta_c & + \quad \pi's \end{cases} \quad . \tag{17}$$

Since these final states are also CP eigenstates they may prove useful in the search for CP violating signals;[34] however, each exclusive decay mode of this type is expected[22,26] to have a branching ratio of less than a percent.

To test the dependence of annihilation diagrams on the mass of the lighter bound quark, the importance of the final states (17) in B_s–decay should be compared with the partial lifetimes for B_c–decays to final states accessible via CKM allowed annihilation, namely (Figs. 6b and 7a):

$$B_c \to \begin{cases} \text{pions} \\ DK + X \end{cases} \quad . \tag{18}$$

4. Why B's? (Experiment)

The most recent datum supporting the assertion that B–decays are important is that a single experimental measurement, namely of $B_d - \overline{B}_d$ mixing, instantaneously generated a large number of (for the most part good) theoretical papers.

In fact there have been three recent experimental measurements of prime importance for probing the standard model, namely:

1. The observation[35] of B–decay into a noncharmed final state ($p\bar{p} + X$). This (almost certainly) demonstrates the existence of a direct $b\bar{u}W$ + coupling, without which CP violation would be inexplicable in the framework of the standard model.

2. The observation[36] that $\epsilon'/\epsilon \neq 0$. This is the first positive indication for CP violation other than in $K^0 - \overline{K}^0$ (superweak) mass mixing, and is an equally important result for substantiating the standard model.

3. A substantial $B_d - \overline{B}_d$ mixing.[37] This result was at first sight surprising because $B_d - \overline{B}_d$ mixing was predicted[19] to be rather smaller than observed, under the assumption of a relatively light ($m_t \lesssim 40$ GeV) top quark. As I shall outline below, however, the observed values of ϵ'/ϵ and $B_d - \overline{B}_d$ mixing are quite consistent with the standard model, provided that the top quark mass is rather large.[38–40]

The logic of the analysis of these recent results is as follows. The relative yield of same-sign dileptons in $B_d - \overline{B}_d$ events:

$$r_d = \frac{\ell^+\ell^+ + \ell^-\ell^-}{\ell^+\ell^-} \tag{19}$$

determines (neglecting, as argued above, "width mixing," $\Delta\Gamma \simeq 0$) the B mass-mixing parameter which is governed by the diagrams of Fig. 1. For a large top quark mass the dominant contribution is double t–exchange, giving a contribution:

$$\Delta m_{B_d} \propto \theta_{td}^2 f(m_t^2) \quad . \tag{20}$$

Using the standard parametrization[1,2] of the KM matrix in terms of three angles $\theta_1 \simeq \theta_c, \theta_2$ and θ_3 and a phase δ, the $t \leftrightarrow d$ matrix element

$$\theta_{td} \simeq s_c s_2 \tag{21}$$

(here $s_i \equiv \sin\theta_i$) is related by unitarity[2,14] of the CKM matrix to other measured CKM matrix elements. The B–decay lifetime, dominated by the $b \to c$ transition, determines[18,41] the element

$$|\ \theta_{bc}\ | = |\ s_3 + s_2 e^{i\delta}\ | \quad . \tag{22}$$

The CKM suppressed $b \to u$ transition is experimentally bounded. The experimental limit[42] on the branching ratio

$$R = \frac{b \to u}{b \to c} \tag{23}$$

can be, together with B–lifetime measurements,[43] interpreted as a limit on the $b \to u$ transition matrix element:

$$|\theta_{bu}| = |s_c s_3| \quad . \tag{24}$$

The Cabibbo angle, or s_c, is a well-measured quantity. The experimental bounds[42] on the ratio R, Eq. (23), imply a small value for s_3. This in turn, together with a rather long[43] B–lifetime that bounds θ_{bc}, Eq. (22), implies that s_2, and hence θ_{td}, Eq. (21), cannot be very large. As a result, the substantial value observed[37] for $B_d - \overline{B}_b$ mixing implies that the function[16] $f(m_t^2)$, which, for $m_t^2 < m_W^2$, grows with m_t^2, must be large. Numerical analyses have been performed by several groups[38–40,44] who for the most part conclude[38–40] that existing data imply at least $m_t \gtrsim 50$ GeV and, more probably, $m_t \gtrsim 100$ GeV. A dissenting view has been registered by one group[44] that claims that present data allow m_t as low as the roughly 20 GeV limit imposed by the nonobservation of $t\bar{t}$ production at PEP and PETRA. The latter authors, however, allow values for the unknown parameters in the analysis, namely f_B, B_B and the ratio R of Eq. (23), that most theorists would probably consider as unreasonable. I emphasize once again the importance of independent measurements of these parameters.

Once the observed $B_d - \overline{B}_d$ mixing has been assimilated within the standard model, the resulting restrictions on allowed values for the parameters of this model have implications for other measurable quantities. Consider first CP violation in the $K^0 - \overline{K}^0$ system. Superweak CP violation (i.e., CP violation in mass mixing) is determined[17] by the imaginary parts of the diagrams of Fig. 1. The CP violating part of these diagrams involves t–quark exchange; this contribution grows as m_t^2 for $m_t < m_W$. Thus the parameter ϵ, which measures the CP violating component of Δm_K, grows roughly as m_t^2. On the other

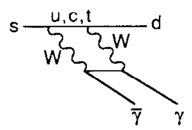

Figure 8: One-loop contribution to the $s \to d\nu\bar{\nu}$ transition in the standard model.

hand, direct CP violation in decays other than the 2π isospin zero mode used to define the superweak CP violating phase, and in particular the parameter ϵ' which measures the CP violating phase in the 2π $I = 2$ mode relative to the $I = 0$ phase, is governed[45] by Penguin diagrams, as in Fig. 3, that grow only logarithmically with m_t. Thus the ratio ϵ'/ϵ decreases[46] with increasing m_t for $m_t < m_W$. As a consequence, the large value for m_t inferred from the $B_d - \overline{B}_d$ mixing measurement[37] is consistent[38] with the small observed[36] value for ϵ'/ϵ in the context of the standard model.

This picture implies predictions for as yet unmeasured quantities. For example, it is inferred[38,39] that $B_s - \overline{B}_s$ mixing should be nearly maximal. In addition, the $K + \to \pi + \bar{\nu}\nu$ branching ratio prediction is sharpened. This occurs[13,47] in the standard model through the loop diagram of Fig. 8, and, since it is GIM suppressed, grows in importance for large m_t. One finds[38]

$$B(K^+ \to \pi^+\nu\bar{\nu}) \simeq (1-8)10^{-10} \tag{25}$$

for $m_t = (50 - 200)$ GeV. (The experimental bound on the parameter $\rho - 1$ where $\rho = m_W/m_Z \cos\theta_w$ implies[48] an upper limit of about 200 GeV on m_t.) It has also been pointed out[49] that a top quark mass as large as 200 GeV could give a possibly observable branching ratio for the rare neutral current flavor changing B–decay:

$$B(B^+ \to K^+ + \ell^+\ell^-) \sim 10^{-5} \quad . \tag{26}$$

More generally, the measured $B_d - \overline{B}_d$ mixing[37] tightens the values of the CKM matrix elements and hence the quark mass matrices, which, when diagonized, determine the CKM matrix. A recent analysis[50] has all but ruled out specific conjectures for the form of the quark mass matrices, partially based on GUTs models.

The implications of this measurement[37] for physics beyond the standard model has also been analyzed.[39] Contributions from supersymmetric partners of ordinary particles and/or additional Higgs scalars are found to enhance $B - \overline{B}$ mixing. Thus a smaller value of m_t than that inferred in the standard model would be compatible with the data if either of these effects are present.[39] On the other hand, $B\overline{B}$ mixing is found to be relatively suppressed in left–right–symmetric extensions of the electroweak gauge theory; an even higher top quark mass limit is inferred in the context of these theories.[39]

5. A Superstring–Inspired Example of Exotic Physics

Models inspired by the $E_8 \times E_8$ heterotic[51] superstring[52] theory end up in four dimensions[53] with an (already broken) $E_8 \times E_6$ gauge theory. Here E_8 (or a subgroup thereof) describes a pure supersymmetric Yang Mills theory of a so-called "hidden sector" that interacts only gravitationally with observed matter, and E_6 is the GUT of the observed world. The unbroken subgroup of E_6 at scales just below the compactification scale must contain the observed gauge group $SU(3)_c \times SU(2)_L \times U(1)$. Each matter generation fills a 27–plet of E_6 which decomposes under $SU(5)$ as:

$$27 = (\bar{5} + 10) + (5 + \bar{5}) + 1 + 1 \quad . \tag{27}$$

In (27) the $(\bar{5} + 10)$ supermultiplets contain quarks (q) and leptons (ℓ) and their superpartners, squarks ($\tilde{q}$) and sleptons ($\tilde{\ell}$). Each $(5 + \bar{5})$ supermultiplet contains a Higgs (H) and Higgsino ($\widetilde{H}$) super-multiplet that is a weak isopin doublet, as well as a color triplet supermultiplet $(D, \widetilde{D})$ which has the same flavor quantum numbers under $SU(3)_c \times SU(2)_L \times U(1)$ as the right-handed d–quark. There are as many $(5 + \bar{5})$ supermultiplets as matter generations. This means that there is a large number of physical Higgs particles as well as other exotic states. If there are no discreet symmetries to forbid them, there will be generation mixing couplings among the $(\bar{5} + 10)$ and $(5 + \bar{5})$ multiplets, which, if the masses of the later are not very large, will induce[54] effective Flavor Changing Neutral Current (FCNC) transitions among light particles, via the diagrams of Figs. 9 (a–c). In addition, the possibility of d–D mixing potentially spoils[54] the GIM mechanism that in the standard model forbids the tree level FCNC process of Fig. 9d, where Z' represents on additional neutral gauge boson that is present if the surviving gauge group in four dimensions is larger than the standard one. If present, all of the processes of Fig. 9 would contribute to Δm_B (and Δm_K), and therefore to the parameter r_d of Eq. (19). Neglecting $\Delta\Gamma_B$, the experimental result[37] implies a bound[54]

$$r_d \simeq \frac{1}{2}\frac{\Delta m_B}{\Gamma_B} \lesssim 0.3 \tag{28}$$

or

$$\Delta m_B \lesssim 4 \times 10^{-13} \text{ GeV} \tag{29}$$

which is in the ballpark of

$$\Delta m_K = 3.5 \times 10^{-15} \text{ GeV} \quad . \tag{30}$$

This means that constraints on new phenomena from Δm_B are comparable to those from Δm_K. For example, assuming $m_{H,\widetilde{H}} \simeq 100$ GeV, $m_{D,\widetilde{D}} \simeq 300$ GeV $\simeq m_{Z'}$ the bounds[54] on new couplings λ involving external b–quarks in the diagrams of Fig. 9:

$$\lambda_b < 10^{-4} - 0.1 \tag{31}$$

are comparable to these involving external s–quarks:

$$\lambda_s < 10^{-5} - 0.1 \quad . \tag{32}$$

Note moreover that (31) and (32) are independent, since couplings involving different matter generations are *a priori* independent.

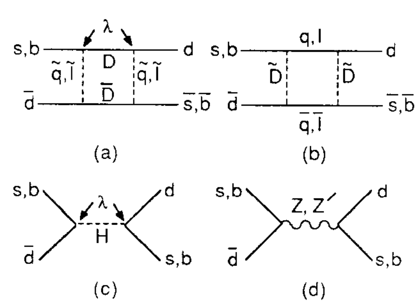

Figure 9: Diagrams that can generate $B_d^0 - \overline{B}_d^0$ and $K^0 - \overline{K}^0$ mixing in superstring-inspired models.

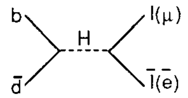

Figure 10: Diagram that can generate $B \to X + \ell^+\ell^-$ or $\mu^\pm e^\mp$ in superstring-inspired models.

The new couplings suggested by superstring-inspired theories should also induce FCNC semi-leptonic decays. For example, the experimental branching ratio bound

$$B(B \to \ell^+\ell^- + X) < 6 \times 10^{-3} \qquad (33)$$

implies[54] the limit

$$\lambda_b \lambda_\ell < (0.06)^2$$

on the couplings of b-quarks and leptons to additional Higgs bosons with $m_H \simeq 100$ GeV, Fig. 10, as suggested by some superstring-inspired models.

6. Conclusions

I hope that I have made it clear that any data on B-decays is at present extremely interesting, in that it provides powerful new constraints in analyses of the standard model and extensions thereof.

Thinking about future detectors and/or facilities for B-meson studies should have as the primary objective the ability to study CP violation. This will be difficult. Bjorken[55] has estimated that at least 3×10^7 $B\overline{B}$ production events are needed for meaningful CP violation studies. This is actually his optimistic estimate, revised upward because of the observed substantial $B_d - \overline{B}_d$ mixing that may facilitate observation of CP violating effects in neutral B-decays. Bjorken's reasoning[55] is as follows:

a) A specific state must be reconstructed. This involves either a CKM-forbidden noncharmed final state, a somewhat phase-space suppressed $c\bar{c}$ final state, or a decay chain $B \to D + f$, $D \to f'$ entailing the product of two small branching ratios for fixed f and f'. Therefore, the overall branching ratio for any given final state will be no larger than $10^{-3} - 10^{-4}$.

b) The associated B or $\overline{B}$ must be flavor-tagged by identifying the charge of a decay lepton and/or the strangeness of the hadronic decay products. This will entail another suppression factor of at least 10^{-1}.

c) Sufficient statistics, at least 10^3 events, must be accumulated for a meaningful search for CP violation in a particular channel.

A necessary prerequisite for CP violation studies is a good knowledge of production rates and distributions and decay branching ratios. Production and decay branching ratios will provide important data for the standard model, as well as sharpen the choices for the best line of attack on CP violation.

A secondary goal for new facilities or detectors is to push, as far as possible, limits on rare decays. These can provide powerful constraints on proposed extensions of the standard model — or perhaps one day provide a real signal for new physics.

References

1. For reviews see, L. -L. Chau, Phys. Rep. **C95**, 1 (1983); A. J. Buras, Proc. 1985 International Europhysics Conference on High Energy Physics, L. Netti and G. Preparata, Eds. (Lazarus, 1985) p. 1035.

2. N. Cabibbo, Phys. Rev. Lett. **10**, 531 (1963); M. Kobayashi and T. Maskawa, Prog. Theor. Phys. **49**, 652 (1973).

3. For reviews see, M. K. Gaillard, Proc. 1978 Summer Inst. on Particle Physics, SLAC Report No. 215, Martha Zipf, Ed. (1978) p. 397; R. Rückl, Ph. D. Thesis (CERN preprint, 1985); A. J. Buras, Ref. 1.

4. N. Cabibbo, G. Martinelli and R. Petronzio, Nucl. Phys. **B244**, 381 (1984); R. C. Brower, G. Maturana, M. B. Gavela and R. Gupta, Phys. Rev. Lett. **53**, 1318 (1984); C. Bernard, G. Hockney, A. Soni and T. Draper, Proc. Tallahassee Conf. (1985) p. 113.

5. E. V. Shuryak, Nucl. Phys. **B198**, 83 (1982); A. R. Zhitnitskii, I. R. Zhitnitskii and V. L. Chernyak, Sov. J. Nucl. Phys. **38**, 773 (1983); T. M. Aliev and V. L. Eletskii, Sov. J. Nucl. Phys. **38**, 936 (1983); M. A. Shifman and M. B. Voloshin ITEP–54 (1986); L. J. Reinders, H. Rubenstein and S. Yazaki, Phys. Rep. **127**, 1 (1985); A. Pich and E. de Rafael, Phys. Lett. 158B, 477 (1985); S. Narison, CERN–TH 4768/87 (1987).

6. A. J. Buras and J. -M. Gerard, Nucl. Phys. **B264**, 371 (1986).

7. See A. Soni, these preceedings.

8. S. Weinberg, Phys. Rev. Lett. **40**, 223 (1978); F. Wilczek, Phys. Rev. Lett. **40**, 279 (1978).

9. R. D. Peccei and H. R. Quinn, Phys. Rev. **D16**, 1791 (1977).

10. For a review, see R. N. Cahn and H. Harari, Nucl. Phys. **B176**, 135 (1980).

11. F. Wilczek, Proc. 1983 Erice Summer School on Subnuclear Physics, p. 157.

12. See, Dynamical Gauge Symmetry Breaking, E. Farhi and R. Jackiw, Eds. (World Scientific, Singapore, 1982).

13. M. K. Gaillard and B. W. Lee, Phys. Rev. **B10**, 897 (1974); A. I. Vainshtein and J. B. Khriplovich, JETP Lett. **18**, 83 (1973).

14. S. L. Glashow, J. Iliopoulos and L. Maiani, Phys. Rev. **D2**, 1258 (1970).

15. J. S. Hagelin, Phys. Rev. **D20**, 2893 (1979).

16. T. Inami and C. S. Lim, *Prog. Theor. Phys.* **65**, 297 (1981).

17. J. Ellis, M. K. Gaillard and D. V. Nanopoulos, Nucl. Phys. **B109**, 213 (1976).

18. J. Ellis, M. K. Gaillard, D. V. Nanopoulos and S. Rudaz, Nucl. Phys. **B131**, 285 (1977).

19. J. Hagelin, Nucl. Phys. **B193**, 123 (1981); T. Brown and S. Pakvasa, Phys. Rev. **D31**, 1661 (1985); I. I. Bigi and A. I. Sanda, Phys. Rev. **D29**, 1393 (1984); V. Barger and R. J. N. Phillips; Phys. Lett. **143B**, 259 (1984); A. Ali and C. Jarlskog, Phys. Lett. **144B**, 266 (1984); A. J. Buras, W. Slominski and H. Stegel Nucl. Phys. **B238**, 529 (1984) and **B245**, 369 (1984).

20. A. Pais and S. B. Treiman, Phys. Rev. **D12,** 2744 (1975).

21. M. A. Shifman, A. I. Vainshtein and V. I. Zakharov, Phys. Lett. **65B**, 255 (1976).

22. J. D. Bjorken, *A Forward Spectrometer for B Physics,* Talk at the Berkeley SSC Workshop, July 1987.

23. R. E. Shrock and S. B. Treiman, Phys. Rev. **D19,** 2148 (1979); J. Trompetic, Phys. Rev. **D27,** 1656 (1983); P. Colic et al., Nucl. Phys. **B221**, 141 (1983).

24. M. I. Vysotskii, Sov. J. Nucl. Phys. **31,** 797 (1980).

25. F. J. Gilman and M. B. Wise, Phys. Rev. **D27,** 1128 (1983).

26. J. D. Bjorken, *Estimates of Decay Branching Ratios for Hadrons Containing Charm and Bottom Quarks,* Fermilab Internal Report (1986).

27. M. K. Gaillard, B. W. Lee and J. L. Rosner, Rev. Mod. Phys. **47**, 277 (1975).

28. G. Altarelli, N. Cabibbo and L. Maiani, Phys. Rev. Lett. **35**, 635 (1975).

29. J. Ellis, M. K. Gaillard and D. V. Nanopoulos, Nucl. Phys. **B100**, 313 (1975).

30. N. Christ, private communication to M. K. Gaillard; Proc. 9th International Symposium on Lepton and Photon Interactions at High Energy, T. B. W. Kirk and H. D. I. Abarbanel, Eds. (Fermilab, 1979) p. 397; S. P. Rosen, Phys. Rev. Lett. **44,** 4 (1980); M. Bander, D. Silverman and A. Soni, Phys. Rev. Lett. **44,** 7 (1980); H. Fritzsch and P. Minkowski, Phys. Lett. **90B,** 455 (1980); V. Barger, J. P. Leveille and P. M. Stevenson, Phys. Rev. Lett. **44,** 226 (1980); W. Berenreuther, O. Nachtmann and B. Stech, Zeit. fur Physik **C4,** 257 (1980); K. Shizuya, Phys. Lett. **100B**, 79 (1981).

31. B. Guberina, S. Nussinov, R. D. Peccei and R. Rückl, Phys. Lett. **89B**, 111 (1979); Y. Koide, Phys. Rev. **D20,** 1739 (1979); K. Jagannathan and V. S. Mathur, Phys. Rev. **D21,** 3165 (1980).

32. See, for example, B. Steck, Non Leptonic Weak Decays, HD–THEP–87–18, San Miniato Topical Seminar on Heavy Flavors, 1987.

33. See, for example, B. Guberina, Fizika **16**, 49 (1984).

34. See, I. I. Bigi, these proceedings.

35. Argus collaboration, B. D. Mac Farlane, Proc. SLAC Flavor Workshop, Sept. 1987.

36. NA–31 collaboration (CERN–Dortmund–Edinburgh–Mainz–Orsay–Pisa–Siegen), A. Nappi, Proc. SLAC Flavor Workshop, Sept. 1987.

37. Argus collaboration, H. Albrecht et al., Phys. Lett. **192B,** 245 (1987).

38. J. Ellis, J. S. Hagelin and S. Rudaz, CERN preprint CERN–TH. 4679/87, MIU–TPH–87/011, UMN–TH–602/87 (1987).

39. G. Altarelli and P. Franzini, CERN preprint CERN–TH–4745/87 (1987).

40. L. -L. Chau and W. -Y. Keung, Davis preprint UCD–87–02(1987); I. I. Bigi and A. I. Sanda, SLAC–PUB–4299 (1987); D. -S. Du and Z. -Y. Zhao, IASSNS–HEP–87/23 (1987); W. A. Kaufman, H. Steger and Y. -P. Yao, Michigan preprint UM–TH–87–13 (1987); L. Angelini, L. Nitti, M. Pellicoro and G. Preparata, Phys. Lett. **195,** 469 (1987).

41. N. Cabibbo and L. Maiani, Phys. Lett. **79B**, 109 (1978); M. Suzuki, Nucl. Phys. **B145,** 420 (1978).

42. CUSB Collaboration, C. Klopfenstein et al., Phys. Lett. **130B,** 444 (1983); CLEO Collaboration, A. Chen et al., Phys. Rev. Lett. **52,** 1084 (1984); E. H. Thorndike, Proc. Int'l Symposium on Lepton and Photon Interactions at High Energy, Kyoto, Japan (1985).

43. Mark II Collaboration, T. Schaad et al., Phys. Lett. **160B**, 188 (1985).

44. J. R. Cudell, F. Halzen, X. -G. He and S. Pakvasa, Madison preprint MAD/PH/353, UH–511–622–87 (1987).

45. F. J. Gilman and M. B. Wise, Phys. Rev. **D20,** 2392 (1979).

46. F. J. Gilman and J. S. Hagelin, Phys. Lett. **133B,** 443 (1983); A. J. Buras et al., Ref. 19; L. Wolfenstein, Comments Nucl. Part. Phys. **14,** 443 (1983); J. F. Donoghue, B. R. Holstein and G. Valencia, UM HEP 272 (1987) (to be published in J. Mod. Phys. A).

47. F. J. Gilman and J. Hagelin, Ref. 46; J. Ellis and J. S. Hagelin, Nucl. Phys. **B217,** 189 (1983).

48. M. Veltman, Nucl. Phys. **B123,** 89 (1977); M. S. Chanowitz, M. A. Furman and I. Hinchliffe, Nucl. Phys. **153,** 402 (1979).

49. X. -G. He and S. Pakvasa, Hawaii preprint, UH–511–619–87 (1987).

50. H. Harari and Y. Nir, Phys. Lett. **195,** 586 (1987).

51. D. J. Gross, J. A. Harvey, E. Martinec and R. Rohm, Phys. Rev. Lett. **54,** 502 (1984).

52. M. B. Green and J. H. Schwarz, Phys. Lett. **149B,** 117 (1984).

53. P. Candelas, G. Horowitz, A. Strominger and E. Witten, Nucl. Phys. **B258,** 46 (1985).

54. B. Campbell et al., International Journal of Modern Physics **A2,** 831 (1987).

55. J. D. Bjorken, talk presented at the International Symposium for the Fourth Family of Quarks and Leptons, UCLA (1987).

BEAUTY PHYSICS AT FERMILAB FIXED TARGET ENERGIES

B. Cox
Fermi National Laboratory,
Batavia, IL 60510

Summary

The very high luminosities ($\gg 10^{32}$ cm^{-2} sec^{-1}) available in the Fermilab fixed target experimental areas offer immediate opportunities for producing large samples ($> 10^8$) of B–hadrons in individual experiments. The possibilities of accumulating large samples of B–decays are limited by experimental techniques and trigger strategies and not by available luminosity. At the present time one experiment, E771, is approved to begin B physics experimentation and several other experimental possibilities are being discussed. Some of the problems and the potential of B–experiments at fixed target energies as b–factories are discussed.

1. Introduction

The weak decays of B–hadrons offer perhaps the one remaining experimental opportunity to study CP violation. To date, CP–violation effects have been observed only in the decays of K–mesons. Since the observation of CP effects will require substantial statistics, a great deal of attention has been devoted recently to evaluating the possibilities of accumulating large samples of B–decays at the SSC[1,2,3] and at the TEV I collider.[4,5] The possibilities for various types of e^+e^- B–factories[6] have also been extensively discussed. All of these possibilities must be considered to be relatively far in the future. A much more immediate possibility for attaining large samples of B–hadrons is available using the hadron beams in the Fermilab TEV II fixed target experimental areas.[7,8] Indeed, the experimental configurations necessary to perform such experiments at TEV II bear a striking resemblance to those necessary for SSC experiments. This similarity adds extra impetus to the investigation of the TEV II possibilities. It is the purpose of this paper to investigate the potential and discuss some of the problems of fixed target B–experiments.

2. Comparison Yields of $B\overline{B}$ for Various Experimental Options

The comparison of fixed target options for B physics and various hadron and e^+e^- collider options is a complex enterprise. There may be no clear cut global choice based solely on experimental feasibility and physics if we ignore cost comparisons and possible schedules for implementation. We show Table I, extracted from Ref. 7, which gives the $B\overline{B}$–event yields for 10^7 seconds of operation of experiments at TEV II (Fermilab fixed target), TEV I (Fermilab collider) and the SSC. In a similar spirit, Table II, extracted from Ref. 6, compares the yields of B's for 200 days of operation of various e^+e^- experimental options to E771[8] (the only TEV II fixed target B experiment approved thus far) and to future possible Fermilab collider experiments. Several general conclusions can be drawn from these tables, ignoring for the time being all the complex differences and relative feasibilities of the various experiments that must be mounted to take advantage of these yields.

First, it is clear that the ultimate B–hadron yields of the present and the various future e^+e^- options lie considerably below the potential yields of all the hadroproduction experiments because of the luminosities of electron-positron colliders and the much lower cross sections for electroproduction of B's. The most promising e^+e^- options in Table II (which are far in the future) are at least an order of magnitude lower in yield of B's than the yield that is expected for the fixed target hadroproduction experiment, E771. In addition, while one might think that e^+e^- production of B's would be a somewhat cleaner process that hadroproduction, thereby allowing a greater percentage of the B's decays to be detected and

Table I. Comparison of Beauty Hadroproduction at Different Machines (from Ref. 7).*

	TEV II	TEV I	SSC
$\sqrt{s}$ (TeV)	.041	1.8	40
$\sigma(b\bar{b})$ (cm^2)	$\approx 2.4 \times 10^{32}$	$\approx 1.5 \times 10^{-29}$	$\approx 1.0 \times 10^{-28}$
$\sigma(b\bar{b})/\sigma_T$ (pN)	$\approx 0.75 \times 10^{-6}$	$\approx 1.5 \times 10^{-4}$	$\approx 10^{-3}$
$\#b\bar{b}/10^7$ sec	$\approx 0.75 \times 10^8$	$\approx 1.5 \times 10^9$	$\approx 10^{11}$
Int/10^7 sec	$\approx 10^{14}$	$\approx 10^{13}$	$\approx 10^{14}$
$\langle p_b \rangle < 45°$	145 GeV/c	38 GeV/c	130 GeV/c
$\langle p_B \rangle$ into det.	118 GeV/c	32 GeV/c	60 GeV/c
$\langle n \rangle$ into det.	≈ 8	≈ 100	≈ 35
$\gamma\beta c\tau$	$\approx .7$ cm	$\approx .2$ cm	$\approx .3$ cm

* For purposes of estimating the detector dependent entries in this table, the detectors for TEV II (Fermilab Experiment E771[8] is taken as a model) and the SSC[1,2,3] have been taken to be relatively forward along a given beam direction. Because of the low momentum and wide angular distribution of the B–hadrons at TEV I, the TEV I detector has been assumed to be a 4π detector. The calculation of the average momentum of the b–quark has been done for b's in an angular cone of 45° around the beam direction for all three experimental configurations.

Table II. Various Future (Mid 1900's) B Sources (from Ref. 6).

Sources	E_{cm} (GeV)	σ_T (nb)	Frac$_{B's}$	Luminosity/ day	BB/ 200 day
TEV II (Fixed Target)	40	5×10^7	5×10^{-7}	2.8 pb^{-1} (E771)	$1.6 \times 10^{7**}$ (E771)
TEV I (Collider)	2000	1×10^8	5×10^{-5}	0.03 pb^{-1}	3×10^7
SIN New CESR	10.6 (4S)	3.9	0.26	15 pb^{-1}	3×10^6
SFB-Multi Bunch PEP	26	0.5	0.09	175 pb^{-1}	1.5×10^6
SLC (SLD)	92	40	0.13	0.2 pb^{-1*}	2×10^5
LEP	92	40	0.13	0.6 pb^{-1}	6×10^5

* For SLC $\langle L \rangle = L_{peak}/2$, for storage rings $\langle L \rangle = L_{peak}/3$.

** As an example of fixed target experiments, this number is appropriate to the updated E771 experiment objectives, assuming operation at 10^6 int/sec with 23 seconds of spill every 60 seconds. The intention of the experiment, however, is to attempt to move toward operation at 10^7 int/sec.

reconstructed (especially since operation at the Υ (4S) resonance produces events with only a B and $\overline{B}$), there are formidable problems reconstructing B's in this type of experiment. The fact that the B and $\overline{B}$ are produced at rest with respect to one another in e^+e^- interactions at the 4S leads to great difficulties in untangling their decay products, since the secondary vertices cannot be distinguished. This combinatorial difficulty has resulted in only a couple of hundred B's reconstructed out of the quarter of a million produced during the lifetimes of the ARGUS and CLEO experiments at DESY and at Cornell.[9] In addition, no B–hadron has been reconstructed thus far at the higher energy e^+e^- machines, PEP and PETRA. This is partially because of the much smaller cross sections for electroproduction of B's other than that of the Υ (4S) resonance, but mainly because secondary vertices are not observed.

The development of microstrip detectors, fast online trigger processors, fast data acquisition systems and sufficient computing power to compute 10^8–10^9 trigger experiments, together with the unique features of the B–decays (especially the long lifetime[10] of 1.42×10^{-12} seconds) have given rise to the possibility that hadroproduction of B's may be the optimal way of obtaining a large sample of B–decays. The fixed target photoproduction experiment, E691, has demonstrated the power of microvertex detectors in detecting and reconstructing charm through detection of the charm secondary vertices. However, the low-yield, high-energy photons (due to the tertiary nature of Fermilab fixed-target photon beams) and the small cross sections for B–photoproduction does not point us toward photoproduction as the optimal place to accumulate large numbers of B's.

Instead, attention has slowly been focused on hadroproduction, both at the CERN SPS and Fermilab TEV II fixed target experiments and at the TEV I and CERN colliders as the most promising possibilities for producing large B–samples. The presence of a resolvable secondary vertex coupled with clever trigger strategies can help overcome the small size of the B–hadroproduction cross section relative to the large hadronic total cross section. The ratio of these cross sections, as shown in Table I, varies between 10^{-6} at the Fermilab fixed target hadroproduction energies and 10^{-3} at the SSC. Therefore, the hadroproduction experiment which seeks to study a particular exclusive mode (typically having a 10^{-4} branching ratio) must be able to select one in ten billion interactions at TEV II. There is thus a premium on good triggers to select the appropriate interactions and striking features of desired exclusive decays to allow offline separation of signal from backgrounds. While the ratio of cross sections (approximately 10^{-4}) is more favorable at present collider energies, the relatively low momentum of the large majority of the B's produced at TEV I and the CERN collider, and the presence of the huge multiplicities in the high-energy interactions, present daunting experimental obstacles to both online triggering and separation of the B's from backgrounds offline. Not until one reaches SSC energies (as shown in Table I) does the average momentum of the B's approach the momentum of the Lorentz-boosted TEV II B–mesons and does the decay product momenta become appreciable.

While formidable, the difficulties of selecting the B–production from the large hadronic total cross section in fixed target experiments are not insurmountable. Strategies, involving single lepton and lepton pair triggers,[8,11,12] have already been discussed (and, in the case of E771, the J/Ψ trigger strategy has been approved for experimentation). Such trigger strategies have the potential of rejecting the total cross section at the level of 10^6 while preserving a substantial fraction of interesting B–decays. We concentrate on fixed target options for B–experiments in this paper.

In the following discussions we will briefly weigh the various fixed-target hadroproduction options. More detailed work will have to be done by the advocates of any approach to

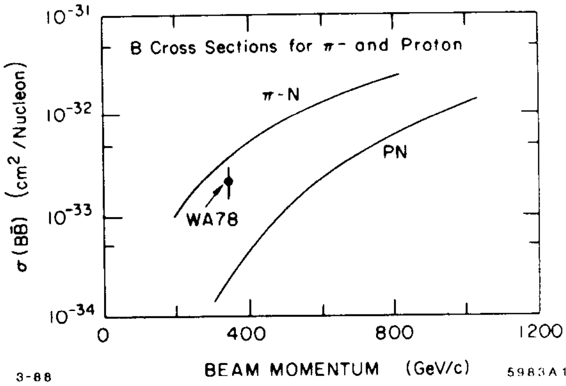

Fig. 1. B–hadroproduction cross sections for π^-N and pN interactions at fixed target experiment energies.

B physics experimentation (including e^+e^- experiments) to completely evaluate the different techniques by the correct meter stick, the number of fully reconstructed B–decays. Indeed, an even more stringent meter stick must be applied in the search for CP–violating effects in B–decay, i.e., the number of fully reconstructed B–decays in a particular exclusive mode that can be both fully reconstructed and tagged as being a B or $\overline{B}$ at $t = 0$ (at production).

3. Features of Hadroproduction of Beauty Hadrons

There is only a small amount of data available on hadroproduction of beauty at fixed-target energies at the present time. The WA78 experiment at CERN has inferred[13,14] the cross section for B–production in 320 GeV/c π^-U interactions from a measurement of the di- and tri-muon yields. They quote a result of $(2.0 \pm 0.3 \pm 0.9)$ nb per nucleon assuming a linear A–dependence of the B–hadroproduction cross section. The QCD cross section calculated by E. Berger[15] agrees roughly with this result (using a K–factor of 2). In Fig. 1 we show the B–hadroproduction cross sections for π^-N and pN interactions calculated by E. Berger, together with the WA78 data point. We will use these calculated cross sections later to estimate the B–hadron yields of π^-N and pN interactions for fixed target B–experiments.

The general features of B–hadroproduction have been reported in several places.[1,2] The dominance of gluon fusion mechanism at collider energies leads to several salient features. This mechanism produces strong correlations between the b– and $\bar{b}$–quark directions such that both quark and antiquark are produced in the same direction strongly peaked along one or the other beam. In addition, the momentum of the b–quarks is appreciable only in the forward direction. Thus, the b–quarks in the very high-energy collisions at the SSC mimic the Lorentz-boosted TEV II fixed-target b–quarks and make the spectrometers required for B physics at the SSC and TEV II quite similar in configuration. This is discussed more fully in Refs. 1, 2 and 3.

The hadronization of the b–quark into one of the various species of B–meson or baryon proceeds by gluon radiation and in the process softens the spectrum of B–hadrons. The decay of the B–hadrons into the various exclusive final states further degrades the energy of the particles that must be detected. As an example of the effect that this multistage process can have, we have calculated the momentum spectra of the leptons from the semileptonic and the J/Ψ–decays of the B's using the PYTHIA Monte Carlo.[16] Both of these modes figure prominently in trigger strategies which have been proposed for B's. In Fig. 2a, b and c we show the momentum spectra of the electrons from the semileptonic decay of the $B \to De\nu$ for the B's produced at the SSC, TEV I and TEV II, respectively. In Fig. 3a, b and c we show the momentum spectra of the muons from the decay $B \to \Psi K\pi$ followed by the subsequent decay of the $\Psi \to \mu^+\mu^-$.

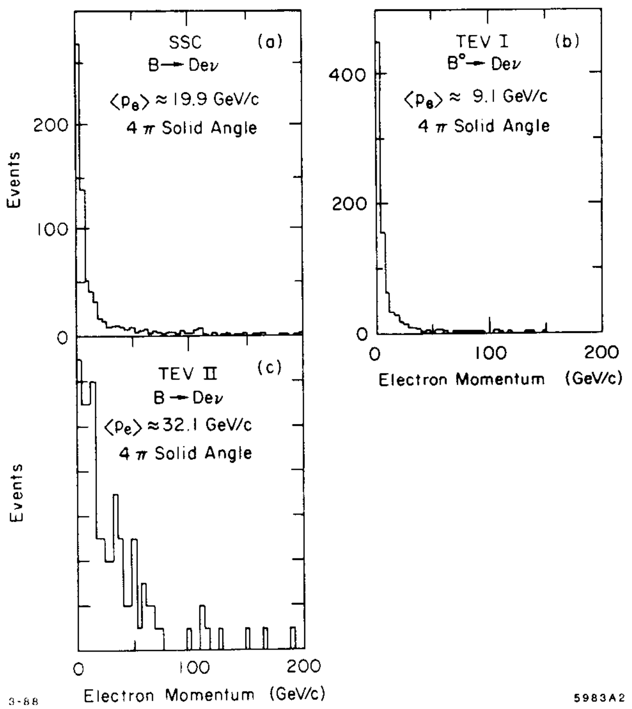

Fig. 2. Momentum spectrum of electrons from the semileptonic decay, $B \to D e \nu$ for B-production a) at the SSC, b) at the TEV I and c) at the TEV II.

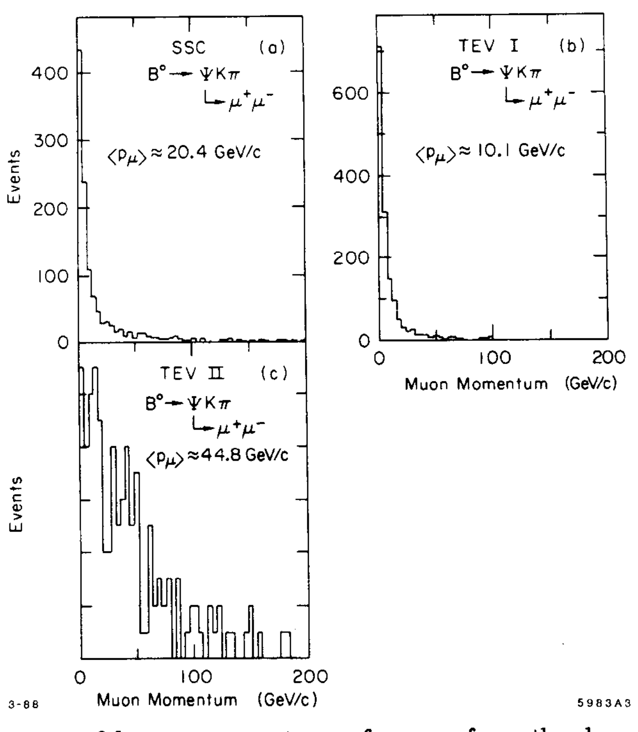

Fig. 3. Momentum spectrum of muons from the decay, $B \to \Psi K \pi \to \mu\mu K\pi$ for B-production a) at the SSC, b) at the TEV I and c) at the TeV II.

In both cases, the TEV II leptons have higher momentum than those produced at the SSC and much higher momentum than those produced in TEV I collider energies. The higher momentum of the B-decay products makes possible a clean lepton trigger for TEV II and SSC experiments as has been discussed in Ref. 2.

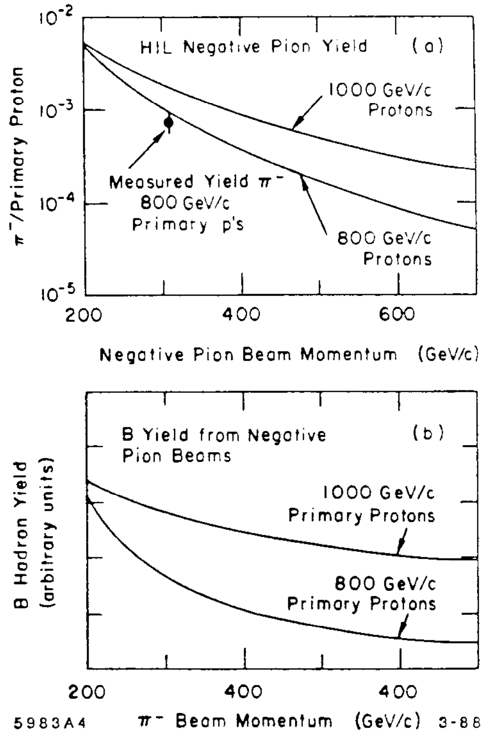

Fig. 4. a) Negative pion yield per incident proton for the Fermilab High Intensity Laboratory beam transport as a function of beam momentum; b) $B\overline{B}$ yield as a function of secondary negative pion beam momentum for the Fermilab HIL secondary pion beam transport.

4. Fixed Target *B* Physics Hadron Beam Options

Having rejected photoproduction as a possibility in our search for methods of accumulating large numbers of B-decays, there still exist many different hadron beam options to choose from for experiments seeking to produce large numbers of B's. Among these are neutron and pion secondary beams. In addition, primary proton beams from the accelerator can be used.

We will not quantitatively evaluate the possibilities of using neutron beams for B-hadroproduction experiments since such an evaluation is an intricate task which must take into consideration the backgrounds from beam halo which couple to particular experiments in a complex and experiment specific way. The neutron beam is unique in its neutral nature. It also has a relatively high-energy spectrum. On the other hand, it has all of the bad features of a secondary pion beam, i.e., large hadronic total cross sections, copious hadron and muon halos, and restricted yields. In addition, neutron beams have some particularly nasty features such as relatively uncontrollable beam spot size. We will leave it to others to argue that the neutral nature of neutron beams outweigh their negative aspects.

We will concentrate instead on comparing the use of secondary pion beams (and in particular negative pion beams) with the use of an extracted proton beam for B-experiments. In Fig. 4a we give, as an example, the negative pion yield of a relatively high intensity pion beam, the Proton West High Intensity Laboratory transport. When combined with the $\pi^- N \to B$ production cross section of Fig. 1, the yield curve of B's shown in Fig. 4b results. The B-yield curve resulting from the product of the production cross section and the pion beam yield curve is relatively flat. Choosing 500 GeV/c (in order to stay away from the region of rapid increase of the production curve for B's and to enhance the ratio of B cross section to total cross section as much as possible) as the beam momentum for π^- production of B's, we can calculate the yield of $B\overline{B}$'s per second as shown below.

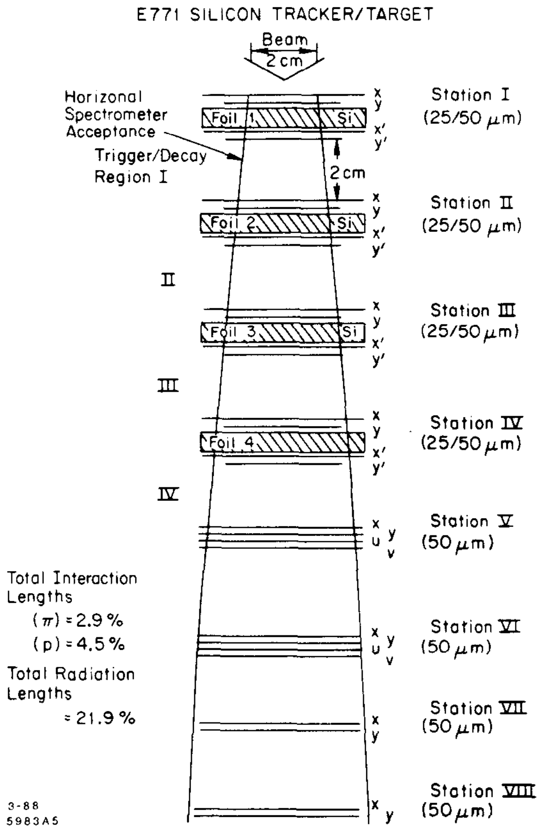

Fig. 5. E771 Silicon Tracker/Target

The number of π^-'s available for a given experiment is dictated by the number of primary protons available for a given experiment. In general, proton "economics" at Fermilab has made it difficult to obtain more than 2×10^{12} protons per minute from the Tevatron. Using this number of protons as a limit, we could expect 2.6×10^7 pions per second of spill (assuming 900 GeV/c primary protons) leading to approximately 7.5×10^5 interactions per second for an optimized silicon tracker target such as that of E771 shown in Fig. 5 (2.9% of an interaction length for pions). Since the E771 spectrometer can already operate at rates above 10^6 interactions per second, this means that the available pion beams cannot saturate the spectrometer. The ratio of $B\overline{B}$ cross section per nucleon at 500 GeV/c (approximately 10 nb as calculated by Berger) to the total πN cross section of 22 mb per nucleon is approximately 0.5×10^{-6}. In correcting this ratio to allow for operation with a nuclear target, the relative A dependence of the total cross section and the B cross section is taken to be $A^{0.28}$. For the silicon foils used in E771, the allowance for the relative A dependence results in an increase in the ratio to 1.3×10^{-6}. So finally, 7.5×10^5 interactions per second of spill results in 0.38 $B\overline{B}$/sec for operation with a pion beam.

In contrast, experiments using the extracted proton beam suffer no lack of available flux. For the case of the E771 target (4.5% of an interaction length for protons), 10^7 interactions per second can be achieved with approximately 2×10^9 protons per second. Using the calculation of Berger to get a $pN \to B$ cross section of approximately 8 nb at 900 GeV/c and using 32 mb for the pN total cross section per nucleon, we calculate a ratio of $.25 \times 10^{-6}$. Correcting for the use of a heavy target (silicon), we get 0.63×10^{-6} for the ratio of B cross section to total cross section for pN interactions. If we can operate at 10^7 interactions per second this will result in 6.3 $B\overline{B}$/sec or almost 10^8 $B\overline{B}$'s per 10^7 seconds of beam. Even if we can only operate at 10^6 interactions per second, we will still produce 0.63 $B\overline{B}$/sec, still a factor of two higher than the rate that can be achieved with pions.

The potential of the extracted proton beam for higher B-production rates than can be attained with a pion beam can only be realized if the maximum beam flux usable by an experiment is not limited by other factors. The radiation damage sustained when operating at 10^7 interactions per second (with 2×10^8 protons per second of spill distributed in a 1 cm radius spot) is at the level of a few times 10^{14} minimum ionizing particles per cm^2. This is the level where leakage current may begin to increase and the performance of the detector may begin to degrade but is probably still bearable. In addition, the average number of interactions per bucket, 0.2, is still tractable. The power of the trigger system, as discussed below, can be a limitation but, at least for some trigger strategies, 10^7 interactions per seconds seems to be reasonable. Finally, the individual elements of a given spectrometer may suffer rate effects but, presuming that these can be handled in some way, it seems clear that the proton beam offers the most potential for a high rate experiment. Indeed, the relative cleanliness of the extracted proton beam which has very little halo in comparison to a pion beam is a very little halo in comparison to a pion beam is a very attractive feature especially when trigger rates are considered. When the cleanliness of the proton beam is coupled to higher rates of $B\overline{B}$-production which are attainable, the extracted proton beam seems to be the optimum choice for fixed target experimentation.

5. Fixed Target Experimental Techniques

At present there are several approaches to fixed target B physics under investigation. They range from a totally "open geometry" experiment such as that of experiment E771[8], which might hope to observe both the B and $\overline{B}$, to a "semiclosed geometry" inclusive B-experiment[20] of P789 which seeks to observe the inclusive B-spectrum via two-body decay modes. The interaction rates required for the various experimental techniques will depend on the techniques and acceptances of individual spectrometers. We will not attempt to evaluate all of these techniques. Rather, we will attempt instead to outline some general features of the fixed-target experiments.

The most important aspect of these fixed-target experiments are the trigger strategies. At present there are a number of triggers that are being discussed by the various experiments. These triggers can be characterized as "physics" triggers and as "generic" triggers in the manner of Ref. 8. The physics triggers prejudice the physics *a priori* while the generic triggers do not select a particular mode except through second order acceptance effects. We list below some of the more widely discussed triggers:

1. Di-muon or J/Ψ trigger strategy (Fermilab Experiment E771, Ref. 8).
2. Single lepton trigger (Refs. 11, 12).
3. Secondary vertex triggers.
   - *a.* Multiplicity change trigger (Ref. 18).
   - *b.* Impact parameter trigger (CERN Experiment WA82, Ref. 17).
4. Intermediate p_t trigger (CERN Experiment WA84, Ref. 19).

The boundary conditions for such trigger systems are 1) the interaction rate that is required to accumulate the desired statistics for the experiment and 2) the amount of data than can be written on tape. The trigger system must make these two rates compatible. In the case of E771, they expect to eventually operate at 10^7 interactions per second. Since the data acquisition system (limited by tape writing speeds) can operate continuously at approximately one megabyte per second which is equivalent to a few hundred events per second of spill, the trigger system must produce a reduction of interaction rate by a factor of 10^{-4} to 10^{-5} without losing signal.

These types of considerations are common to all the trigger systems. In the case of each of the triggers mentioned above, the problem of matching the suppression of the interaction rate to data handling capability must be addressed to determine the sensitivity of the experiment. Again, in the case of E771, the J/Ψ trigger strategy is powerful enough to contemplate operation at 10^7 interactions per second. The requirement that there be two or more muons in an event will produce a few times 10^{-4} reduction by itself. The additional requirement that the two muons have an invariant mass greater than 2.4 GeV/c^2 should produce a factor > 10 further reduction in trigger rate, producing a total suppression of the interaction rate in the range 10^{-4}–10^{-5}. This can be done while losing only a small fraction of the $B \rightarrow J/\Psi + x$ signal. The number of produced $B \rightarrow J/\Psi + x$ events should be in the few tens of thousands per species of B per 10^7 seconds of operation if 10^7 interactions per second is, indeed, an achievable operating point.

Finally, there have been discussions of experiments which might go considerably beyond 10^7 interactions per second into the regime where we will see several interactions overlap within a single bucket. They range from the suggestion that one might be able to distribute the beam over a much larger spot in order to separate decays in space, rather than in time, in order to work at 10^9 interactions per second (Sandweiss) to the proposition that a double arm focusing spectrometer might be able to select two-body decay modes of the B's and operate at a rate greater than 10^{12} interactions per second by detecting the presence of the B secondary vertex early in the trigger sequence (Bjorken). These ambitious speculations await further definition.

6. Conclusions

We can draw several conclusions from this quick inspection of the possibilities for fixed target B physics experiments. First, given the low multiplicity of events at fixed-target energies and the relatively high momentum of the B–hadrons relative to the high multiplicities and quite low average momentum of the B's at TEV I, the fixed target experiments seem quite attractive in spite of the lower B cross sections at fixed target energies. It may well be that fixed target hadroproduction is the optimum place to do B physics until the era of the SSC. Of the possible methods advanced for executing hadroproduction experiments at TEV II, the hadroproduction experiments which use the primary proton beams offer the promise of the highest yield of B's if the spectrometers can be made to operate at high rates and the trigger systems powerful enough to suppress the total cross section interaction rate and to preserve the B events.

Second, the experiments at TEV II, because of the similarity of B–event configuration (ignoring the much higher multiplicity at the SSC), the similarity of RF bucket structure (15 ns at the SSC versus 18.7 ns at TEV II), and the similarity of rates at which the experiments are intended to operate (10^7 interactions per second and above at TEV I which is equivalent to luminosities of greater than 10^{32} cm^{-2} sec^{-1} at the SSC), provide an excellent school for learning to do the comparable experiments at the SSC. The similarity of spectrometers proposed for the SSC for B physics attest to this.

Finally, there is relatively unlimited luminosity available for B–experimentation at TEV II. The facility exists here and now and not in some future era. The limitations are the spectrometers and the cleverness of the experiments.

References

1. B. Cox, F. Gilman and T. Cottshalk, Proceedings of the 1986 Summer Study on the Physics of the Superconducting Collider, Snowmass, Colorado, **33** (1986).
2. B. Cox and D. E. Wagoner, Proceedings of the 1986 Summer Study on the Physics of the Superconducting Collider, Snowmass, Colorado, **83** (1986).
3. K. Foley et al., *Report of the Intermediate $p_\perp$ Detector Group: A Beauty Spectrometer for the SSC*, to be published in the Proceedings of the Berkeley Workshop on Detectors for the SSC, Berkeley, CA (1987).
4. N. Lockyer et al., *A Proposal for A Bottom Collider Detector* (1987).
5. N. W. Reay, *Letter of Intent for a Tevatron Collider Beauty Factory* (1987).
6. E. D. Bloom, *The PEP Option*, *B*–Meson Factory Workshop, SLAC (1987).
7. B. Cox, *Experimental Possibilities for Observation of CP Violation in B Decay,* invited talk to be published in the proceedings of the International Symposium on Heavy Flavors, Stanford University, Stanford, CA (1987).
8. B. Cox et al., *A Proposal to Study Beauty Production and Other Heavy Quark Physics Associated With Dimuon Production in 800-925 GeV/c PP Interactions,* Fermilab Proposal 771 (1986).
9. K. Berkelman, *The Future Cornell Program or CESR as a B-Factory, B*–Meson Factory Workshop, SLAC (1987).
10. Review of Particle Properties, Phys. Lett. **170B**, 15 (1986).
11. S. Conetti, B. Cox, W. Selove and D. E. Wagoner, *A Single Muon Trigger for E771,* to be published in the proceedings of the Fermilab Beauty Workshop (1987).
12. R. J. Morrison, S. McHugh and M. V. Purohit, *A Semileptonic Electron Trigger for Recording B^0, $\bar{B}^0$ Events,* UCSB–HEP–87–14, to be published in the Proceedings of the Berkeley Workshop on Detectors for the SSC, Berkeley, CA (1987).
13. M. G. Catanesi et al., WA78 Collaboration, Phys. Lett. **187B**, 431 (1987).
14. M. G. Catanesi et al., WA78 Collaboration, CERN–EP/87 (1987).
15. E. Berger, *Heavy Quark Production in Hadron Collisions,* ANL–HEP–PR–87–53 (1987); E. Berger, *Momentum Correlations in Heavy Quark Hadroproduction,* ANL–HEP–PR–87–113 (1987); E. Berger, talk given at Fermilab Beauty Workshop (1987).
16. H. U. Bengtsson and G. Ingelman, Computer Phys. Comm. **34** (1985) 351.
17. L. Rossi et al., *Proposal for a Test of an Impact Parameter Trigger Aimed at a High Statistics Heavy Quark Study,* CERN/SPSC 85–62, SPSC/P218 (1985).
18. W. Selove, *A Multiplicity Change Trigger for Fermilab Experiment E771,* to be published in the Proceedings of the Fermilab Beauty Workshop (1987).
19. C. Fisher et al., *A Proposal to Study the Production and Decay Properties of Beauty Flavored Hadrons,* CERN/SPSC 87–2, SPSC/P 226 (1987).
20. D. Kaplan, Fermilab Proposal P789, *A Proposal to Measure the Production and Decay into Two-Body Modes of B-Quark Mesons and Baryons* (1987).